UNIVERSITY OF PARDUBICE

Faculty of Chemical Technology

Adaptation of conventional and modern non-invasive methods for analysis of photoaged human skin barrier

Author: Mgr. Marek Svoboda

Supervisor: prof. RNDr. Zuzana Bílková, Ph.D.

Co-Supervisors: Mgr. Iva Dolečková, PhD. and Mgr. Tomáš Muthný, Ph.D.

DECLARATION

I hereby declare that I have written this doctoral thesis independently. All sources and information that have been used are listed in the bibliography – reference list. I am aware that my work is to abide by the rights and obligations under Act No. 121/2000 Coll. – Copyright law, especially with the fact that the University of Pardubice is entitled to the concession contract for this work such as school work according to § 60, Section 1 of the Copyright Act, and that if this work will be used by me or licensed to use by another entity, University of Pardubice is entitled to demand a reasonable reimbursement covering the incurred costs for funding this work up to their actual amount and according to circumstances. I agree with full disclosure to the public in the University Library and via the Digital Library of the University of Pardubice in agreement with the article 47b of the Act No. 111/1998 Coll., on Higher Education Institutions, and on the Amendment and Supplement to some other Acts (the Higher Education Act), as subsequently amended, and with the University of Pardubice's directive no. 9/2012.

ACKNOWLEDGEMENT

I am compelled to state my full acknowledgements and show my unreserved gratitude to all who supported me in this long journey as this would not be possible if it was not for every single one of them.

First of all, I would like to thank Professor Zuzana Bilkova for making my doctoral studies in Contipro happen and for being the role-model professor to whom every student can look-up to.

The main acknowledgement belongs to Contipro family, where I grew-up as a scientist and where I progressed as a person. As a former team-member of Cosmetology team, I want to show my appreciation for their commendable hard-work, knowledge, innovation and guidance. Special thanks belongs to Dr. Jana Matonohova, Dr.Paulina Orzoł, Marketa Maresova, Dr. Lenka Sucha, Lenka Machkova, Sona Moravcikova and my co-supervisors Dr. Iva Doleckova and Dr. Tomas Muthny as they brought so much joy, confidence, respect, perspective and experience to my daily scientific life and beyond. It has been an honor to spent four great years with them.

Also, I am obliged to pay respect to Contipro CEO and co-founder Professor Vladimir Velebny for what he has done for the whole community and for supporting my project.

Furthermore, I would like to thank Professor Katerina Vavrova and Professor Michal Holcapek for the collaboration on lipidomics. Also, special thanks belong to my fellow friend Dr. Jakub Novotny for constructive debates, his unmatched wit and much more.

The warmest thanks belong to a special person to me, Hana Ohnoutkova. For over seven years, her unyielding faith, resolve, companionship and love has been the greatest support to me beyond any recognition. I wish I could repay the depth. My heartful appreciation for the support, inspiration and so much more also belongs to her mother and family of Hegar.

At last, my thanks go to my beloved family and friends for the endless support, understanding and great deal of patience. I hereby dedicate this thesis to my greatest benefactor, scientist at heart and grandad all in one person. I wish I could have finished the thesis earlier.

PODĚKOVÁNÍ

Nemohu jinak než vyjádřit svůj neskonalý vděk všem, kteří mě během této náročné cesty podporovali. Těžko bych uspěl, nebýt každého jednoho z těchto lidí.

Nejprve bych velice rád poděkoval profesorce Zuzaně Bílkové za uskutečnění mého doktorského studia ve firmě Contipro a také za její přístup, který je vzorem mnoha kolegům a studentům.

Hlavní poděkování patří rodině Contipro, kde jsem vyrostl jako vědec a pokročil jako osobnost. Jako bývalý člen týmu Kosmetických surovin bych rád vyjádřil uznání před jejich tvrdou prací, znalostmi, inovací a vedením. Obzvláště děkuji Dr. Janě Matonohové, Dr.Paulině Orzoł, Markétě Marešové, Dr. Lence Suché, Lence Machkové, Soně Moravčíkové a mým vedoucím Dr. Ivě Dolečkové and Dr. Tomáši Muthnému, že (nejen) do mého života vědce přinášeli tolik radosti, důvěry, respektu, perspektivy a zkušeností. Bylo mi ctí strávit s nimi čtyři skvělé roky v jednom týmu.

Musím také prokázat obrovský respekt řediteli a spoluzakladateli Contipro docentu Vladimíru Velebnému za jeho přínos vědecké komunitě a také za podporu mého projektu.

Dále bych rád poděkoval profesorce Kateřině Vávrové a profesoru Michalovi Holčapkovi za spolupráci v oblasti lipidomiky. Zvlášť děkuji mému blízkému příteli a kolegovi Jakubu Novotnému za konstruktivní debaty, za jeho bezkonkureční intelekt a mnohem více.

Nejvřelejší vděk patří osobě mně nejdražší, Haně Ohnoutkové. Více než sedm let byla pro mě její nezdolná víra, odhodlání, společnost a láska tou největší oporou jakou jsem mohl mít. Kéž bych to mohl oplatit. Mé srdečné díky za podporu, zázemí a inspiraci a mnoho dalšího patří i její mamce a rodině Hegarových.

Nakonec bych chtěl poděkovat své milované rodině a mým přátelům za jejich nekonečnou podporu, pochopení a velkou dávku trpělivosti. Tímto bych rád věnoval tuto dizertační práci mému hlavnímu patronovi, který měl srdce vědce, mému dědovi. Lituji, že jsem práci nedokončil dříve.

ANNOTATION

This doctoral thesis deals with the phenomenon of unchanged or even decreased trans-epidermal water loss (TEWL) in the aged skin despite a decreased skin barrier lipids content. To address this task, analysis of structural components of the skin barrier was performed along with analysis of the skin barrier properties by using a wide range of methods. Optimal procedures for the skin sampling and subsequent sample handling and analysis were established as the first step. The second step included the analysis of the epidermal tight junction (TJ) proteins expression, lipid content and the skin barrier properties in the skin affected by ageing to select a potential target responsible for this phenomenon. The last part of this thesis challenged the target molecule occludin with regard to TEWL in the skin with diminished lipid barrier by using an *ex vivo* porcine skin model.

Keywords: confocal microscopy, immunochemistry, lipids, PCR, skin barrier, thin-layer chromatography, TEWL, tight junctions

ANOTACE

Tato dizertační práce se zabývá fenoménem stabilní nebo dokonce snížené transepidermální ztráty vody (TEWL) ve stárnoucí kůži navzdory nižšímu obsahu bariérových lipidů. K řešení této problematiky bylo nutné analyzovat strukturální komponenty kožní bariéry a biofyzikální parametry kůže, k čemuž byla použitá celá řada analytických metod. Jako první krok byla provedena optimalizace postupu pro odběr vzorku a jeho následného zpracování a analýzy. Další krok zahrnoval analýzu exprese proteinů epidermálních těsných spojů, analýzu obsahu lipidů a analýzu bariérových vlastností v kůži ovlivněné stárnutím, což bylo použito k následné selekci možných cílových molekul zodpovědných za výše uvedený fenomén. Poslední část této práce zkoumá potenciální molekulu okludin ve vztahu k TEWL v kůži se sníženým obsahem lipidů za použití *ex vivo* modelu prasečí kůže.

Klíčová slova: imunochemie, konfokální mikroskopie, kožní bariéra, lipidy, PCR, tenkovrstevná chromatografie, TEWL, těsné spoje

ABSTRACT

A photoaged skin is able to maintain its water barrier as trans-epidermal water loss (TEWL) remains constant or even decreases throughout the skin aging. Since tight junctions (TJs) can restore the skin barrier after an acute damage, we addressed the potential ability of TJs to regulate the water barrier in the aged skin.

First of all, several optimization procedures of analytical methods as well as sampling methods were required to gain relevant and reproducible results, which is a must when working with skin samples. Suction-blistering and tape-stripping were tested as sampling techniques for the suitability of subsequent extraction and analysis. Although punch biopsy is a golden standard in dermatology, it is significantly more invasive than the latter and may pose serious ethical concern. Therefore, for the purpose of this study, the suction blistering was selected as a sampling method of the first choice as it provides better analysis capabilities of the epidermis than the tape-stripping and is less invasive than the punch biopsy.

Microarray analysis of young and aged human epidermis provided from a local surgery clinic has been used to map the gene expression of all TJs-associated proteins. Claudin-1, occludin and ZO-2 were selected for further study based on a difference in the expression between the two age groups and their connection to the skin barrier as known from previous studies. These TJ proteins were analyzed on the mRNA and protein level along with epidermal lipids in the sun-exposed (dorsal forearm) and sun-protected (volar forearm) area of the young and aged human skin in the epidermal samples acquired by suction blistering from healthy human volunteers.

The sun-exposed, but not sun-protected, aged skin had lower total amount of epidermal lipids than the young skin. Next, a significant overexpression of occludin and ZO-2 was found in the sun-exposed aged skin, but ZO-2 was also overexpressed in the sun-protected aged skin. Furthermore, an *ex vivo* model, a delipidated porcine epidermis, was used to study the occludin-driven restoration of TEWL. A previously reported, occludin-stimulating NPWDQ casein-derived peptide induced occludin overexpression in this model as well, which was accompanied by amelioration of the water barrier in the delipidated porcine epidermis. Taken together, these results suggest that occludin plays an important role in the water barrier maintenance of the photoaged skin.

ABSTRAKT

Kůže ovlivňovaná slunečním zářením v průběhu stárnutí je schopna udržet neporušenou vodní bariéru, kdy hodnoty transepidermální ztráty vody (TEWL) zůstávají stejné nebo se i snižují v průběhu tohoto procesu. Vzhledem k tomu, že těsné spoje jsou schopny kompenzovat kožní bariéru při akutním poškození, byla tato jejich schopnost zkoumána i ve stárnoucí kůži.

Nejprve byly optimalizovány procesy odběru vzorku epidermis a analytické metody, což je obzvláště nutný krok pro zisk relevantních a reprodukovatelných výsledků při práci s kožními vzorky. Techniky v anglickém jazyce označovány jako „suction-blistering“ a „tape-stripping“ byly testovány jako odběrové techniky pro vhodnost k extrakci a analýze. I když technika tzv. punch-biopsie je zlatým standardem odběru vzorků kůže v dermatologii, představuje mnohem invazivnější techniku, a podléhá tak přísnějším etickým zásadám. Pro účely této studie byla nakonec vybrána technika „suction-blistering“, která je pro analýzu epidermis vhodnější než tape-stripping a zároveň je méně invazivní než tzv. punch-biopsie.

Pomocí „microarray“ analýzy byla zmapována genová exprese proteinů asociovaných s těsnými spoji ve vzorcích staré a mladé epidermis poskytnuté z lokální plastické chirurgie. Na základě rozdílů genové exprese mezi těmito věkovými skupinami a také předešlých znalostí o jednotlivých proteinech těsných spojů byly pro další analýzu vybrány „claudin-1“, okludin a ZO-2. Tyto proteiny byly dále analyzovány pro jejich expresi na úrovni mRNA a proteinu spolu s epidermálními lipidy v lidské staré a mladé epidermis v místech sluncem exponovaných a před sluncem chráněných, které byly získány technikou „suction-blistering“ z vnitřního a vnějšího předloktí zdravých dobrovolníků.

Stárnoucí kůže, sluncem exponovaná, vykazovala celkově nižší obsah epidermálních lipidů než mladší kůže a zároveň i zvýšenou expresi okludinu a ZO-2. Exprese ZO-2 byla zvýšená i v části před sluncem chráněné. Pro další postup byl připraven *ex vivo* model prasečí epidermis se sníženým obsahem bariérových lipidů, který byl použit pro zkoumání možné obnovy poškozené bariéry indukované occludinem. V literatuře popsaný NPDQW kaseinový peptid byl použit k indukci exprese okludinu, což bylo doprovázeno zlepšením vodní bariéry modelu poškozené prasečí epidermis. Tyto výsledky naznačují možnou roli okludinu při udržení vodní bariéry ve stárnoucí kůži exponované slunečnímu záření.

TABLE OF CONTENT

LIST OF FIGURES

LIST OF TABLES

LIST OF ABBREVIATIONS

3D	three dimensional
AA	9-aminoacridine
APCI	atmospheric pressure chemical ionization
aSE	aged sun-exposed
aSP	aged sun-protected
CholS	cholesterol sulfate
CLSM	confocal laser scanning microscopy
C_t	threshold cycle
Ceramide Nomenclature	sphingoid base (S: sphingosine, P: phytosphingosine, H: 6-hydroxysphingosine, DS:sphinganine) N-acyl residue (A:α-hydroxy-FA, O: ω-hydroxy-FA, N: no hydroxy-FA) E: acylated with linoleic acid in ω-OH position
DAPI	4′,6-diamidino-2-phenylindole
DHB	2,5-dihydroxybenzoic acid
DNA	deoxyribonucleic acid
EDTA	2,2',2",2'"-(Ethane-1,2-diyldinitrilo) tetraacetic acid
ESI	electrospray ionization
FA	fatty acids
FFA	free fatty acids
FRET	fluorescence resonance energy transfer
FT	Fourier transform ion cyclotron resonance
GAPDH	glyceraldehyde 3-phosphate dehydrogenase
GCer	glucosyl ceramide
HILIC	hydrophilic interaction chromatography
HPLC	high performance liquid chromatography
HPTLC	high performance thin layer chromatography
IHC	immunohistochemistry

IgG (M)	immunoglobulin G (M)
IPA	isopropanol
IR	infrared
JAM	junction adhesion molecule
LB	lysis buffer
MALDI	matrix associated laser desorption ionization
MS	mass spectrometry
NARP	Nonaqueous reversed phase
NP-HPLC	normal phase high performance liquid chromatography
RP-HPLC	reversed phase high performance liquid chromatography
OECD	The Organization for Economic Co-operation and Development
PC	phosphatidylcholine
PI	phosphatidylinositol
PL	phospholipids
PS	phosphatidylserine
PVDF	polyvinylidene difluoride
Q (QQQ)	quadrupole (triple quadrupole)
qRT-PCR	quantitative reverse transcription polymerase chain reaction
RCM	reflectance confocal microscopy
RHE	reconstructed human epidermis
RHS	reconstructed human skin
RNA	ribonucleic acid
RT	room temperature
SB	suction blistering
SC	stratum corneum
SDS-PAGE	sodium dodecyl sulfate–polyacrylamide gel electrophoresis
SFC	supercritical fluid chromatography
SG	stratum granulosum
SM	sphingomyelin

TBS	tris buffered saline
TEWL	trans epidermal water loss
TG	triacylglycerols
TJ	tight junctions
TLC	thin layer chromatography
TOF	time-of-flight
TS	tape-stripping
UV	ultraviolet
WB	western blotting
ySE	young sun-exposed
ySP	young sun-protected
ZO	zonulin

1 INTRODUCTION

The skin as an external organ creates a crucial barrier in the human body. The barrier function of the skin is fulfilled by its outermost skin layer, the epidermis, where the stratum corneum (SC) plays a key role (Elias 2005; Pouillot et al. 2008; Proksch et al. 2008). The skin as the barrier protects the organism from biological and chemical threats, regulates the passage of molecules and protects against physical insults such as UV-light. However, these external factors damage the skin triggering respective cellular responses which over time cause the skin aging. Up to 90% of the skin aging features may be attributed to the photoaging and its most significant factor, the UV irradiation (Gilchrest 2013; Kohl et al. 2011; Shah and Rawal Mahajan 2013).

The aged skin has a deteriorated barrier function with an altered permeability to various substances (Farage et al. 2008; Hung et al. 2012; Vinson and Anamandla 2006), which is thought to be caused by a decreased lipid content in the SC. More specifically, a generally accepted idea is that the aged skin losses approximately 30% of ceramides (Coderch et al. 2003). Paradoxically, the water barrier does not show any signs of deterioration associated with aging as trans-epidermal water loss (TEWL) remains constant or even decreases with age (Kottner et al. 2013b; Luebberding et al. 2013a; Luebberding et al. 2013b). Although several hypotheses have been introduced, this phenomenon has not been elucidated yet. After an acute damage to the skin barrier either by tape-stripping (TS), organic solvents or by UV-light, TEWL significantly increases in the damaged area and returns to normal after 10 days, even though the SC is not fully recovered suggesting some sort of compensatory mechanism (Jiang et al. 2007; Kottner et al. 2013b; Malminen et al. 2003; Yuki et al. 2011).

The debate puts forward a role of tight junctions (TJs). TJs were shown to be an important contributor to the barrier function of the skin (Kirschner et al. 2013; Yuki et al. 2007). A knockdown or downregulation of most TJ proteins is associated with the barrier dysfunction, as reviewed in (Svoboda et al. 2016). In this regard, TJs have shown the ability to compensate for damaged or even completely missing SC. During this process, some of the TJ proteins such as zonulin (ZO)-1 or occludin exert an increased expression resulting in a blockage of the passage of various molecules at TJ positive sites (Celli et al. 2012; Malminen et al. 2003). We aimed to investigate whether the same mechanism works also in the photoaged skin affected by years of the chronic UV exposure or in the intrinsically aged skin, and whether TJs can regulate TEWL of the photoaged skin or intrinsically aged skin in such manner. We analyzed TEWL,

lipid composition and organization, and expression of claudin-1, occludin and ZO-2 in the young and aged, both sun-protected (volar) and sun-exposed (dorsal) forearm skin.

Such an approach requires a sampling from various skin regions. Due to regional epidermal differences, the sampling techniques must be flexible and performable almost anywhere on the skin area (Sandby-Møller et al. 2003; Tagami 2008). A few techniques, invasive and non-invasive, are used for the skin sampling, where punch biopsy dominates as a quick and reliable technique providing a substantial amount of a full-thickness skin sample. However, punch biopsy represents a painful intervention into the body causing a permanent skin damage and brings along the potential health risks such as infection, nerve damage or allergy to anesthetics, which should not be neglected (Nischal et al. 2008; Zuber 2002). Moreover, punch biopsy must be performed by an acknowledged physician. Altogether, punch biopsy is highly demanding on research laboratories to meet the ethics committee requirements, and thus research laboratories might find it rather difficult to acquire a biopsy of intended both quality and quantity. Therefore, techniques with minimalized invasiveness such as suction blistering (SB) and TS, which are less painful and leave no permanent damage (Serup et al. 2006), are more suitable for common research laboratories. Generally, SB and TS techniques do not provide full-thickness skin samples, which is not imperative for the epidermal analysis. However, it is a question what the possibilities and limits of these techniques for the analysis of the epidermis are. To ensure reliable analysis of epidermal lipids and TJ proteins, reproducible sampling process and detection methods must be established and optimized.

2 TIGHT JUNCTIONS IN THE SKIN

2.1 The human skin

The skin is an indispensable human organ that creates an important barrier protecting the human body against external threads and the interface with the outer environment. It is a complex arrangement of structures with a wide range of different functions. The skin accounts for approximately 5-15% of total bodyweight of an adult, weighing twice as much as the brain, and covers up to $2m^2$ (Sontheimer 2014).

The skin consists of two individual and unique, but cooperating layers, the dermis and epidermis. The third layer that underlies the skin, the hypodermis (or subcutaneous tissue), is considered by some experts as a part of the skin, but others say otherwise. The skin as a quite adaptable organ varies in thickness and other features according to function and area of the body (McLafferty et al. 2012). For a detailed description of individual skin compartments see following references (Burr and Penzer 2005; James et al. 2006; Kanitakis 2002; Kolarsick et al. 2011).

The complex skin system fulfills several functions, including barrier, sensory, secretory, thermoregulatory, immunological and psychological function. However, the barrier function is a primary purpose of the skin above all else (McLafferty et al. 2012; Venus et al. 2011).

2.2 Barrier function of the skin

Two distinct aspects of the skin barrier function are recognized: “outside-in” and “inside-out” barrier. The skin not only prevents microorganisms, xenobiotics or UV-rays from entering the organism (outside-in), it also regulates movement of water, ions or metabolites from the inside to the outer environment (Natsuga 2014). Both aspects can be readily analyzed. “Outside-in” barrier analysis involves either *in vivo* or *ex vivo* penetration of a reference compound (dye, caffeine, testosterone) into the skin. “Inside-out” barrier is measurable either by a tracer injected into the dermis or by TEWL. TEWL is commonly used as an indicator for the skin barrier function since it is easy and quick to perform (Fluhr et al. 2006; Indra and Leid 2011).

Several pathways exist that lead in or out of the skin barrier, see Figure 1. The first pathway is transepidermal, which includes transcellular (or intracellular) and paracellular (or intercellular) route. The second pathway is called as appendageal (or shunt) (Ng and Lau 2015).

The skin barrier function is primarily fulfilled by the epidermis whose unique structure and composition is highly specialized to do so.

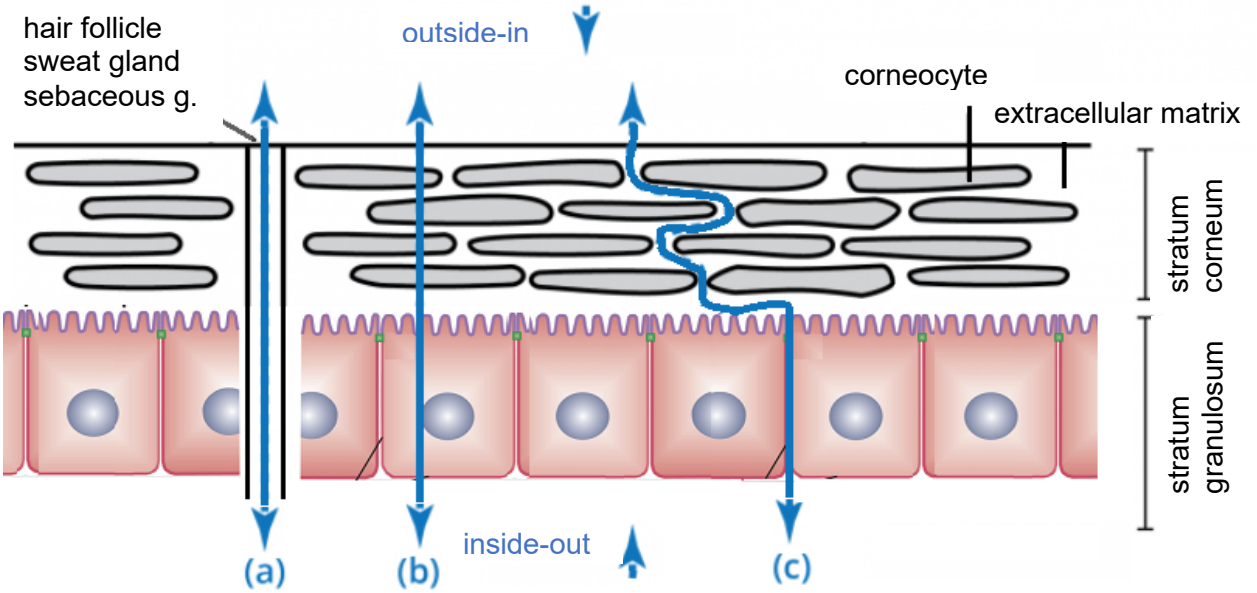

Figure 1: Illustration of outside-in and inside-out skin barrier function. *a) appendageal pathway; b) transcellular pathway; c) paracellular pathway. Modified from (Wilbur 2017).*

2.3 Epidermis

The epidermis, the outermost layer of the skin, is composed of stratified keratinized squamous epithelium, which is approx. 100µm thick. Four main cell types can be found in the epidermis: Merkel cells, dendritic (Langerhans) cells, melanocytes and keratinocytes that represent the majority (up to 95%). The epidermis itself is divided into a number of layers, including the stratum basale, stratum spinosum, stratum granulosum (SG), stratum lucidum (only present at finger tips, palms and soles), and SC (Tortora and Derrickson 2009). These layers are designated by the different stages of keratinocyte maturation. Therefore, each layer has a unique structure and function.

The stratum basale is a bottom epidermal layer made up of a single row of columnar keratinocytes, a.k.a. epidermal stem cells that are capable of division. However, not all of them can divide (Jones et al. 1996). These stem cells are clonogenic cells with a long lifespan that progress through the cell cycle very slowly under normal conditions. Basal keratinocytes are scaffolded together by the basement membrane, which creates an interface between the epidermis and dermis. As the daughter cells of the keratinocytes move into the next layer, the

stratum spinosum, they lose their ability to divide. Keratinocytes in this layer resemble spines due to desmosomal connections with adjacent cells that are continuously broken and reformed. Also, a production of lamellar granules is initiated in the upper stratum spinosum. The last epidermal layer containing living cells, the SG, is composed of flattened cells harboring large quantities of keratohyaline granules and lamellar granules (see Figure 2). Keratinocytes in this layer initiate the terminal differentiation, a specific type of apoptosis. By this stage, keratinocytes lose their nucleus, lose their metabolic functions, become keratinized and enter the SC, which is the uppermost layer of the epidermis. It is up to 400 µm thick, containing 25-30 layers of dead, flattened and anucleated cells, a.k.a. corneocytes, which eventually shed off in the process called desquamation. Keratinocyte proliferation and differentiation secures perpetual renewal of the epidermis, which takes approx. 28 days (Kolarsick et al. 2011).

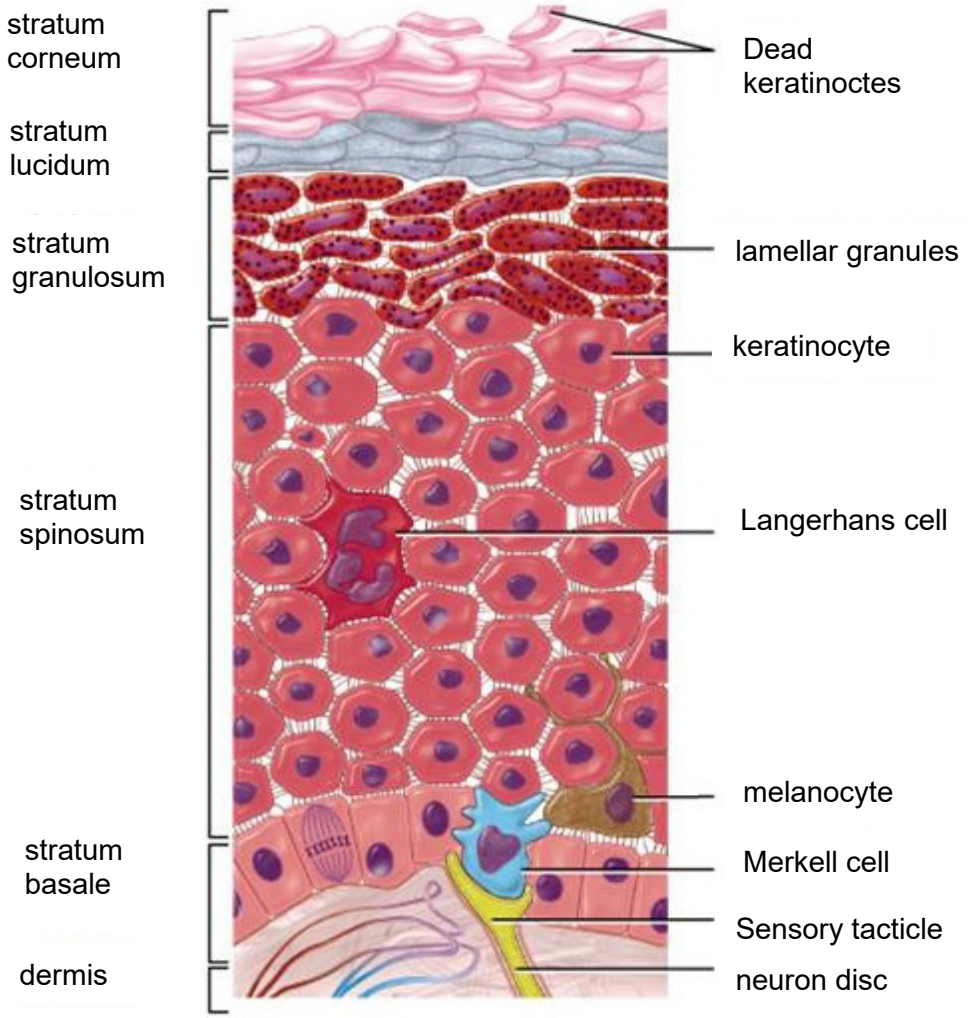

Figure 2: Schematic illustration of cross-sectioned epidermis. *Modified from:* (Earthslab).

2.4 Stratum corneum: the first and critical barrier

Although the SC constitutes only around 10 % of the skin, it contributes to over 80 % of the skin barrier function (Pouillot et al. 2008). The SC has a unique structure and composition and forms a multi-layered sheet of protein-rich corneocytes connected by corneodesmosomes and embedded in the intercellular lipid matrix.

After the terminal differentiation, corneocytes are substantially enriched with proteins. Alongside a protein enhancement of the corneocyte‘s cytosol with keratins and filaggrin (almost 90 % of all protein content) (Sandilands et al. 2009), a cornified envelope is being assembled on the corneocyte‘s plasma membrane during the differentiation process.

Cornified envelope is a tough protein complex structure that essentially contributes to biomechanical properties of SC, and that provides an anchor point for lipid matrix. Cornified envelope consists of specialized proteins such as involucrin, loricrin, elafin, desmoplakin and other that are highly cross-linked, for review see (Eckert et al. 1993; Nithya et al. 2015; Proksch et al. 2008; Yoneda et al. 1992). Along with transglutaminase, involucrin initiates the assembly of cornified envelope. Furthermore, involucrin but also periplakin, envoplakin and loricrin provide an anchor for ω-hydroxyceramides, which create a lipid envelope that further establishes an interface for lipid fraction of the SC (Kalinin et al. 2002).

2.5 Stratum corneum: barrier lipids

Lipids greatly vary in structural and functional features and physical properties. A comprehensive classification organizes lipids into eight categories which include fatty acyls (FA), glycerolipids, glycerophospholipids, sphingolipids, sterols, prenols, saccharolipids and polyketides, for a review see (Fahy et al. 2005).

Skin surface lipids are found in the upper layers of epidermis where they have number of specific roles. Skin surface lipids include epidermal lipids and sebaceous lipids. Mixture of skin surface lipids has a unique composition as compared to lipids in serum or in other tissues (De Luca and Valacchi 2010). Lipid mass of SC comprises of 50 % ceramides, 25 % cholesterol, 10 % FA and the rest consists of cholesterol sulfate and cholesterol esters (Madison 2003). Epidermal lipids contain mainly saturated FA and very long chain FA (C20-28). However, unsaturated and essential FA are needed for proper epidermal integrity as well. Linoleic acid is the most abundant FA in human epidermis (Ziboh et al. 2002).

Ceramides are very important class of epidermal lipids. Besides their crucial role in the formation and maintenance of epidermal barrier function, ceramides and their metabolites possess cell signaling abilities that affect differentiation, apoptosis etc. (Rabionet et al. 2014). Twelve ceramide fractions that vary in hydroxylation and FA moiety can be extracted from the SC (Kindt et al. 2012; Ponec et al. 2003; van Smeden et al. 2011a). Ceramide nomenclature is based on chromatographic migration as proposed by Motta et al., see Figure 3 (Motta et al. 1993). In total, there are already 342 identified ceramide species in human SC (Breiden and Sandhoff 2014; Rabionet et al. 2014). Epidermal ceramides contain unique acylglycosylceramides which binds linoleate via ω-hydroxy group. Two major and distinctive classes of skin ceramides derive from esterification of the ω-hydroxyl group: ultra-long chain ceramides and protein bound ceramides. Ultra-long chain (C28-36) ceramides are thought to be responsible for the formation of lamellar granules. Furthermore, after hydrolysis, acylceramides have the same effect for lamellar bilayer formation in the SC. Terminal hydrolysis causes binding of free ω-hydroxy ceramides to the protein envelope of corneocytes which creates linked interface between bricks and mortar (Feingold 2007; Madison 2003). For detailed description of ceramide synthesis in the epidermis, see following references (Elias and Wakefield 2014; Ishida-Yamamoto et al. 2004; Rabionet et al. 2014; Zheng et al. 2011).

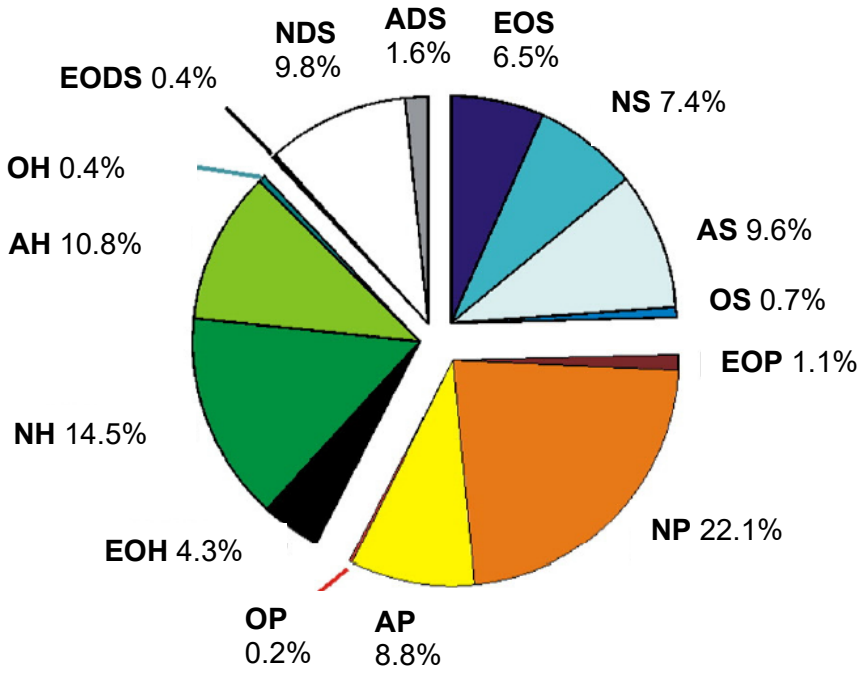

Figure 3: Molecular distribution of different ceramide species in human SC. *The structures are classified according to the sphingoid base (S: sphingosine, P: phytosphingosine, H: 6-hydroxysphingosine, DS:sphinganine) and the N-acyl residue (A:α-hydroxy-FA, O: ω-hydroxy-FA,N: no hydroxy-FA). E: acylated with linoleic acid in ω-OH position. Modified from* (Breiden and Sandhoff 2014).

Epidermal lipids represent crucial component of the SC. The barrier function is severely disrupted in number of skin diseases with disordered lipid metabolism. Psoriatic skin or skin with atopic eczema were found to have significant changes in ceramide subclasses (Jungersted et al. 2010; Mallbris et al. 2006). Aged epidermis also exhibits aberrant lipid composition. Number of studies showed that altering lipid content or metabolism in the epidermis results in impaired barrier function (Li et al. 2007; Radner and Fischer 2014). Ceramide subclasses and chain length have been found to affect lipid lamellar organization in the SC and also the barrier function of the skin. Increased content of short-chained ceramides decreased the skin barrier function (Janssens et al. 2012) and another study observed impaired barrier function when a content of very long-chain ceramides was lowered (Li et al. 2007). However, minor lipid classes such as triglycerides are also important. Impaired metabolism of triglycerides negatively affected barrier function as well (Radner and Fischer 2014).

2.6 Tight junctions in the epidermal barrier

TJs are type of cell-cell junctions sealing an intercellular space between adjacent cells (Tsukita et al. 2001). TJs are complex structures comprised of various transmembrane, scaffolding and cell polarity proteins, see Figure 4 (Brandner 2009; Brandner et al. 2008). While TJ structures are strictly formed only within one cell layer, expression pattern of individual TJ proteins is more complex (Kalinin et al. 2002).

Claudins, occludin, and tricellulin are tetraspan transmembrane proteins with two extracellular loops which act mainly as physical barrier in TJ complexes (Ebnet 2004; Furuse et al. 1993; Ikenouchi et al. 2005; Krause et al. 2008; Turksen 2004). Claudin-1 and claudin-7 are expressed in all living epidermal layers, while occludin and claudin-4 is only present at the SG (Brandner 2007; Peltonen et al. 2007; Pummi et al. 2001). Tricellulin is predominantly expressed in the SG at tricellular contacts but can also be found in lower layers of the epidermis (Schlüter et al. 2007) . Junctional adhesion molecules (JAMs) have two extracellular Ig-like domains and also create physical barrier in the intercellular space. JAM-A is present in all living epidermal layers (Brandner 2009). Scaffolding proteins localized peripherally to the cell membranes are tightly associated with transmembrane proteins, and anchor the whole protein complex to actin component of the cytoskeleton (O'Neill and Garrod 2011). ZO-1, ZO-2, cingullin and symplekin belong to the scaffolding proteins and reside at the SG with faint expression pattern in the lower layers (Langbein et al. 2002; Peltonen et al. 2007; Pummi et al.

2001). Functional TJ structure is formed where all TJ proteins co-localize, which is in the uppermost living cell layers of the epidermis (Haftek et al. 2011; Langbein et al. 2003). Recent studies demonstrated that TJ barrier is single layered and formed in the second SG layer in rodent (Furuse et al. 2002; Kubo et al. 2009) as well as in the human epidermis (Yoshida et al. 2013).

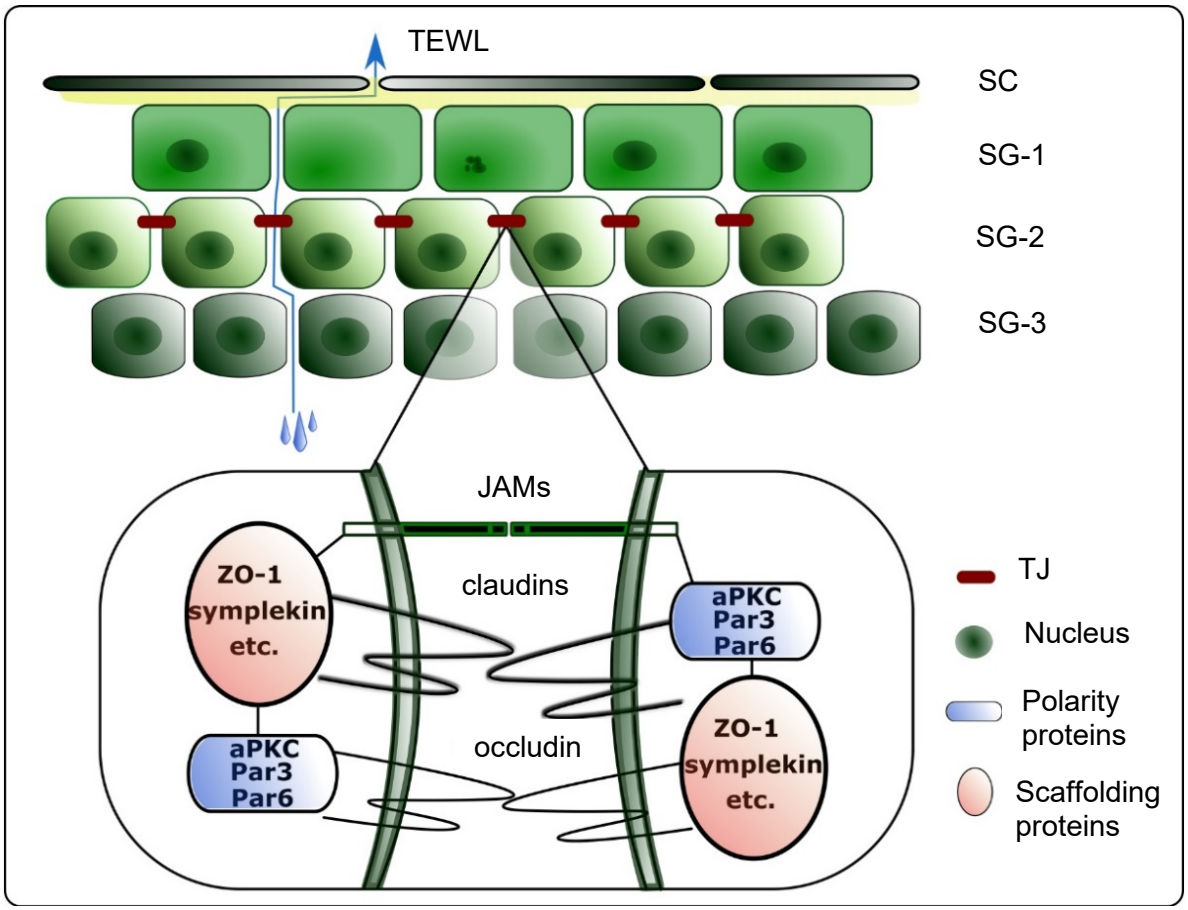

Figure 4: Localization, structure and protein composition of epidermal TJ. *JAM, junctional adhesion molecules; Par, partitioning defective; aPKC, atypical protein kinase; SC, stratum corneum; SG, stratum granulosum; TEWL, trans epidermal water loss; TJ, tight junction.*

2.7 Functions of the tight junctions in the skin

Skin TJs represent multifunctional elements, which are involved in the barrier function of the skin, regulation of epidermal homeostasis and differentiation of the epidermis. TJs are associated with establishment of epithelial polarity that helps to facilitate these functions. The second SG layer containing TJs exhibited cellular polarity maintained by Par3/Par6/aPKC protein complex (González-Mariscal et al. 2008; Matter et al. 2005), which is also responsible for the correct assembly of the whole TJ structure (Anderson et al. 2004; Denning 2007; Hirose

et al. 2002; Horikoshi et al. 2009; Suzuki 2002). TJ proteins were shown to have impact on the composition of SC, and localization of other TJ proteins by using knockdown models. Barrier capabilities of TJs were studied in several experiments where molecules of various size were used in knockdown models. TJs also maintain epidermal calcium gradient. For review, please see Table 1 and (Svoboda et al. 2016).

Table 1: Summary of epidermal barrier alterations in experimental models of TJ proteins.

Protein	**References**	**Downregulation associates with**		
		↑Permeability	**↑TEWL**	**Deregulation of**
Claudin-1	Furuse et al., Sugawara et al., Kirschner et al., Yamamoto et al., Yuki et al.,	Na^+, Ca^{2+}, Cl^-, fluorescein, FD4, FD40	yes	Ceramides Involucrin Filaggrin TJ proteins Transglutaminase1
Claudin-4	Itallie et al., Kirschner et al., Stremnitzer et al., Yuki et al.	Na^+, Ca^{2+}, Cl^-, fluorescein, FD4, FD10, Sulfo-NHS-LC-biotin	yes	-
Claudin-6*	Turksen et al.	-	yes	SC TJ proteins
Occludin	Kirschner et al., Saitou et al., Stremnitzer et al., Yuki et al.	-	yes	TJ proteins
Tricellulin	Krug et al., Ikenouchi et al.	FD4, FD10	-	-
ZO-1	Kirschner et al., Stremnitzer et al., Yamamoto et al.,	Na+, Ca2+, Cl-, fluorescein, FD4, FD40	yes	TJ proteins
aPKC/Par6	Gao et al., Helfrich et al.	inulin	-	TJ proteins

**overexpression. FD4, 4 kDa FITC-dextran; FD10, 10 kDa FITC-dextran; FD40, 40 kDa FITC-dextran; TEWL, transepidermal water loss; TJ, tight junction; SC, stratum corneum.*

2.8 Challenging the barrier and tight junctions

Skin structure and physiology can be affected by various external factors and TJs are no exception. Several factors have been described to be associated with disorganization or decreased number/abundance of TJ components. UV-light is the most significant environmental factor affecting the skin as it is the major cause of its extrinsic ageing and our skin is exposed to UV-light almost permanently. Skin ageing is a natural process that ultimately changes skin physiology at several different levels. Two ageing processes have been distinguished, intrinsic and extrinsic. The hallmark of intrinsic ageing is cellular senescence where telomere shortening plays an important role (Gilchrest 2013). The skin extensively suffers by extrinsic ageing (also photoaging) mainly because of substantial exposure to UV-light. Two types of UV-light reach the skin, UV-A and UV-B. UV-A irradiation (320-400 nm) penetrates deeper into the skin and approx. 50 % of UV-A photons enter the dermis (Fourtanier et al. 2008). Short-wave UV-B photons (290-315 nm) are mostly absorbed by the epidermis, however, UV-B is far more energetic. Generally, photoaging contributes to over 80 % of the skin ageing. For review see references. (Ichihashi et al. 2003; Kammeyer and Luiten 2015; Pillai et al. 2005; Rittié and Fisher 2002; Xu and Fisher 2005; Yaar and Gilchrest 2007).

Several studies have been conducted to evaluate the changes in TJs in the skin exposed to different intensities and types of UV-light in relation to the skin barrier function. Some of the studies independently reported that UV exposure diminished TJs in the skin along with its water barrier. Moreover, the water barrier was deregulated and restored in a similar pattern as TJs suggesting their tight relationship. However, these experiments used only a single-dose UV-light simulating the acute UV exposure, and not addressing the chronic UV exposure. The information regarding the chronic exposure of TJ to UV-light and its relationship with barrier function is scarce. From what the literature conveys, the lipid content of the SC is essential for the skin barrier. However, elderly people with the diminished epidermal barrier and altered permeability for some substances showed no deterioration of the water barrier. Also, a chronically UV-exposed skin showed a restoration of the water barrier although the lipid content remained deteriorated. With additional evidence from other studies, this suggest that skin utilizes a compensatory mechanism where TJs might play an important role. For a review see reference (Svoboda et al. 2016).

3 SKIN MODELS FOR THE SKIN RESEARCH

Throughout the history of the skin research number of different skin models have been developed to suit the needs of investigators. Following categories cover most of the skin models that are used today: *in vivo* animal models, *in vivo* human studies, *in vitro* 2D cell cultures, *in vitro* 3D models, *ex vivo* skin tissue and human-on-animal xenografts. The selection of model should be justified by the relevant scientific need and underlying background, and it should be clear that the use of the model can address the scientific hypothesis. Every model has its disadvantages that must be considered, including also the ethical principles.

3.1 Human skin *in vivo*

No doubt the human skin is the best possible model. However, human *in vivo* studies run only under very strict supervision of the ethic committee, where the scientific goal must be justified with relevant medical purpose, benefit/risk ratio evaluated, and safety of the human volunteers assured – most often under the supervision of a medical doctor. The European Union also prohibits financial gain from providing human tissue, making a widespread use of this model no matter for which purpose very complicated (Netzlaff et al. 2005).

3.2 Animal skin models

In vivo animal skin models are widely used in the basic research. Mice and pigs are preferred over the others as their skin resemble the human one the most. The greatest advantage of these models is that the skin is examined under *in vivo* conditions. Moreover, animal material is easy to come by. Nevertheless, together with the studies on human volunteers, an extensive use of animal models imposes serious ethical issues and the need for alternatives has been raised. Cosmetic industry and its adjacent research fields has already banned animals as a test model according to EU regulation (76/768/EEC, Feb. 2003). Furthermore, the relevance of conclusions drawn from animal data for human skin has always been questionable. There are high failure rates in clinical testing because of the poor transferability of animal data to human skin (Hartung et al. 2013; Hartung 2007), both with respect to rodents (Seok et al. 2013), and the dog (Bailey et al. 2014). Despite the obvious resemblance with human skin, mouse or pig skin differs from human skin histologically and physiologically, including thickness, vascularity, and pH (Park et al. 2015).

3.3 Two-dimensional models *in vitro*

Two-dimensional cell cultures are groundwork for almost every biological research field, including the skin research. Even before hindering animal testing in cosmetic industry, *in vitro* skin testing was perhaps the most common from all the alternative testing methods. Human keratinocyte and fibroblast monolayer cultures are well-established, particularly NIH/3T3 mouse embryonic fibroblasts and the spontaneously transformed, immortalized human keratinocyte cell line HaCaT derived from adult human skin. Co-cultures of different cell types (e.g. with melanocytes) are also frequently used. However, these models do not reflect the primary cells *in situ*, for example due to chromosomal aberrations. Moreover, monolayer cell cultures cannot be used to investigate percutaneous absorption. In addition, monolayer cell cultures do not mimic cell-cell interactions of a multilayer tissue consisting of different cell types. Several types of cells contribute to skin function in order to prevent damage by UV irradiation, xenobiotics or microorganisms. Skin morphology also varies during lifetime and according to the body site (Alépée et al. 2014).

3.4 Three-dimensional models *in vitro*

Organotypic 3D skin models are state-of-the-art models used in the skin research *in vitro* and dermal tissue engineering. In most 3D-models, a scaffold provides the geometrical structure for tissue growth. Moreover, scaffolds can provide markers and proteins to facilitate cell adhesion and to guide the tissue development. Furthermore, a scaffold can support the development of sophisticated co-culture systems. Basically, there are two types of 3D-models of the skin, reconstructed human epidermis (RHE) or reconstructed human skin (RHS) (Alépée et al. 2014).

RHE constructs are built from keratinocytes isolated most commonly from juvenile foreskin or adult abdominal/breast skin and expanded in culture media. The cells are seeded into trans-wells, and after a submersed cultivation an airlift is performed to induce keratinocyte differentiation, which is a continuous process. After about two weeks keratinocytes are fully differentiated and all the epidermal layers found in the human skin are present (Gazel et al. 2003).

RHS are started by adding fibroblasts to vacant scaffolds, ranging from a simple collagen gel made freshly in the laboratory or an array of commercially available premade matrices, to the actual, decellularized skin dermis. Fibroblasts are allowed to populate the scaffold, at which

point epidermal keratinocytes are seeded on top of it and stratification is induced in the same way as with RHE models, see Figure 5 (Oh et al. 2013).

Primary human skin cells are used predominantly when building up these models. Primary human skin cells preserve better the structural and biochemical complexity found *in vivo*. However, a donor availability and variation are a considerable limitation on reproducible results when using primary human skin cells. Recently, RHS model made completely of cell lines was developed (Reijnders et al. 2015).

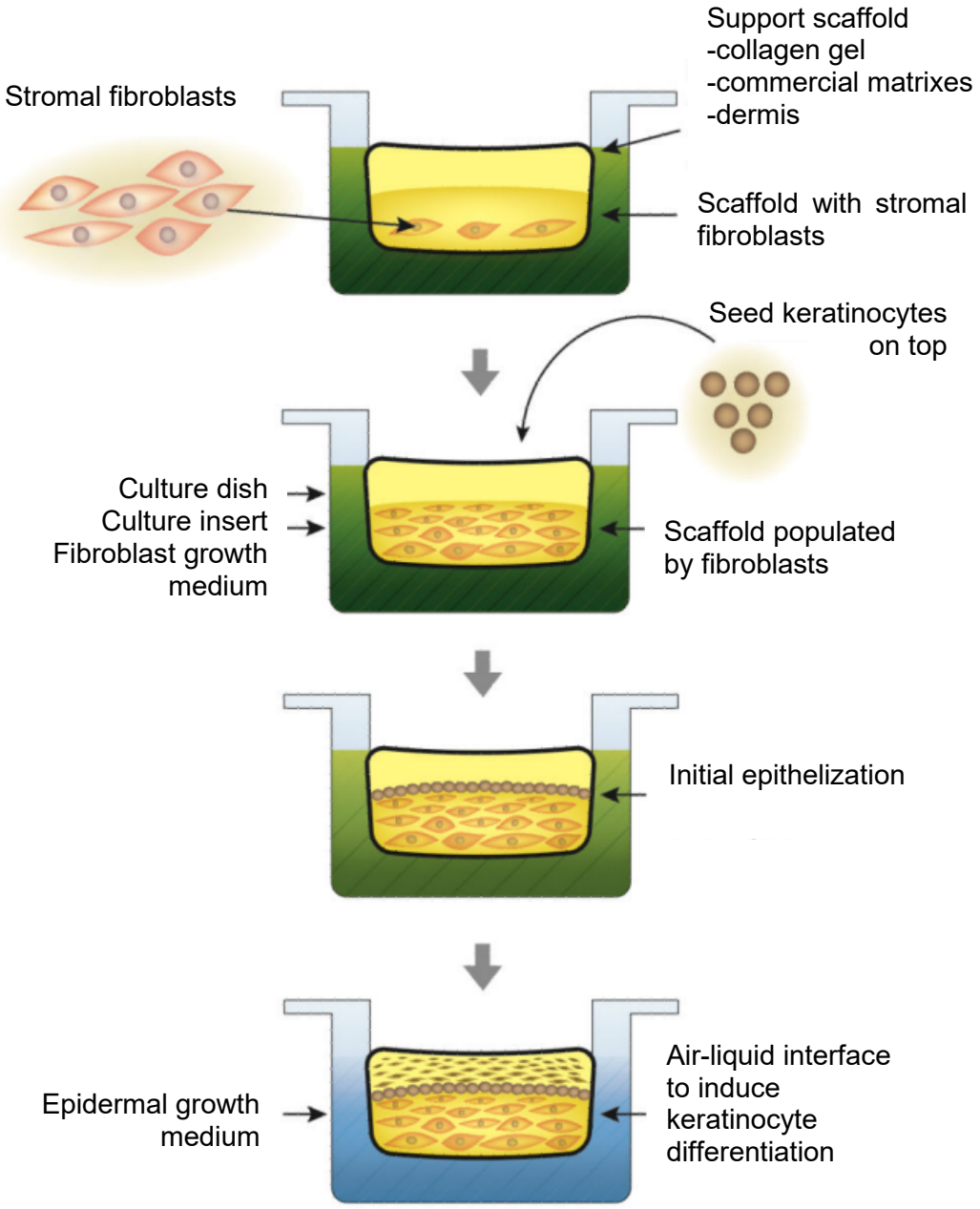

Figure 5: Flowchart of organotypic epidermal culture system. *Modified from* (Oh et al. 2013).

RHE/RHS closely mimics the native human skin, are stable up to six months and enable the investigation of dermal penetration and various biological processes. Although several studies have shown that RHE/RHS is able to reproduce the differentiation process, exhibit all the different layers of a normal epidermis and general features of the native human skin, there are still limitations to be considered when using RHE/RHS. These constructs suffer of lower barrier function when compared to native human skin (Netzlaff et al. 2005). Impaired barrier function in RHE/RHS is probably due to lower content and different profile of free fatty acids (FFAs) and some of the constructs also display lower content of polar ceramides 5 and 6, while ceramide 7 is completely missing. Different lipid profile of individual RHE/RHS results in hexagonal packing of lipids in lamellar phases while human *in vivo* skin shows rather orthorhombic packing (Ponec et al. 2002; Ponec et al. 2001). Furthermore, these constructs do not contain all the appendages and cell types that contribute to the skin homeostasis. The expression of differentiation markers (filaggrin, transglutaminase) reflects hyperproliferative state seen in a healing process. A comprehensive analysis of the proteome is yet to be done. RHE/RHS constructs also do not desquamate (Alépée et al. 2014). Using OECD TG 428 protocol, the permeation of RHE was similar to the permeation of the human epidermis and the absolute cut-off level of permeated substance's molar mass (800 g. Mol^{-1}) of the skin and RHE was in accordance as well (Schäfer-Korting et al. 2008a). The OECD TG 428 protocol was transferable for RHS (Ackermann et al. 2010; OECD 2004; Schäfer-Korting et al. 2008b).

3.5 Human skin *ex vivo*

Another option of a skin model for the skin research is *ex vivo* human skin or a human skin explant, which can be processed as a full-thickness skin or as an epidermal sheet only. Skin explants represent a model that is closer to *in vivo* human skin than RHE/RHS, consisting of keratinocytes, melanocytes, Langerhans cells in the epidermis, and containing the whole dermal structure including dermal fibroblasts and extracellular matrix. Although tissue explants cannot completely reproduce *in vivo* conditions because of a lack of intact nervous and vascular tissues, they are useful nonetheless (Park et al. 2015). Skin explants have recently been utilized in various areas in dermatologic research, including immunology, microbiology, and dermal sensation (Eaton et al. 2014; Lebonvallet et al. 2014; Phillips et al. 2013). The key issues of the skin explants are their reproducibility and viability. According to some studies, the unchanged structure and viability can be maintained for up to seven days. Viable explants were maintained for 75 days. However, a histological evaluation showed structural changes, see Figure 6 (Frade et al. 2015).

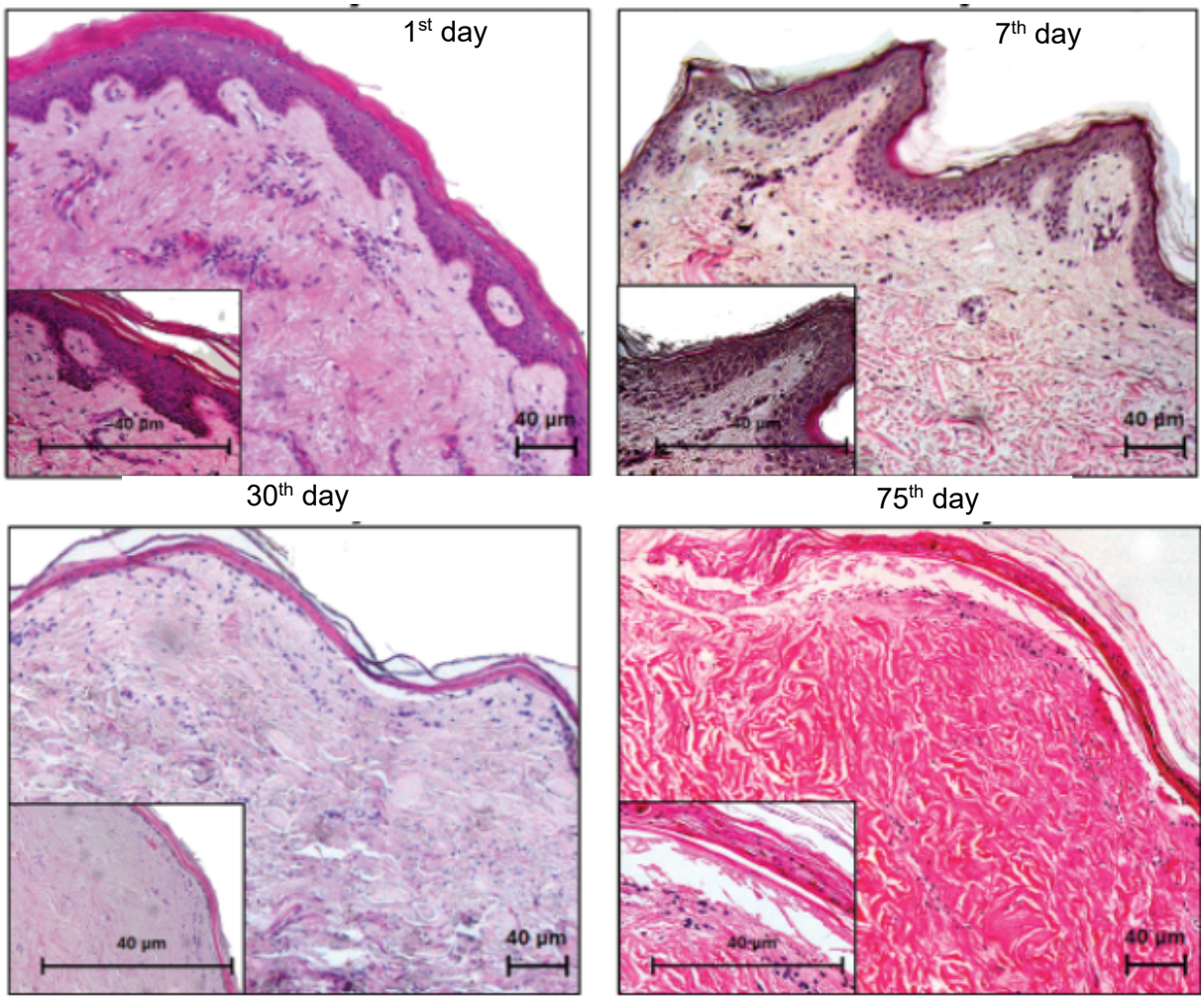

Figure 6: Viability of human skin explants *as showed by hematoxylin eosin staining. Modified from* (Frade et al. 2015).

3.6 Human-on-mouse xenografts

One of the last options that closes to the human skin *in vivo* even more are xenografts. Theoretically, any explant or type of 3D model can be used for xenografting, while mouse is a predominant host. To prepare the recipient mouse a full thickness wound is made on the dorsal back skin between the shoulder blades that matches the size of the donor skin biopsy or 3D construct. After 4-6 weeks, the healed transplanted skin graft closely resembles normal human skin histologically and maintains human vasculature, with minimal ingrowth of murine vascular endothelium into the graft. 3D construct xenografts indeed only contain a portion of the cellular and extracellular components of the human skin (Salgado et al. 2017). Xenografts are suitable for studying even more complex issues such as cell interactions, immunology, TJs, diseases and more (Boyman et al. 2004; Kim et al. 1992; Nosbaum et al. 2016; Yan et al. 1993; Yuki et al. 2011).

4 SKIN ANALYSIS - SAMPLE PREPARATION

4.1 Skin sampling

Several skin sampling techniques have been developed to deal with the diversity of the skin. Some of the techniques have wider range of applications, others are designed for specific use only. Sampling techniques vary in the degree of invasiveness, reproducibility, analytes or targets of interest that can be obtained etc.

Latest research trends regarding skin sampling techniques on humans are focused on using non-invasive techniques or at least on reduction of the technique's invasiveness as much as possible. Non-invasive approach reduces the risk of health complications and increases patient's comfort. Hence, it is more ethically acceptable and less demanding on research staff specific qualifications. Also, more sampling procedures can be performed at the same time or during given period of time. Needless to say, some aspects of the skin can be analyzed without any skin sampling by using non-invasive methods, e.g. tewametry for TEWL determination, sebumetry for the skin sebum quantification, methods based on the electric properties of the skin (e.g. electric capacitance), ultrasonography or reflectance confocal microscopy (RCM). On the other hand, if structural components on molecular level are the target of research, invasive methods usually provide more relevant sample. Also, for some research purposes excisions from surgeries or cadaver skin are used. However, the sources are limited by number and specific area of the body (auricles, eyelids, foreskin, abdominal excision). Research projects based on animal subjects or human skin analogue models are not restricted by invasiveness in terms of ethical concern (Svoboda et al. 2017; Wang and Maibach 2011).

4.1.1 Invasive sampling techniques

Invasive techniques of the skin sampling are represented by skin biopsies, suction blistering (SB) and tape-stripping (TS) that has substituted scrapping some time ago.

Skin biopsies provide full-thickness skin sample as the only skin sampling technique. Although biopsy is usually a safe procedure, complications such as bleeding, infection and scarring may occasionally occur in the facility with basic infrastructure. There are various methods of performing skin biopsy including punch biopsy, shave biopsy, saucerization biopsy, wedge biopsy, incisional and excisional biopsy. All methods include prior anesthesia either local or total and post-treatment with hemostatic substances or suturing. Therefore, all skin biopsy methods should be carried out by a qualified healthcare professional. Biopsies are

performed mainly in clinical practice as a diagnostic tool but are utilized in the dermatology research as well (Alguire and Mathes 1998; Nischal et al. 2008). Since biopsies provide undamaged full-thickness skin, they are ideal for analyzing structural components of all skin compartments – epidermis, dermis and hypodermis by imaging methods such regular light microscopy, immunohistochemistry (IHC) with fluorescence microscopy, electron microscopy, etc. Application of skin biopsies is broader of course, but invasiveness should be taken into consideration, especially in human studies. To reduce the invasiveness micro-biopsy technique was introduced as an upgrade, which is based on a sub-millimeter punch biopsy device that yields enough of material for DNA and RNA analysis (Lin et al. 2013).

Another skin sampling technique is SB. Blisters are induced by applying a constant negative pressure on a skin surface by specialized vacuum pump. This technique provides samples of epidermis and interstitial fluid for the analysis. In SB samples, various cluster of designation molecules were analyzed by immunostaining or flow cytometry (Leitch et al. 2016) and specific antigen PGP 9.5 was used to quantify nerve fibers (Panoutsopoulou et al. 2015; Panoutsopoulou et al. 2009). SB sampling is preferentially used for analyses of the blister fluid rather than the blister roof (Macdonald et al. 2006; Varila et al. 1995). SB is less invasive than biopsies but cannot provide full-thickness skin sample.

Last widely used invasive method is TS which is considered to be even less invasive than SB. TS provides mainly SC cells as a sample by consecutively removing the layers of corneocytes using a glue on a platform. Specialized TS discs were developed that consist of plastic disc of standardized diameter and attached layer of the glue. In TS samples, various keratin proteins (Chao and Nylander-French 2004; Thiele et al. 1999), aquaporins 3 and 10 (Jungersted et al. 2013) were detected by western blotting (WB) or IHC. Human beta-defensin-2 peptide was quantified by ELISA kit in TS samples of atopic dermatitis and healthy skin (Clausen et al. 2016). Broccardo et al. identified 104 proteins from 20 consecutive tape strips (D-Squame) of atopic dermatitis and healthy skin using high-performance liquid chromatography (HPLC) coupled with mass spectrometry (MS) approach (Broccardo et al. 2009).

Apart from structural studies on a molecular level SB and TS are common dermatological techniques with a wide range of applications such as the vitiligo and chronic wound treatment (Gupta et al. 1999), wound models (Brönneke et al. 2015; Leitch et al. 2016) or they are used for a sampling of the skin after topical drug delivery (Benfeldt et al. 1999; Lademann et al.

2012). Additionally, TS was proposed as a tool for bioequivalence and dermato-pharmacokinetic studies (Benfeldt et al. 1999; Clausen et al. 2016).

4.1.2 Non-invasive sampling techniques

Various non-invasive techniques were developed that are mostly focused on a specific target of interest e.g. sweat patches based on occlusion and passive diffusion (Jadoon et al. 2015), abrasion techniques, swabbing, agar-contact plate method for collecting microbiome, and others. One of the most sophisticated skin sampling method is reverse iontophoresis. A low electric current is applied to the skin surface to promote transdermal molecular transport driving small, polar, charged and uncharged molecules across the skin via electromigration and electroosmosis. Reverse iontophoresis is technology behind a continuous glucose monitoring device that had opened a new opportunity for diabetology patients to measure plasma glucose comfortably and continuously. One of the drawbacks, however, is a lag time caused by transport from the blood across the skin which in the case of glucose is 5-20 minutes on average. Also, reverse iontophoresis has been used to monitor skin inflammation by extracting prostaglandins, as well as to monitor urea or amino acids (Delgado-Charro 2015; Leboulanger et al. 2004; Wang and Maibach 2011).

4.2 Skin sample homogenization

The skin represents very complex biological matrix for analytical procedures. The skin is tough for homogenization, contains resident bacterial microflora and potential interference, such as auto-fluorescence, enzyme inhibitors or xenobiotics.

The skin sample homogenization is usually achieved via mincing with razor blades, using mechanical homogenizers (bead homogenizers), using a mortar and pestle in combination with liquid nitrogen, which is an efficient, but time-consuming process, or cryogenic grinding can be utilized as well (Berglund et al. 2007; Gardner et al. 2006; Keermann et al. 2015; Reimann et al. 2012; Samadani et al. 2015).

Additionally, enzymatic digestion of hyaluronic acid-collagen matrix with collagenase and hyaluronidase prior to mechanical homogenization might increase the efficiency of homogenization. Two commonly used solutions for homogenization contain phenol and guanidine thiocyanate, which commercial lysis buffers often combine with beta-mercaptoethanol, and which have both lysis and RNA inhibiting capacities (Reimann et al. 2019).

5 SKIN LIPID ANALYSIS

Lipidomics is defined as study of lipidome that tries to completely characterize lipid molecular species, their metabolic roles and pathways in various biological systems such as cells, tissues and body fluids. A number of analytical techniques are used for lipid analysis: nuclear magnetic resonance, spectroscopy, fluorescence-based analysis and most widely used mass spectrometry (MS) analysis (Park et al. 2012; Watson 2006; Wolf and Quinn 2008). For a schematic overview of the most common approaches used in lipidomic studies see Figure 7.

5.1 Lipid extraction techniques

Extraction and separation of skin lipids is problematic part due to a wide range of lipid species polarity. The analysis of lipids has been performed by a diverse variety of approaches reflecting the diverse chemical subclasses. Following lipid extraction techniques are used most frequently or they create a basis for many modifications: Folch extraction using chloroform : methanol (2:1,v:v), Bligh&Dyer using chloroform : methanol (1:1,v:v), Shevchenko using methyl tert-butyl ether : methanol (5:1, v:v) and non-polar extraction based on hexane : methanol : water (2:1:0.1,v:v:v). The Folch method is considered the gold standard of lipid extraction, regardless of lipid yield, but is considered time-consuming to perform. The Methyl tert-butyl ether lipid extraction protocol was found to be a suitable substitute for a rapid lipid extraction for high throughput mass spectrometric analyses and was considered superior to the Bligh and Dyer method. However, in low lipid yield tissues as in the eye (<2% lipid composition), the Bligh and Dyer method is as effective and rapid as the Folch and methyl tert-butyl ether lipid extraction protocols, respectively (Bhattacharya 2017). Most “lipid-analyzing” studies rely on methanol or chloroform as an extraction solution. To optimize the extraction, other reagents are used as well, i.e. tetrahydrofuran, ethyl acetate, ethanol, or hydroxides.

5.2 Lipid separation techniques

Several separation techniques can be used when analyzing lipids. Gas chromatography and Gas chromatography coupled with MS approaches provide a rapid, sensitive, and relatively cheap method, but require prior time-consuming chemical derivatization which can lead to inter laboratory variations. (Camera et al. 2010a; Rainville et al. 2007).

Solid-phase extraction (SPE) chromatography is useful for rapid, preparative separation of crude lipid mixtures into different lipid classes. This involves the use of prepacked columns containing silica or other stationary phases to separate glycerophospholipids, fatty acids, cholesteryl esters, glycerolipids, and sterols from crude lipid mixtures (Laboureur et al. 2015).

The high-performance liquid chromatography (HPLC) is the most common separation method for epidermal lipids and three types dependent on preferences are applied, namely normal phases, reversed phases and hydrophilic interaction chromatography (HILIC). Lipids have been successfully analyzed by normal-phase HPLC (NP-HPLC) and NP-HPLC coupled with MS - this method of analysis has high sensitivity and does not require any sample derivatization. However, peak resolution is typically poor. Reversed-phase HPLC (RP-HPLC) has been the technique of choice in general, which is due to the high efficiency of the separations, the compatibility of the mobile phase with biological and lipophilic samples, and the easy interfacing with a variety of detectors including UV, fluorescence, evaporative light scattering detection, radio-chemical detection, MS, and nuclear magnetic resonance (Rainville et al. 2007; Sandra and Sandra 2013). Both NP-HPLC and RP-HPLC have been employed to separate neutral lipids (including acylglycerols, wax esters, and esters of cholesterol) from complex mixtures that were subsequently characterized using MS. NP-HPLC has the advantage of reducing the analysis time and ensuring the separation of each of the lipid classes. However, the resolution between members of the same class is often unsatisfactory (Hutchins et al. 2008; Sommer et al. 2006). RP-HPLC is a suitable system for the separation of lipid mixtures with a relatively broad range of hydrophobicity. RP-HPLC has been used to separate complex natural lipid mixtures, including triacylglycerols, which were subsequently detected using a mass analyzer (Holčapek et al. 2003; Nagy et al. 2005). Additionally, RP-HPLC has proven effective in the separation of FFA, which can be detected in negative ion atmospheric pressure chemical ionization (APCI) (Nagy et al. 2004). Non-aqueous RP-HPLC coupled with APCI is ideal for the analysis of the hydrophobic features of neutral lipids (Lísa and Holčapek 2008). Reversed phase ultra-performance liquid chromatography (RP-UPLC) with sub 2 μm particle size (p.s.) C18 stationary phase has been successfully employed to separate glycerol esters. Most liquid chromatographic separations used today are based upon reversed phases. However, due to the lipid diversity every LC separation has its application (Camera et al. 2010a). See Table 2 for overview of the lipid separation as proposed by Holčapek et al.

Table 2: Preferred lipidomic approaches for analysis of lipid classes or lipid species *according to Holčapek and his group (Holčapek et al. 2012).*

Lipid class approach			
Approach	**Suitable for**	**Stationary phase**	**Mobile phase**
HILIC-LC/ESI-MS	polar lipid classes	Si, NH2 or diol columns	acetonitrile, methanol, 2-propanol, hexane and ≥ 2.5% water
NP-LC/APCI-MS	nonpolar lipid classes	Si or NH2 columns	hexane, 2-propanol, chloroform, heptane
SFC/MS	all lipid classes	C18 or Si columns	supercritical CO2 with polar organic modifiers
Lipid species approach			
RP-LC/ESI-MS	all lipid species	C18 and C8 columns	aqueous mixtures of acetonitrile, methanol or 2-propanol, often with volatile buffers
NARP-LC/APCI-MS	nonpolar lipid species	C18 columns	2-propanol, acetonitrile, acetone,dichlormethane
Ag-LC/APCI-MS	nonpolar lipid species	ion-exchange column with Ag+	acetonitrile (+2-propanol) or dichlormethane – acetonitrile
Chiral-LC/APCI-MS	nonpolar lipid species	chiral columns	system with hexane and 2-propanol
SFC/MS	all lipid species	C18 columns	supercritical CO2 with polar modifiers

APCI-atmospheric pressure chemical ionization, ESI-electrospray ionization, HILIC-hydrophilic interaction chromatography, LC-liquid chromatography, MS-mass spectrometry, NP-normal-phase, NARP-non-aqueous reversed phase, RP-reversed-phase, SFC-supercritical fluid chromatography

5.2.1 Thin layer chromatography

As already mentioned, HPLC/MS is an ultimate tool for lipid analysis, not only for an identification of lipid species and lipid profiling but for the lipid quantitation as well. However,

the high-cost HPLC/MS instrumentation and operation, and extensively time-consuming method development renders HPLC/MS unfeasible for being the method of the first choice in every laboratory. Moreover, information about each detected lipid species and its role in the physiology of the skin is still rather limited. Therefore, most of dermatology scientists still rely on established methods that are easy, quick and cheap rather than full-scale lipidomics.

Thin layer chromatography (TLC) is the classic standard in lipid analysis. The most popular stationary phases for lipid separations are alumina, kieselguhr and silica gel, which is a predominantly selected stationary phase. Silica can be additionally modified by impregnation with other substances to provide optimum results regarding the separation of a certain lipid class. Based on their surface characteristics these phases can be classified as "normal" or "reversed" phases. 10–50 µm particles are regularly used for purposes of TLC, while about 5 µm particles with narrow size distributions are used in high performance thin layer chromatography (HPTLC). These smaller particles result in higher separation quality. Additionally, smaller sample amounts are sufficient in the case of HPTLC and smaller detection limits can be achieved. To separate very complex mixtures two-dimensional TLC or HPTLC can be utilized. Although the quality of separation is highly improved by 2D TLC, this method has also a serious disadvantage – only one sample per plate can be run at a time. Large number of protocols have been developed to separate and detect various lipid classes, for a review see (Fuchs et al. 2011).

For the detection of TLC-separated lipids various (non-) destructive and (non-) specific techniques and agents are used. In recent years, TLC has also been successfully coupled with MS techniques mainly after the introduction of desorption ionization techniques such as matrix-assisted laser desorption ionization (MALDI) or desorption electrospray ionization. Desorption ionization enables the analyte to be analyzed without eluding it from TLC stationary phase by a suitable solvent (Fuchs et al. 2011).

Series of studies analyzed epidermal lipids with a simple method where lipids were separated on TLC with standards, visualized and evaluated by photo-densitometry. With specialized HPTLC approaches, it is possible to separate most of the lipid classes and easily quantify them (Epp et al. 2007; Hatano et al. 2005).

Although TLC disadvantages are obvious when compared to conventional LC-MS techniques, TLC has notable advantages over the HPLC/MS. Apart from being simple and inexpensive, TLC is certified for several processes across various industries, including the

pharmaceutical analyses. Furthermore, TLC is faster than HPLC/MS and does not provide any "memory" effect of the stationary phase. Last but not least, TLC consumes significantly lower amount of solvents than LC-MS (Fuchs et al. 2009).

5.3 Mass spectrometers in lipidomics

With development of new MS technologies, possibilities of lipidomics have dramatically increased (Wenk 2005). Currently, two (or three) MS-based approaches are used in lipidomics, namely non-targeted lipidomics, targeted lipidomics and lipid imaging, see Figure 7. Non-targeted approach is generally used for first surveys when lipid composition is unknown, or it is applied for a monitoring of aberrant changes in the lipid metabolism. A full scan can encompass hundreds of lipid species. Therefore, MS method should have got high mass resolution and accuracy (Lam and Shui 2013). Targeted approach is focused on a precise characterization and quantification of lipids of interest (Lam and Shui 2013). Lipid imaging has found its place particularly after development of MALDI. Imaging MS enables mapping of lipid species in tissues, their distribution *ex vivo* with no need for extraction or separation (Goto-Inoue et al. 2011; Sparvero et al. 2012).

In general, three ionization techniques are: electrospray ionization, MALDI and APCI (Sandra and Sandra 2013). These are the exemplars of the modern desorption ionization and the spray ionization classes of methods.

In spray ionization, the sample is introduced as a solution which is nebulized. Resulting charged droplets undergo desolvation and the resulting gas-phase ions are then mass analyzed. The role of matrix in the spray ionization is essentially provided by the solvent in which the sample is carried. To successfully analyze the sample, solvent must be completely removed. Complete solution removal is a demanding task if the analyte itself is to be preserved intact (Kebarle and Verkerk 2012).

In desorption ionization, by contrast, condensed phase samples are examined by the impact of energetic particles. Analyte is dislodged from the surface and ionized by the input of sufficient amount of energy. Sample is protected from high energy input by matrix that is present in great excess. The matrix absorbs the direct incoming energy and transforms into a form that enables a gentle desorption of an analyte (Knochenmuss 2012).

The most noteworthy difference between the spray ionization desorption methods is the charge state in which the analyte is formed. The coulomb energy spent on removing charged ions from surrounding counterions causes the spectra of desorption ionization experiment are being dominated by singly charged ions. In spray ionization experiments, the analyte tends to take several charges that is roughly in proportion to the size of the molecule due the evaporation of water from a microdroplet that has ionic constituents. This dramatic difference in charge states has a profound effect on the most appropriate type of mass analyzer for each type of ionization method. The desorption ionization methods demand an instrument with a large mass/charge range, whereas the spray ionization methods yield ions for molecules of the same mass using mass analyzers with much smaller mass/charge ranges (Cole 2010).

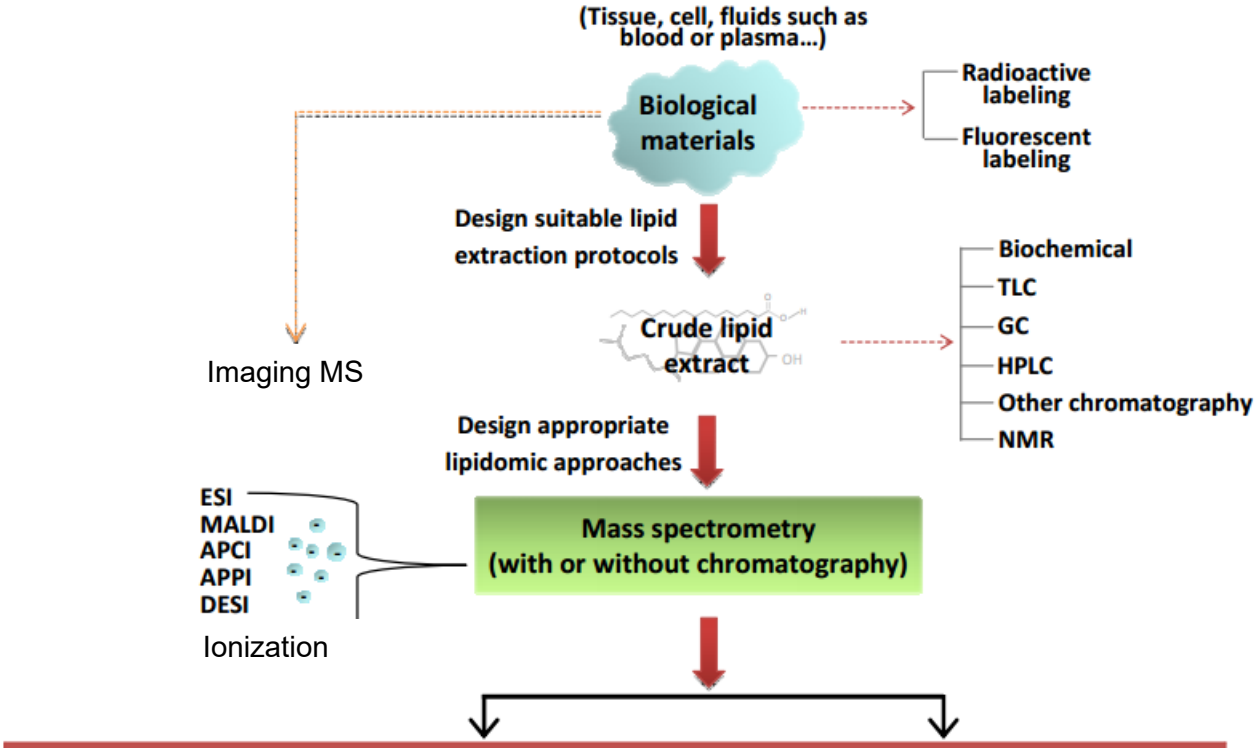

	Non-targeted MS approaches	Targeted MS/MS approaches
Advantages	• Excellent for discovery of novel lipids or unexpected lipid metabolites	• Highly sensitive • Relative ease of data handling and processing
Disadvantages	• Further MS/MS or other analytical approaches are required for complete characterization	• Lose information pertaining to unusual or new lipids • Specific MS/MS fragmentations are required a priori

Figure 7: Classification of lipidomic approaches. *Modified from* (Lam and Shui 2013).

Both, electrospray ionization and MALDI can be coupled with most of mass analyzers such as the quadrupole (Q) mass filter, 3D-quadrupole ion trap, linear quadrupole ion trap, time-of-flight (TOF), etc. In the skin lipid analysis, tandem (MS/MS) analyzers such as triple quadrupole (QQQ) and Q-TOF, or high-end analyzers such as Orbitrap or Fourier transform ion cyclotron resonance (FT) are preferentially selected (Camera et al. 2010b; Köfeler et al. 2012; van Smeden et al. 2011b). Orbitrap was originally designed for small molecule identification and quantitation, this technology has a lot of advantages in store for lipidomic applications, especially when hyphenated with the fragmentation power of linear ion trap or quadrupole technology. Before introducing Orbitrap technology, tandem LQT-FT was also used. Although LQT-Orbitrap resolving power and mass accuracy are less than the LQT-FT, it is still sufficient to provide unambiguous elemental compositions at higher scan rate for most applications (Köfeler et al. 2012).

There are also other approaches for lipidomics apart from MS techniques such as Nuclear Magnetic Resonance, which provides a relatively fast method of profile analysis that can generate information on a range of lipids including lipoproteins, but the disadvantage of this approach is the difficulty in separating multiple overlapped lipidic species (Watson 2006).

5.4 Quantification techniques in lipidomics

The basic prerequisite of any lipidomic quantification is the use of at least one non-endogenous internal standard per each lipid subclass. The data processing is an important step which is highly demanding on keeping the integrity and quality of lipidomic data. An automated data processing should be implemented in each lipidomic workflow to deal with the enormous data output. Also, the full method validation is an indispensable part of any quantification as required by respective authorities in the pharma industry. The method validation has not yet been frequently performed in lipidomic analyses, although several recent studies have used their own validation protocols, which included parameters like LOD, LOQ, linear dynamic range, matrix effect, intra- and inter-day reproducibility, etc. (Holčapek et al. 2018).

6 SKIN BARRIER ANALYSIS

Since both the “inside-out” and “outside-in” skin barrier function must be considered, different methods have been developed to cover both aspects of the skin barrier function.

6.1 Molecule permeation techniques

One of the methods for an assessment of the skin barrier function is permeation of various chemical molecules. This approach is a common technique in the pharmaceutical industry for the assessment of drug pharmacokinetics and is also known as percutaneous absorption or transdermal drug delivery. With use of reference molecules such as caffeine, benzoic acid or testosterone, whose permeability is well-described, the outside-in barrier function can be analyzed. This can be done either *in vivo* or *ex vivo* with skin samples or with special synthetic membranes, where various diffusion cells can be utilized. OECD guidelines provides instructions for performing the percutaneous absorption (Levin and Maibach 2005; OECD 2004). The molecule permeation can be also utilized for the inside-out barrier function assessment, when injected intradermally. Special compounds with a fluorescence feature and exact mass have been designed for this purpose (Kirschner et al. 2013).

6.2 TEWL measurement

TEWL is a widely used non-invasive biophysical method that quantifies amount of water passing through the skin, which primarily indicates the state of the inside-out barrier. TEWL values representing the amount of condensed water diffused through the skin per a defined area and time are measured indirectly as the water vapor flux in the air immediately adjacent to SC (Imhof et al. 2009; Jansen van Rensburg et al. 2019). Different approaches are used to measure TEWL: closed-chamber method measuring the increase of relative humidity, unventilated-chamber method measuring amount of condensed water, and open-chamber method estimating vapor pressure gradient (Farahmand et al. 2009; Imhof 2007; Laudanska et al. 2003; Luebberding et al. 2013a). TEWL can be measured in both, *in vivo* skin and *in vitro* skin explants. TEWL is commonly used as a research tool to objectively assess skin barrier function in clinical practice (Alexander et al. 2018).

In an open-chamber device both lower and upper orifice are open. When used in still conditions, the air inside the chamber is stationary and the water vapor from the skin surface

diffuses through the chamber and into the ambient atmosphere. The humidity near the skin surface increases, while the humidity at the exhaust rim remains close to that of ambient air. This humidity gradient provides the means for measuring the flux density by the diffusion-gradient method. The gradient is calculated from readings of relative humidity and temperature provided by two on-axis sensors that are spatially separated. The open-chamber method relies on steady-state diffusion for flux measurement (Imhof et al. 2009).

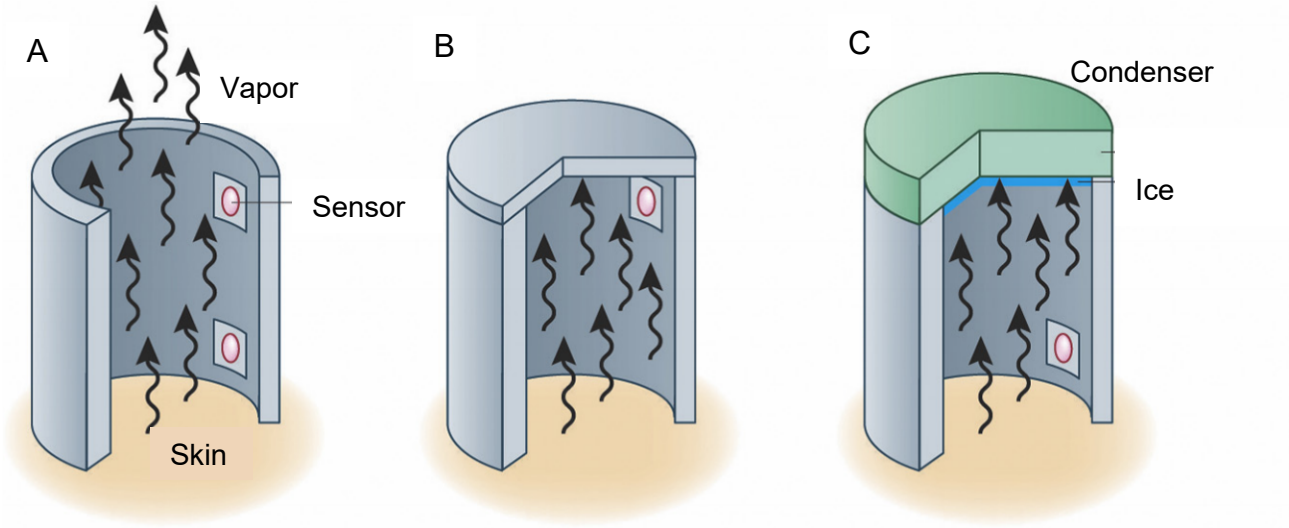

Figure 8: Schematic illustration of following TEWL devices *: a) open-chamber, b) unventilated-chamber, c) condenser-chamber. Modified from* (Alexander et al. 2018).

The main feature of the condenser-chamber method (Imhof et al. 2002), illustrated in Figure 8, is that natural convection and other forms of air movement are dampened, leaving a diffusion as the only transport mechanism. The condenser maintained at controlled temperature below the freezing point of water closes the upper end of the chamber. The lower end of the chamber is open and in contact with the skin. Condenser controls the microclimate humidity within the chamber independently of ambient humidity. Furthermore, the condenser maintains humidity gradient. So, the humidity at the skin surface increases with increasing water vapor flux, whereas the humidity at the condenser remains low and stable, irrespective of water vapor flux. Like the open-chamber, the condenser-chamber method also relies on steady-state diffusion for flux measurement and can therefore be characterized by a diffusion resistance (Imhof et al. 2009).

In unventilated-chamber method, one end of the cylinder is closed, the other end has a measurement orifice that can be placed in contact with the skin. The chamber is equipped with sensors for relative humidity and temperature. Water vapor from the skin surface accumulates

in the chamber, which causes the humidity to rise over time. After the measurement is complete, the chamber needs to be lifted from the skin to allow the accumulated water vapor to escape, otherwise the humidity would rise towards saturation level. Unlike the open-chamber and condenser-chamber methods, the unventilated-chamber method does not rely on steady-state diffusion for flux measurement and its measurement chamber cannot therefore be characterized by a diffusion resistance. It determines the vapor flux from the rate at which vapor accumulates in an unventilated chamber (Nuutinen et al. 2003).

In the head-to-head comparison, the open-chamber device seems to be superior to the unventilated-chamber device in a term of sensitivity as the open-chamber device was able to detect smaller differences and also fluctuations (e.g. due to temperature variations, blood perfusion, sweat rate, circadian rhythms etc.) during the time (De Paepe et al. 2005). In another study, the condenser-chamber device was shown to be superior to the open-chamber and unventilated-chamber devices in discriminating the effect of the TS and moisturization on TEWL values. Moreover, the values obtained from all three instruments correlate well with each other (Farahmand et al. 2009). All the devices are more or less prone to a biased measurement due to an angle, temperature and pressure dependence (Pinnagoda et al. 1990). TEWL measurements can be also significantly affected by several other factors that does not arise from the device itself: the anatomical site, sweating, skin surface temperature, inter- and intra-individual variation, air convection, ambient air temperature and humidity. Therefore, a highly experienced and trained individual should perform the TEWL measurement. Also, guidelines have been developed to help control external factors affecting TEWL in research studies and achieve consistency and accuracy (Alexander et al. 2018). Even though TEWL may be influenced by many variables, experiments show that evaporimeter measurements are reproducible *in vitro* and *in vivo*. Simplicity and speed at which you can obtain data make TEWL the first-choice indicator of the skin barrier function. Several studies also showed that TEWL correlates with percutaneous absorption of hydrophilic to slightly lipophilic compounds (Levin and Maibach 2005).

6.3 Reflectance Confocal Microscopy

Reflectance confocal microscopy (RCM) is a non-invasive technique for *in vivo* examination of the skin. Near-infrared (IR) light from a diode laser is focused on a microscopic skin target in a defined skin depth. As this light passes through cellular structures having different refraction indexes, it is naturally reflected, and this reflected light is then detected, Figure 9.

Wavelength range and power of the laser have a critical importance. Light transmittance in Caucasian skin increases progressively with wavelength in the near-IR region (700–1400 nm), though longer wavelengths provide limited lateral resolution. The power of the laser light-source which can be utilized is limited by the hazard of tissue damage and the skin sensitivity. In the skin, light is focused on a small tissue spot a few microns of diameter. Reflection occurs at the boundary between two cellular structures having different indexes of refraction, such as cell membranes, keratohyalin granules and melanosomes. Strong signal and bright contrast are obtained particularly from melanin, keratin, collagen and hemoglobin. Reflectance can also occur when the object viewed has a size similar to the illuminating wavelength. After the reflection, light travels through the objective lens and pinhole to a photodetector. The pinhole is providing the optical sectioning like in conventional CLSM (Calzavara-Pinton et al. 2008; Rajadhyaksha et al. 2017).

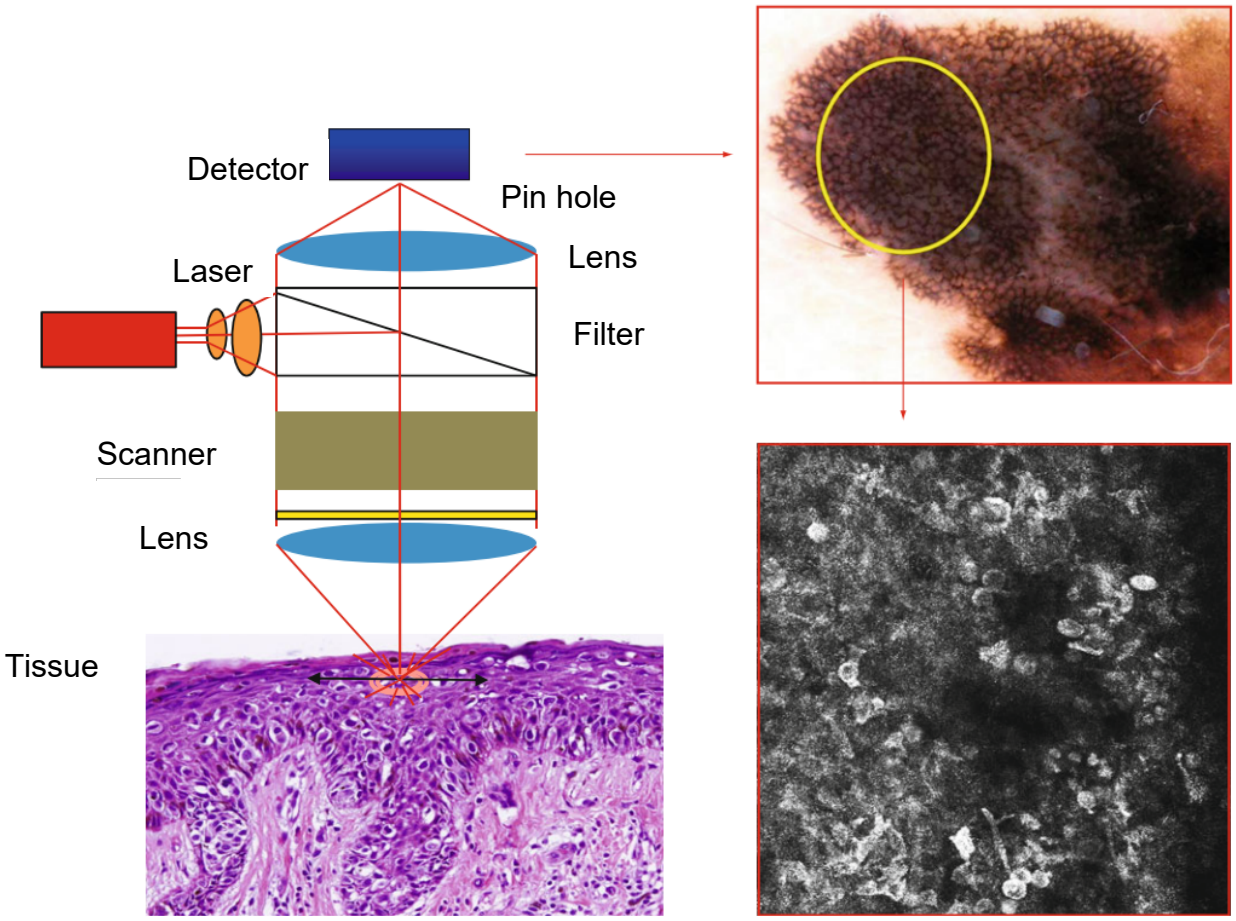

Figure 9: Schematic illustration of reflectance confocal microscope*. Modified from* (Hofmann-Wellenhof et al. 2012).

The commercially available near-IR reflectance microscopes are equipped with a diode laser with peak emission usually at 830 nm and has a maximum power of 35 mW. With this system, each image has an effective 500x500 μm field of view and the imaging depth in normal skin is 200–300 μm, which is roughly between papillary and reticular dermis and spatial resolution in lateral dimension 0.5 to 1 μm (Branzan et al. 2007). This allows reliable imaging of individual epidermal layers from the SC to the stratum basale, dermo-epidermal junction and upper layers of the dermis. Each layer, each cell, appendage and structure have its distinct pattern in an RCM image. SC layer is displayed as large bright, anucleated cells with polygonal shapes (diameter, 10-30 μm) with dark outlines. The underlying SG layer is located 15-20 μm below the skin surface and typically presents large polygonal cells (diameter, 10-25 μm) with bright granular cytoplasm and dark nucleus. The stratum spinosum located 20-50 μm below the skin surface consists of smaller cubical cells (diameter, 15-25 μm) with bright cellular borders. Structure of the SG and stratum spinosum resemble so called "honeycomb pattern" in an RCM image. The basal layer is located approximately 40-100 μm below the skin surface. Cells of the basal layer have a diameter of about 7-12 μm and typically appear as solitary bright, round to oval shapes in RCM images forming the "cobblestone pattern". Pigmented keratinocytes, as well as melanocytes, appear very bright in RCM, due to the high refractive index of melanin. In normal skin, it is difficult to clearly distinguish melanocytes and pigmented basal keratinocytes, because melanocytes rarely show branching outlines that may correspond to their dendrites and appear as round to oval structures (Ahlgrimm-Siess et al. 2008).

RCM is predominantly used in clinical practice by dermatologist to reveal or confirm potential melanomas or other skin carcinomas (Levine and Markowitz 2018). These are usually confirmed via invasive skin biopsies. Furthermore, inflammatory skin conditions such as psoriasis or contact dermatitis, and cutaneous infections can be examined with RCM (González and Gilaberte-Calzada 2008; Hofmann-Wellenhof et al. 2009). RCM is being used by cosmetologists to describe immediate changes in the skin induced by new substances, or to characterize and quantify histological changes of the epidermis and papillary dermis caused by aging. Moreover, RCM has been successfully utilized in UV-irradiation, acne or pigmentation studies (Nakano et al. 2006; Torres et al. 2004; Yamashita et al. 2005).

The greatest advantage is the RCM's non-invasive character which preserves the skin tissue during the examination. It also allows to examine the skin tissue in real-time and over-time at the same place. Therefore, a progression of diseases, aging, etc. can be studied within one selected skin site during the experiment (Hofmann-Wellenhof et al. 2009). RCM also has

its limitations. The main limitation is the imaging depth which with a maximum of 300 μm prevents from examining deeper dermis. Another limitation is imaging the hard-to-reach areas such as ocular canthi, nasal alae, etc. which can be partially solved using the smaller handheld probes. In RCM, there is also chance for false-positives since some of the specific cells or structures in some cases are indistinguishable from one another (Levine and Markowitz 2017).

7 ANALYSIS OF EPIDERMAL TIGHT JUNCTIONS

Four parameters are the main interest when studying TJs, including quantity, structure, localization and functionality. Since TJs are variable complexes of proteins, individual TJ proteins must be analyzed. Due to a large number of TJ proteins, which have different function and localization within TJs, individual proteins must be chosen carefully for the analysis. TJ protein expression can be analyzed on protein as well as mRNA level. For this purpose, common techniques of molecular biology are used, including qRT-PCR and microarray analysis in case of mRNA, or WB and IHC in case of protein level. All these methods provide mainly relative quantification, i.e. a comparison between two groups with a correction by house-keeping gene or protein.

7.1 Real-time reverse transcription-polymerase chain reaction

The introduction of polymerase chain reaction (PCR) has been an important milestone in the field of molecular biology. PCR is a powerful research tool that allows an exponential amplification of DNA copies of a specific DNA segment. Principle of the PCR uses the knowledge of nucleic acid features and its denaturation and renaturation kinetics. Essential components of PCR are DNA templates, DNA polymerase, primers, nucleotides, magnesium cations (Mg^{2+}) and buffer (Freeman et al. 1999). There are many applications of the PCR such as DNA cloning for sequencing, gene manipulation, functional analysis of genes, diagnosis of diseases, DNA profiling, detection of pathogens and analysis of the gene expression (Ninfa et al. 2009).

The gene expression analysis has been made more accessible mainly after the discovery of reverse transcriptase and its utilization in PCR (RT-PCR). In the RT-PCR, RNA is transcribed into DNA, also called as complementary DNA, which in turn is used for exponential amplification (Freeman et al. 1999). For the quantification in RT-PCR reaction products must be separated so that target and standard can be discriminated and quantified. There is a variety of systems that can be used. The two broad classes of amplification product detection techniques are the traditional “end-point” measurements of the product and “real-time” monitoring of the product formation. End-point determinations analyze the reaction after it is completed and often requires post-PCR processing. Real-time approaches monitor the reaction as it progresses and minimize the errors in the sample manipulation (Deepak et al. 2007).

Several factors have contributed to the transformation of real-time RT-PCR technology into a mainstream research tool. Firstly, as a homogeneous assay it avoids the need for post-PCR processing. Secondly, a wide (>107-fold) dynamic range allows straightforward comparison between RNAs that differ widely in their abundance. At last, it is a quantitative as well as qualitative assay (Ginzinger 2002). As a detection signal fluorescent dyes are mainly used in the real-time RT-PCR. Earlier, non-specific dyes have been used such ethidium bromide which intercalates into double-strand DNA molecules. Later, sequential specific methods that are mostly based on the fluorescence resonance energy transfer (FRET) were developed, and these include hydrolysis probes, beacon probes and simple-FRET probes.

The quantitative endpoint for real-time PCR is the threshold cycle (C_T). The C_T is an arbitrarily set threshold for the fluorescent signal of the reporter dye during the PCR cycle. The number of amplicons in the reaction is inversely related to the C_T. Real-time PCR data can be reported using absolute or relative expression levels. Absolute expression provides the exact copy number following transformation of the data via a standard curve (Chen et al. 2005). In relative quantification, the real-time PCR data is presented relative to another gene often referred to as an internal control. Several methods have been developed over the years to present the relative gene expression (Schmittgen and Livak 2008). The efficiency correction method uses the real-time PCR efficiencies and the C_T to calculate the relative expression ratio. Since PCR efficiency of the target and internal control genes are included in the equation, differences in the efficiency between the target and internal control will be accounted for in the calculation. On the other hand, efficiencies must be calculated for every experiment making it impractical for large scale analysis. Sigmoidal curve fitting methods predicts the PCR efficiency and estimates the initial copy number of the amplicon by fitting the experimental data to an empirical equation (Rutledge 2004). As a result, PCR efficiency does not need to be calculated by a separate experiment and is estimated during the analysis. The comparative C_T method (also known as the $2^{-\Delta\Delta CT}$ method) method is based on assumptions such as the PCR efficiency is close to 1 and the PCR efficiency of the target gene is similar to the internal control gene (Livak and Schmittgen 2001). The comparative method is easy to use, and data can be presented as "fold change". However, PCR efficiency must hold, or must be further optimized (Schmittgen and Livak 2008).

7.2 Western-blotting basics

The WB is commonly used to identify, quantify, and determine the size of specific proteins. Basically, native or denatured proteins are separated by gel electrophoresis. The proteins are then transferred to a membrane for detection using antibodies specific to the target protein.

7.2.1 Protein isolation

Successful WB begins with thorough and careful sample preparation where the protein degradation should be kept to minimum by rapidly freezing the sample, keeping the freeze/thaw cycles to minimum, and by adding protease and phosphatase inhibitors to the lysis buffer (Mahmood and Yang 2012).

7.2.2 Electrophoresis

Proteins are then usually separated using polyacrylamide gel electrophoresis. The ideal bisacrylamide:acrylamide ratio has to be determined for optimal separation. Proteins can be separated by isoelectric point, molecular weight, electric charge, or a combination of these. The most common type of electrophoresis separates proteins based on the molecular weight using strong anionic detergent sodium dodecyl sulphate (SDS). Hence, the procedure is called SDS-PAGE. SDS agent denatures the proteins and gives them a similar negative charge. When voltage is applied to the gel, proteins migrate at different speeds based on their molecular weight. A two-dimensional gel can also be used. This type of gel spreads out proteins from a sample in two dimensions. Proteins are separated by isoelectric point in the first dimension and by molecular weight in the second dimension. Unlike SDS-PAGE gels, which unfold and denature the native structure of a protein, non-denaturing or native gels can be used to maintain protein complexes for detection after transfer. However, protein complexes may not separate cleanly or predictably (Jensen 2012).

7.2.3 Blotting

The second part of the WB is blotting or transferring the proteins onto a membrane. The transfer is done using an electric field oriented perpendicular to the surface of the gel. The transfer can be either wet or semidry depending on whether the transfer system is immersed, or only soaked paper is used. The effectiveness of protein transfer is dependent on the type of gel used, the molecular mass of the protein, and the type of membrane. Some limitations associated with protein transfer include a lower molecular weight limit (lower than approx. 10 kDa), specialized transfer buffers facilitating transfer of proteins with high isoelectric point, and transfer buffer with a lower pH than the protein's isoelectric point. Membranes used in WB are

usually made of nitrocellulose, polyvinylidene difluoride (PVDF), activated paper, or activated nylon. Nitrocellulose is used for its high affinity for protein and its retention abilities. However, it is brittle, and does not allow the membrane to be used for re-probing. In this regard, PVDF membranes provide better mechanical support and allow the blot to be re-probed and stored. However, the background is higher in the PVDF membranes than in nitrocellulose (Jensen 2012; Mahmood and Yang 2012).

7.2.4 Probing and detection

After the protein transfer, a membrane must be blocked and washed in order to ensure a reliable probing with antibodies. Non-fat dry milk or bovine serum albumin is used most often to prevent the non-specific antibody binding. Both monoclonal and polyclonal antibodies can be used for wester-blotting, with advantages and disadvantages in using either type (MacPhee 2010). The probes that are labeled and bound to the protein of interest need to be detected on the blotting membrane. For detection methods, colorimetric, radioactive, and fluorescent methods can be used. However, chemiluminescent detection is used most frequently. Enhanced chemiluminescence is a sensitive method and can be used for relative quantitation of the protein of interest (Kurien and Scofield 2009; MacPhee 2010). Basically, the primary antibody binds to the protein of interest and the secondary antibody, typically linked to horseradish peroxidase, is used to cleave a chemiluminescent agent. The reaction product generates luminescence, which is related to the amount of protein. Only a single light detector is required, and the light is detected by a photographic film or by a charged-couple device camera. Data produced with a WB is typically considered to be semiquantitative, since it provides a relative comparison of protein levels, but not an absolute measure of quantity. There are two reasons for WB cannot be used for absolute quantitation. Firstly, there are variations in loading and transfer rates between the samples in separate lanes which are different on separate blots. Secondly, the signal generated by detection is not linear across the concentration range of samples (Jensen 2012; Mahmood and Yang 2012).

7.3 Immunohistochemistry basics

Three disciplines are involved in IHC: immunology, histology, and chemistry. The fundamental concept of IHC is the visual demonstration of antigens within the tissue by means of specific antibodies. Antigen-antibody binding is demonstrated with a histochemical reaction visible by light or fluorescent microscopy. In some cases, IHC is considered the gold standard to which

other techniques are compared. In contrast to many detection techniques, IHC allows a co-localization of an antigen with a morphological section, thereby dramatically enhancing diagnostic interpretation.

7.3.1 Fixation

IHC procedure begins with sample preparation where fixation is the main step. Fixation of tissues is necessary to adequately preserve cellular components, including soluble and structural proteins; prevent autolysis and displacement of cell constituents, including antigens and enzymes, see Figure 10. Fixation stabilizes cellular materials against detrimental effects of subsequent procedures; and facilitates conventional staining and immunostaining (Ramos-Vara and Miller 2014). No fixative optimally fulfills all these goals. Tissue samples should undergo immediate processing (fixation or freezing) right after the excision. Delayed fixation can decrease the mitotic index, induce biochemical alterations, cause cellular swelling, activate various enzymes, all of which can change the immunoreactivity of an antigen. Two types of fixatives are used in IHC: cross-linking (non-coagulating) and coagulating. The quality of fixation is influenced by the type of fixative (fixative pH, buffers, concentration, osmolality, and additives), and fixation time and temperature. The choice of fixative also determines the need for pretreatments (e.g. antigen retrieval), titer of the primary antibody, the intensity of the specific reaction versus background (signal-to-noise ratio), and even the detection pattern of antigens. A standard cross-linking fixative is formaldehyde which induces a formation of adducts between formaldehyde and uncharged reactive amino groups that eventually form cross-links. The formation of methylol adducts inactivates nucleases and proteases (O'Leary et al. 2009). Once the addition product (reactive hydroxymethyl compound) is formed, additional cross-links are created. Thus, in the presence of a second reactive hydrogen, the hydroxymethyl group forms a methylene bridge. Fixation with formaldehyde is a three-step process of penetration, covalent bonding, and cross-linking. While these steps happen simultaneously, they do so at different rates. Penetration is approx. 12 times faster than bonding and the latter 4 times faster than cross-linking (Buesa 2008). The most common types of coagulative fixatives are dehydrants (alcohols and acetone) and strong acids (picric acid, trichloroacetic acid) that precipitate proteins by breaking hydrogen bonds without cross-linking proteins. Also, there are specialized fixatives that are superior to other conventional fixatives such as formalin in some specific applications. Weigner's fixative, a mixture of alcohols and pickling salt, is excellent for DNA and RNA studies (Klopfleisch et al. 2012). Carnoy's fixative, a mixture of alcohol–chloroform–acetic acid, and PAXgene fixative, which consists of a fixation reagent (methanol,

acetic acid, and organic solvent) and a post-fixation stabilization reagent (alcohol mixture), may not need antigen retrieval for some antigens (Kap et al. 2011; Koch et al. 2012).

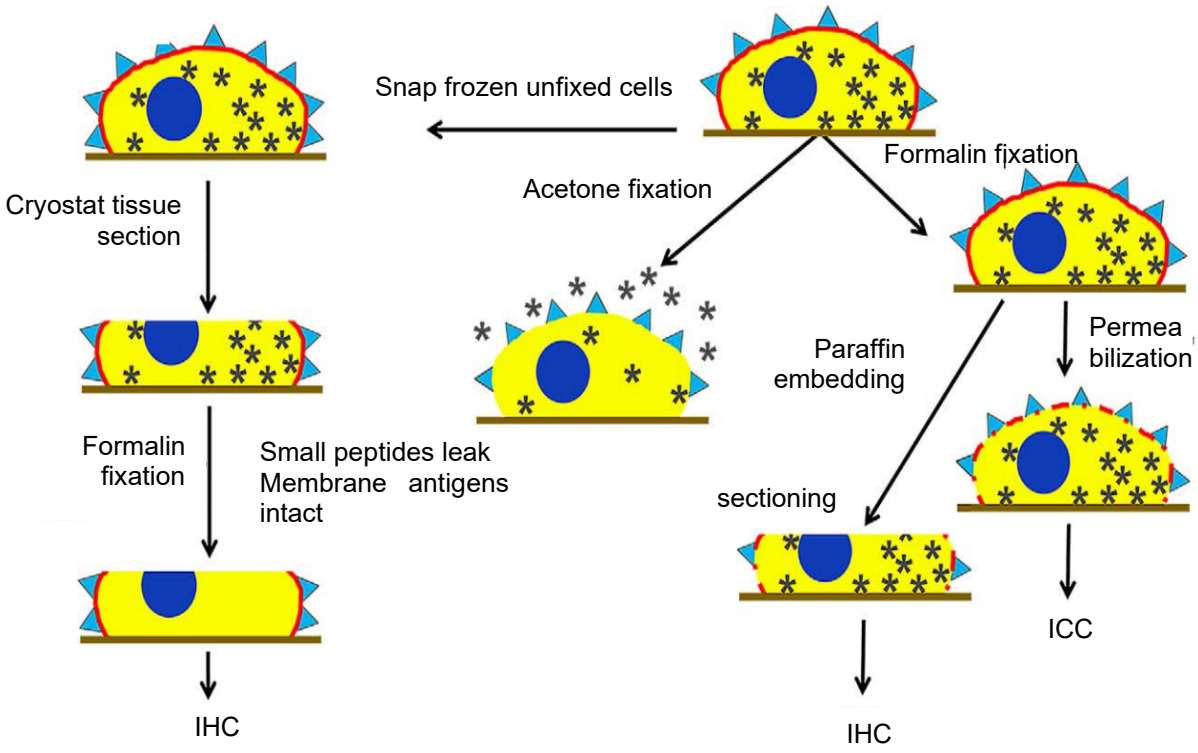

Figure 10: Effects of fixation on small peptides and cell membrane antigen stability. *Modified from* (Ramos-Vara and Miller 2014). **-small peptides, Δ-membrane antigen, IHC immunohistochemistry, ICC-immunocytochemistry.*

7.3.2 Antigen retrieval

Fixation and tissue processing alter the three-dimensional structure of proteins, which can render antigens undetectable by specific antibodies due to change in conformation of the antigen (Huang et al. 1976). The purpose of antigen retrieval procedures is to reverse the changes produced by fixation. Antigen retrieval is important mainly for tissues fixed in cross-linking fixatives. Whereas, tissues fixed in coagulation fixatives do not require the antigen retrieval step prior antibody probing. The two most common antigen retrieval procedures in IHC are enzymatic and heat-based retrieval. Enzymatic retrieval is Protease-induced epitope retrieval where trypsin, proteinase K, pronase, ficin and pepsin are commonly used. However, Protease-induced epitope retrieval is optimal only for a low number of antigens (Ramos-Vara and Miller 2014).

Heat-induced epitope retrieval is based on high-temperature heating or strong alkaline hydrolysis (Shi et al. 1997). These mechanisms are thought to reverse protein-formaldehyde chemical reactions. Although these mechanisms denature tissues, it enhances its immunoreactivity. The mechanism involves the dissociation of irrelevant proteins from target peptides. Heating may unmask epitopes by hydrolysis of methylene cross-links. In fact, there are other hypothesized mechanisms since the heat-induced epitope retrieval enhances immunoreactivity of tissues fixed in ethanol or even of unfixed tissues (Ramos-Vara and Miller 2014).

7.3.3 Detection

The primary, secondary, or tertiary antibodies of a detection system are labeled with reporter molecules to visualize the antigen-antibody complex. Suitable labels include fluorescent compounds, enzymes, and metals. The detection system should maximize sensitivity of an IHC test and optimize visibility of the immune reaction within shortest time possible. Moreover, the detection system must be reproducible, accurate, and provide a high signal-to-noise ratio. Direct detection methods are one-step processes using a primary antibody conjugated with reporter molecules, such as fluorochromes, enzymes, colloidal gold, or biotin (Polak and Van Noorden 2003). The direct method is quick but lacks sensitivity for most antigens in routinely processed tissues. The need for more sensitive antigen detection prompted to develop a two-step method. The primary antibodies are unlabeled, but the secondary ones are labeled. The sensitivity is higher in comparison to the direct method because the unlabeled primary antibody retains full avidity with stronger antigen binding, and the number of labels (e.g. peroxidase) per molecule of primary antibody is higher increasing the reaction intensity (Ramos-Vara and Miller 2014).

7.4 Antibodies as a tool for analysis

Immuno-based analyses such as IHC, WB etc. involves antibody recognition and binding to an epitope on the target antigen. The specificity of the reaction largely depends on qualities of the primary antibody and the ability of the antigen (epitope) to bind it. The most commonly used immunoglobulin (Ig) is IgG; IgM is used less commonly (Ramos-Vara 2005). The antigen-binding site of an antibody is called the paratope, see Figure 11. Epitopes, usually 5 to 21 amino acids long, are the regions of an antigen that bind to antibodies. Epitopes are classified as linear or conformational. Linear epitopes are a group of 5 to 7 contiguous amino acids.

Conformational (discontinuous) epitopes, the typical form, comprise of small groups of amino acids brought together by conformational folding or binding (Bogen et al. 2009). Although most epitopes involved in immune responses are believed to be conformational, data support the concept that antibodies used in IHC or WB tissues recognize mainly linear epitopes.

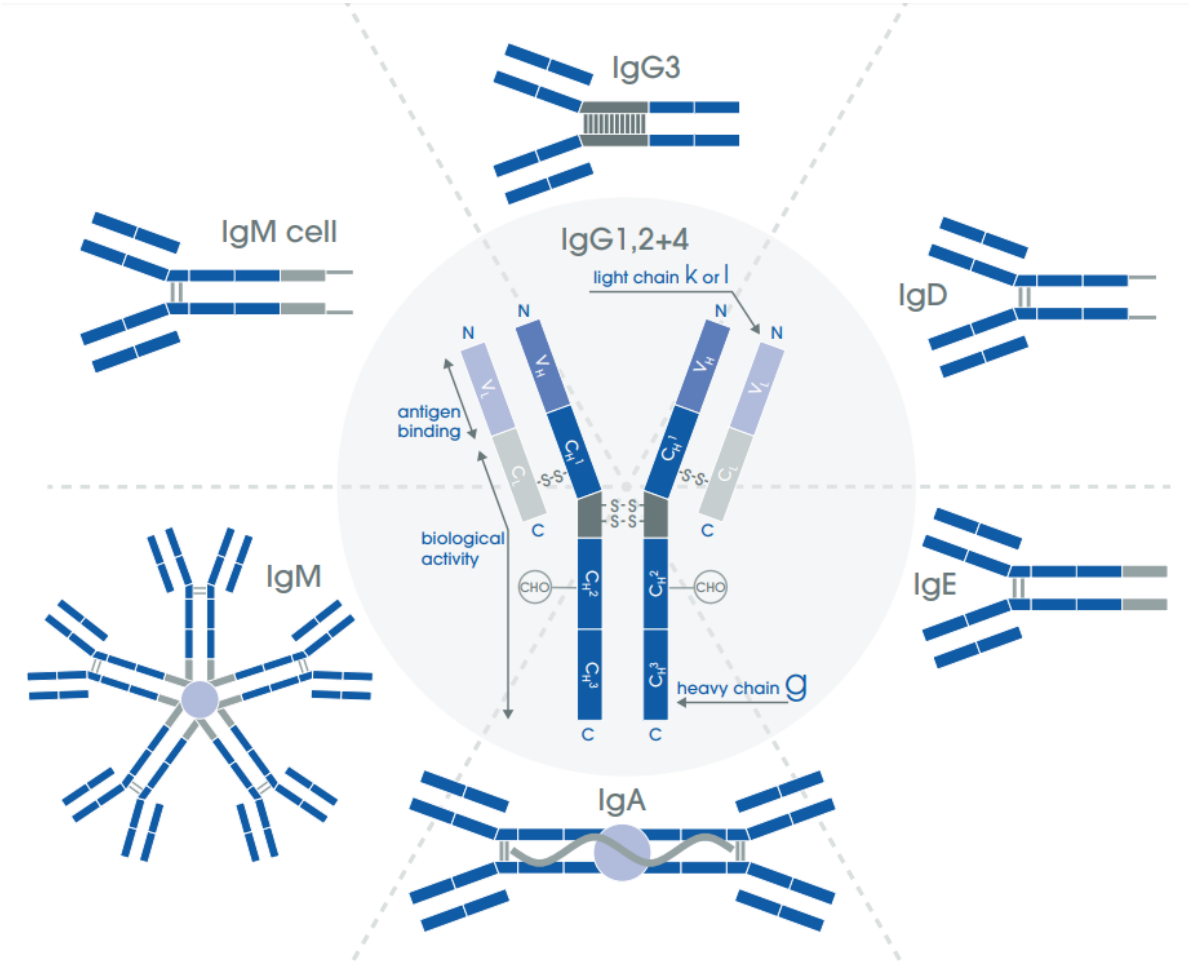

Figure 11: Antibody isotopes and their structure. *Modified from* (Abcam 2010).

Assay validation requires confirmation that the primary antibody is specific, selective, and reproducible for its intended use (Bordeaux et al. 2010). For use as cellular markers, a good starting point is WB to demonstrate reactivity with the designated antigen according to its molecular weight in the tissue and species of interest. Nevertheless, WB immunoreactivity does not necessarily predict immunoreactivity in formalin-fixed tissues. Some antibodies bind only denatured protein immunoblots; others bind only native proteins. The native versus denatured confirmation is further complicated by methods used to fix tissue. Epitopes that are not exposed in the native proteins can be exposed in fixed tissue and vice versa, even though they may not be truly denatured. Thus, an antibody can recognize one epitope in a fresh tissue, but when applied to a fixed tissue it can recognize another epitope (Saper 2009). WB and pre-adsorption

tests are the most widely used methods to determine the specificity of a primary antibody in a diagnostic setting. Other methods that require more sophisticated technology and laboratory capabilities include: use of knockout animal tissues with genetically removed antigen and use of a transfected cell line expressing the antigen for the primary antibody (Ramos-Vara and Miller 2014). In the end, antibody specificity is best documented by the appropriate use of controls: Positive tissue controls assess the performance of the primary antibody; A negative control that verify the specificity of the primary antibody in tissue lacking the antigen of interest; Negative reagent controls (without the primary antibody) are used to confirm test specificity and to assess the degree of non-specific background caused by the secondary or tertiary antibody (Bordeaux et al. 2010; Hewitt et al. 2014).

7.5 Microscopy as a detection technique

IHC outcome greatly relies on the detection method where various microscopy techniques are utilized (Mahmood and Yang 2012; Ramos-Vara and Miller 2014). Basic wide-field fluorescence microscopy is poorly efficient for TJ analysis in tissues. Confocal laser scanning microscopy (CLSM) is the golden standard for TJ analysis as it is the most versatile 3D imaging system with wide range of applications. The optical principle of a CLSM is quite simple, yet elegant. Laser beam is focused down to a small spot in the specimen, exciting fluorescence in the entire cone of illumination. Instead of visualizing the specimen by using a camera, the fluorescence from the sample is collected by the objective lens, rescanned by the galvanometric mirrors, and then focused through a confocal pinhole onto a point detector or photomultiplier tube. Fluorescence from out-of-focus planes is blocked by the pinhole (Jonkman and Brown 2015). The main weaknesses of CLSM are speed and sensitivity. It takes circa 1 s per image to collect a 1024x1024 pixel image with a 1 µs pixel dwell time, which sounds fast enough. However, acquiring 3D images with multiple fluorophore channels, multiple averaging and multiple positions, can take up to tens of minutes or even hours. Furthermore, high intensity lasers cause a lot of phototoxicity when imaging living cells. On the other hand, the CLSM is such a versatile tool that it can be adjusted to various applications. Several parameters such as scan speed, scan averaging, resolution, zoom, laser power, pinhole size, detectors can be modified to work towards ideal set-up in a particular experiment (Waters 2009). However, improving one imaging parameter will be at the expense of others. Nevertheless, thanks to this versatility CLSM can be used for high-resolution imaging, 3D imaging, moderate resolution for cell counting, live-cell imaging, photobleaching etc. (Patterson 2008).

Newly developed technologies such as resonant scanner, white light laser or hybrid detector help to overcome some of the weaknesses of conventional CLSM. The resonant scanning galvanometric mirrors that oscillate at a fixed frequency and undergo gradual acceleration and deceleration while scanning and imaging increases the acquisition of a 512x512 pixel image frame at upward of 30 frames per second. The rapid speed enables imaging of fast biologic processes such as protein transport, lipid diffusion, and calcium fluctuations. Also, the faster scanning of resonant scanners reduces the dwell time on each pixel which in turn suppress the photobleaching and the phototoxicity caused to living samples (Borlinghaus 2006). On the other hand, the resonant-scanning galvanometers are not as flexible as traditional galvanometers: they resonate at a fixed frequency, so the pixel dwell time is fixed by the chosen size of the field of view. In addition, with reduced pixel dwell time, which is under 1 μs, there are very few photons collected in each pixel.

White light lasers consist of a low energy-pulsed IR fiber laser (80 MHz) that is amplified by a diode-pumped laser amplifier. White laser generates the visible spectrum covering wavelengths from 470 to 670 nm. Acousto-optic device is used to select light bands 1–3 nm in width employing acoustic waves across a birefringent crystal changing the crystal's refractive index. Variable frequencies of acousto-optic waves cause refraction and bending of different wavelengths of light, giving rise to highly tunable wavelength-specific bending. Thus, different wavelengths of light can be bent into or out of the light path of the microscope (Jonkman and Brown 2015). Hybrid detector combines a high dynamic range of the photomultiplier tube technology and a high sensitivity of the avalanche photodiode technology, amplifying its signal by approx. 150,000-fold, see Figure 12 (Jonkman and Brown 2015).

With a few exceptions biological tissues strongly scatter light, making high-resolution deep imaging impossible for traditional, including confocal, fluorescence microscopy. Nonlinear optical microscopy, in particular two-photon excited fluorescence microscopy, has overcome this limitation. It differs from traditional fluorescence microscopy as the wavelengths of the two exciting photons are longer than the wavelength of the resulting emitted light. Two-photon excitation microscopy typically uses near-IR excitation light which can also excite fluorescent dyes. However, for each excitation, two photons of IR light need to be absorbed. Using IR light minimizes scattering in the tissue. Due to the multiphoton absorption, the background signal is strongly suppressed. Both effects lead to an increased penetration depth for these microscopes (Denk et al. 1990; Helmchen and Denk 2005).

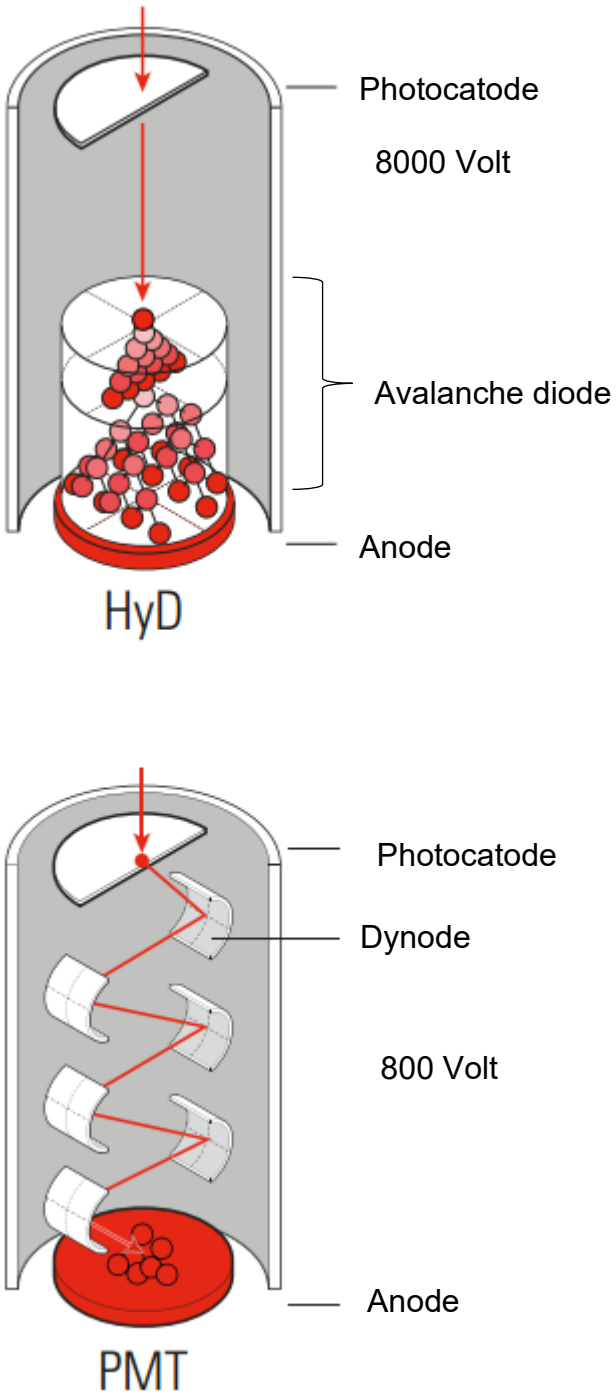

Figure 12: Schematic illustration of Hybrid Detector versus ordinary photomultiplier. *Modified from* (Leica 2014).

8 AIMS OF THE THESIS

This project was focused on setting up methods for analysis of the skin barrier in the process of ageing. First of all, a comprehensive review of the skin barrier topic has been made in order to establish the main hypothesis and list of objectives, which resulted in a published paper. The main hypothesis of this thesis challenges the TJs and their potential capability to regulate the barrier function of the aged skin. Since epidermal TJs, epidermal lipids and their mutual interplay define the skin barrier, these were the main points of interest for the analysis.

One of the first objectives was to narrow down the selection of TJ proteins by analyzing TJ expression differences between young and aged skin samples. Next important objective was to implement a suitable skin sampling technique as a substitution for punch biopsy. Two alternatives, SB and TS have been tested for the purpose of future epidermal analyses and their impact on subject safety and well-being. The results have been used for the next published paper. Subsequent objective was focused on an optimization of the RNA/protein co-extraction workflow from the human and porcine epidermis. Optimization of individual methods for the analysis of TJ protein expression followed afterwards, mainly antibodies and workflow for WB and IHC with CLSM. Results of this progress have been orally presented at a conference. In parallel, another objective dealt with a selection of an optimal analytic method for epidermal lipids. Lipid composition of porcine epidermis has been tackled with shotgun MALDI MS technique (presented via poster). However, gold standard HPTLC proved to be more valuable for analysis of epidermal lipids. Next objective dealt with analysis of the aged human skin barrier. Study design had to be approved be by ethics committee to perform skin sampling and non-invasive measurement on human volunteers. Established analytic methods were used to compare the state of young and aged skin barrier and to pinpoint potential TJ protein targets.

The last objective was to mimic the state of aged skin barrier with decreased content of barrier lipids due to years of sunlight exposure by developing a delipidated porcine ex vivo model. Because occludin as a key member of TJ proteins was found to be upregulated in the aged skin and also as a response to the acute skin barrier damage, we evaluated whether its overexpression could improve the water barrier in our *ex vivo* delipidated skin model as well. For this purpose, a NPWDQ casein-derived peptide previously described as a specific occludin stimulator in epithelial cells (Tanabe 2012) was synthesized and characterized for the induction of occludin overexpression in the delipidated porcine model.

9 MATERIALS AND METHODS

9.1 Methods Optimization

9.1.1 Optimization of protein extraction

For the optimization of protein extraction procedures, skin samples of porcine auricle (obtained from local slaughterhouse) and biopsies of human skin were used. Both types of skin samples were heated in 58°C water bath in order to obtain the epidermis. The epidermises were homogenized in RNAzol® RT (MRC, Cincinnati, OH, USA) reagent by a TissueLyser II homogenizer (Qiagen, Hilden, Germany) with RNAse free stainless-steel beads. The total RNA and protein isolation were performed according to the manufacturer's protocol. Either chloroform or diethylpyrocarbonate-treated water was added to a RNAzol® sample lysate and the mixture was vortexed for 20 seconds and stored for 20 minutes at RT. After collecting the phase containing RNAs, the protein isolation continued by washing the residual pellet twice with 75% ethanol. The pellet was then dissolved using a lysis buffer (150 mM NaCl, 50 mM Tris, 1% Triton-X), or lysis buffers enhanced with either 1% SDS or 1% SDS and 4 M urea. Samples were then heated at 55°C for 20 minutes or stored at RT for 20 minutes. After centrifugation (13,500 g, 15 minutes) the supernatant was collected.

9.1.2 Selection of antibodies used for immunodetection

To obtain reliable results, only tested and validated antibodies were used, that were also previously described in literature of the skin research, see Table 3.

9.1.3 Immunohistochemistry optimization

IHC-Paraffin – skin samples from porcine auricles were fixed in 10% neutral buffered formalin for 24 hours at 4°C. Skin samples were then embedded in paraffin and 10µm thick cross-sections were cut and affixed onto the glass slide. Skin cross-sections were deparaffinated using xylene (2x5 minutes), 100% ethanol (2x3 minutes), 70% ethanol (1x3minutes) and water (1x3 minutes). Antigen retrieval was performed with Tris/EDTA buffer (10mM Tris Base, 1 mM EDTA, 0.05% Tween 20, pH 9). Skin cross-sections were incubated in preheated Tris/EDTA buffer at 95°C for 30 minutes. Skin cross-sections were then cooled and rinsed in water and TBS, both for 3 minutes. Skin cross-sections were incubated in 0.1% Triton X-100 for 15 minutes and rinsed with TBS. Immunostaining procedure followed afterwards.

IHC-Frozen - skin samples were frozen in a Cryomount optimal cutting temperature compound (Histolab, Göteborg, Sweden) and stored at -80°C until further use. Cross-sections

(7 µm) were obtained by a Leica CM1950 cryostat (Leica Biosystems, Wetzlar, Germany) and fixed in acetone at -20°C for 10 minutes. Immunostaining procedure followed afterwards.

Immunostaining procedure optimization was done as follows: skin cross-sections were blocked by 5% BSA in 0.1% TBS-T solution for 60 minutes at RT and probed with the primary antibodies for 30, 60, 90 and 120 minutes for each antibody. After washing with TBS-T, the sections were incubated with the appropriate secondary antibody for again 30, 60, 90 and 120 minutes for each antibody.

Table 3: Primary antibodies used in this PhD project.

Protein	Manufacturer cat.no.	Description	Detection in human skin		Detection in porcine skin	
			IHC	WB	IHC	WB
Claudin-1	Thermo Fisher 37-4900	Monoclonal Mouse, clone 2H10D10	✓	✓	✓	✓
Filaggrin	Thermo Fisher MA5-13440	Monoclonal Mouse, clone FLG01	**N/A**	✓	**N/A**	**N/A**
GAPDH	Sigma Aldrich G8795	Polyclonal Rabbit	**N/A**	✓	**N/A**	✗
Laminin	Abcam Ab11575	Polyclonal Rabbit	**N/A**	✓	**N/A**	**N/A**
Occludin	Thermo Fisher 33-1500	Monoclonal Mouse, clone OC-3F10	✓	✓	✓	✓
Occludin	Thermo Fisher 701161	Monoclonal Rabbit, clone 6H10L9	✗	✗	✗	✗
Occludin	Thermo Fisher 40-4700	Polyclonal Rabbit	✓	✓	✗	✓
ZO-2	Thermo Fisher 71-1400	Polyclonal Rabbit	✓	✓	✓	**N/A**
β-actin	Santa Cruz sc47778	Monoclonal Mouse	**N/A**	✓	**N/A**	✓

✓ -successful detection; ✗ -unsuccessful detection; **N/A**-data not available

9.1.4 Porcine skin lipidomics

Skin samples were obtained from the fresh porcine auricles. The samples were heated for 60 seconds at 60°C and the top layer of the skin, the epidermis was peeled off. Epidermal samples were transferred into a vial and modified Bligh Dyer extraction was performed (Bligh and Dyer 1959). Briefly, 2 mL of chloroform/methanol mixture (1:2) were added and samples were then homogenized using steel beads. After centrifugation, supernatants were transferred into a new vial where 0.5 mL of chloroform and 0.5 mL of water was added. The bottom layer was evaporated under nitrogen and kept under –20°C for further analysis. For non-polar lipids modified extraction of Sun et al. was performed. Briefly, 2 mL of hexane, 2 mL of methanol and 0.2 mL of dH_2O were added to the sample and homogenized. After centrifugation, hexane layer was transferred into a new vial. Additional 2 mL of hexane were added to the sample and extraction was repeated. Total 4 mL of hexane were re-extracted with 2 mL of methanol and the hexane layer was dried under nitrogen. Lipid extracts were reconstituted with 0.8 mL of chloroform/IPA mixture (1:1) and then mixed with equal amount of 10 mg. mL^{-1} MALDI matrixes: α-cyano-4-hydroxycinnamic acid (CHCA), 2,5-dihydroxybenzoic acid (DHB) or 9-aminoacridine (AA). Samples were analyzed using MALDI- LTQ Orbitrap XL (Thermo Fisher). Fullscan in positive-ion and negative-ion mode was obtained in the mass range m/z 180-2000 using appropriate laser settings depending on the matrix used. Individual masses were fragmented (MS/MS) and analyzed.

9.2 Suction blistering and tape-stripping characterization

9.2.1 Donors

20 healthy volunteers were recruited for this study. The volunteers gave written informed consent for epidermal sampling by either SB or TS technique. The group of 10 volunteers for SB consisted of 3 males and 7 females with age average 45 years, range 20-74 years. The group of 10 volunteers for TS consisted of 1 male and 9 females with age average 30 years, range 23-44 years. This study was approved by the Ethical Committee of Contipro a.s. according to WMA Helsinki Declaration.

9.2.2 Epidermal sampling

SB was performed on the left volar forearm of the donors by one person, an acknowledged and well-trained medical laboratory technician. A home-modified syringe with an inner diameter of 0.9 cm was utilized to form the blister as described elsewhere (Gupta et al. 1999). Briefly, the

syringe was connected to a vacuum pump with a CVC 3000 vacuum controller (Vacuubrand, Essex, CT, USA) through a two-way valve. Once a negative pressure of 250 mmHg was developed, the two-way valve was sealed. After the blister formation, the blister fluid was discarded and the blister roof (the epidermis) collected. Each epidermal sample was divided into three parts, one half and two quarters. The half of the sample was used for protein and RNA extraction and the two quarters were used for IHC and lipid analyses, respectively.

TS was also performed on the left volar forearm of the volunteers by one person, an acknowledged medical laboratory technician. 30 D-Squame discs (diameter 1.4 cm, CuDerm, Dallas, TX, USA) were consecutively applied onto the same spot and removed. The obtained material by both techniques was weighed using analytical scales. For the weighing of the TS samples TS discs were pooled by ten (strip number 1-10, 11-20, 21-30).

9.2.3 *In vivo* skin imaging

In vivo RCM imaging was performed on the sampling sites of all volunteers prior to TS and post TS using Vivascope 1500 (Mavig, Munich, Germany). 36 x 3.26 μm stacks were taken from a single spot covering total depth of 114 μm. The same settings were utilized for each imaging.

9.2.4 Protein and RNA extraction and isolation

The obtained material was homogenized in RNAzol® RT (MRC, Cincinnati, OH, USA) reagent either by TissueLyser II (QiaGen, Hilden, Germany) with RNAse free stainless-steel beads in case of SB samples or by vigorous shaking for 30 minutes in case of TS. Total RNA and protein isolation were performed according to the manufacturer's protocol with some modifications to maximize the yield. Briefly, diethylpyrocarbonate-treated water was added to RNAzol® sample lysate and the mixture was vigorously shaken for 15 seconds and stored for 15 minutes at RT. Samples were centrifuged 12,600 g for 15 minutes at 8°C and a water phase containing RNA was collected. The RNA isolation continued by the column extraction protocol on a Qiacube automated isolator (QiaGen, Hilden, Germany). The protein isolation continued by washing the residual pellet twice with 75% ethanol. The pellet was then dissolved using a lysis buffer (4 M urea, 150 mM NaCl, 50 mM Tris, 1 % Triton-X, 1 % SDS). After centrifugation (13,500 g, 15 minutes) the supernatant was collected. Protein and RNA isolates were stored at -80°C until further analysis.

9.2.5 SDS-PAGE and western blotting

Protein concentrations in the protein isolates were assessed by Pierce™ BCA Protein Assay Kit (ThermoFischer Scientific, Waltham, MA, USA). Isolated protein amounts (7 µg for the TS samples and 35 µg for the SB samples) were loaded onto 12% polyacrylamide gel and after the separation, the proteins were transferred to an Immuno-Blot® PVDF membrane (Bio-Rad, Hercules, CA, USA). After blocking for 60 minutes with 5% skim milk in TBS-T, the membranes were incubated with the primary antibodies against claudin-1 (clone 2H10D10, 1:500, cat.no. 37-4900), occludin (clone OC-3F10, 1:300, cat.no. 33-1500), ZO-2 (polyclonal, 1:200, cat.no. 71-1400), filaggrin (mouse monoclonal FLG01, 1:500, cat.no. MA5-13440) (all ThermoFischer Scientific, Waltham, MA, USA), laminin (rabbit polyclonal, Abcam, Cambridge, UK, 1:500, ab11575) and GAPDH (rabbit polyclonal, Sigma-Aldrich, St.Louis, MO, USA, 1:1000, cat.no. G8795) overnight at 4°C. After a subsequent washing in TBS-T, the membranes were incubated for 60 minutes with the respective secondary antibodies conjugated with HRP (anti-rabbit IgG-HRP antibody produced in goat, anti-mouse IgG-HRP produced in rabbit, both Sigma-Aldrich, St.Louis, MO, USA, 1:1000, cat.no. A0545 and A9044). After a subsequent washing with TBS-T, the protein-antibody complexes were visualized with the SuperSignal™ West Pico Chemiluminescence Substrate (ThermoFischer Scientific, Waltham, MA, USA) and detected by an Alliance 4.7 chemiluminescence detector (UVItec Limited, Cambridge, UK).

9.2.6 RNA amplification and quantitative real-time RT-PCR

The concentration and purity of isolated RNA were determined by a Cary50 UV-VIS spectrophotometer (Agilent Technologies, Santa Clara, CA, USA) using the 260/280 absorption ratio. A reverse transcription reaction was performed with 1 µg of isolated RNA using High Capacity RNA-to-cDNA Kit (ThermoFischer Scientific, Waltham, MA, USA) as suggested by the manufacturer. Subsequent qPCR was performed with TaqMan gene expression assays for *FLG* (Hs00856927_g1), *OCLN* (Hs00170162_m1), *CLDN1* (Hs00221623_m1), *LAMA3* (Hs00165042_m1) and *RPL13A* (Hs04194366_g1) genes. For TS samples with low initial concentration of RNA (below 30 $ng.\mu L^{-1}$) we used RNA amplification kit Ovation PicoSL WTA System V2 (NuGen, Manchester, UK) according to the manufacture's manual. After the amplification, we purified the samples on the Agencourt magnetic beads (BeckmanCoulter, Brea, CA, USA) as recommended. Finally, we determined the concentration and purity of the amplified RNA samples, which were then used for the quantitative real-time reverse transcription PCR (qRT-PCR) as described above.

9.2.7 Immunohistochemistry

One fourth of the collected epidermis from SB was frozen in an optimal cutting temperature compound Cryomount (Histolab, Göteborg, Sweden) and stored at -80°C until further use. Cross-sections (7 μm) were obtained by a Leica CM1950 cryostat (Leica Biosystems, Wetzlar, Germany) and fixed in acetone at -20°C for 10 minutes. For the TS samples the 30th TS disc was chosen for the IHC staining. The TS disc was fixed in 4% paraformaldehyde solution for 10 minutes at RT and permeabilized with use of 0.2% solution of Triton X-100 in TBS for 15 minutes. The sections and the TS disc were then blocked by 5% BSA in 0.1% TBS-T solution for 60 minutes at RT and probed with primary antibody against claudin-1 (clone 2H10D10, 1:200, cat.no. 37-4900) for 60 minutes at RT. After washing with TBS-T, the sections and the TS disc were incubated with the appropriate secondary antibody conjugated with Alexa 647 (1:200, cat.no. A-21235) (both ThermoFischer Scientific, Waltham, MA, USA) for 60 minutes at RT. After subsequent washing with TBS-T, the sections and the TS disc were mounted in a Prolong Diamond medium with 4′,6-diamidino-2-phenylindole (DAPI) (ThermoFischer Scientific, Waltham, MA, USA). Images were acquired by a Leica TCS SP8 X confocal laser scanning microscope (Leica Microsystems, Wetzlar, Germany) using a HyVolution mode and deconvoluted by HuygensEssential software (Scientific Volume Imaging, Hilversum, Netherlands).

9.2.8 Fourier-transform infrared spectroscopy

IR spectra of the SB epidermal samples were collected on a Nicolet 6700 FT-IR spectrometer (Thermo Fisher Scientific, Waltham, USA) equipped with a single-reflection MIRacle attenuated total reflectance germanium crystal at 23°C. The spectra were generated by a co-addition of 256 scans collected at 4 cm^{-1} resolution and analyzed with Bruker OPUS software. The exact peak positions were determined from the second derivative spectra and by a peak fitting if needed.

9.2.9 High-performance thin layer chromatography of lipids

For the extraction of the epidermal lipids, a modified Bligh and Dyer method was used (Bligh and Dyer 1959). The epidermal samples were extracted with 1 mL chloroform/methanol ($CHCl_3$/MeOH) 2:1 (v/v) per mg of the epidermis for 90 minutes, filtered, separated and concentrated under a stream of nitrogen. The lipids were dried and stored at -20°C under argon. The lipids were analyzed on silica gel 60 HPTLC plates (20 × 10 cm, Merck, Darmstadt, Germany). The extracted epidermal lipids were dissolved in 100 μl $CHCl_3$/MeOH 2:1. 10 - 30 μL of each lipid sample was sprayed on the plate using a Linomat IV (Camag, Muttenz,

Switzerland). Standards for the HPTLC analysis (ceramide NS, AS, NP and AP), glucosylceramide and sphingomyelin were purchased from Avanti Polar Lipids (Alabaster, AL, USA) or synthesized (ceramide NH (Kováčik et al. 2016), EOS, EOP and EOH (Opálka et al. 2015)). Cholesterol, cholesteryl sulfate, fatty acid standards, L-α-phosphatidylcholine and all other agents were purchased from Sigma-Aldrich (Schnelldorf, Germany) if not otherwise stated. Standard lipids were dissolved in $CHCl_3$/MeOH 2:1 (v/v) (ceramides, cholesterol and free fatty acids), and $CHCl_3$/MeOH 1:1 (v/v) (cholesteryl sulfate, glucosylceramide, sphingomyelin and L-α-phosphatidylcholine), respectively, at 1 $mg.mL^{-1}$. To generate calibration curves, the lipids were mixed in ratios that approximately corresponds to the composition of the human skin (Zoschke et al. 2016). The calibration samples were applied on a HPTLC plate together with the analyzed samples. The major skin barrier lipids (ceramides, free fatty acids and cholesterol) were separated using $CHCl_3$/MeOH/acetic acid 190:9:1.5 (v/v/v) mobile phase twice to the top of the plate (Bleck et al. 1999; Vávrová et al. 2014). The ceramide precursors (glucosylceramide and sphingomyelin), phospholipids and cholesteryl sulfate were separated using a more polar mobile phase ($CHCl_3$/MeOH/acetic acid/H_2O 65:25:6:3) (Vávrová et al. 2014; Wallmeyer et al. 2015). The lipids were visualized by dipping in a derivatization reagent (7.5% $CuSO_4$, 8% H_3PO_4, 10% MeOH in water) for 10 seconds and heating at 160°C for 30 minutes and quantitated by densitometry using a TLC scanner 3 and WinCats software (Camag, Muttenz, Switzerland).

9.3 Skin barrier and tight junctions analysis

9.3.1 Demography of human donors

The study design was approved by the Ethical Committee of Contipro a.s. according to WMA Helsinki Declaration. 20 healthy Caucasian volunteers were recruited and assigned into two groups according to age, young (median 17 years, range 16-21 years; female/male 11/1, n=12) and aged (median 68 years, range 52-84 years; female/male=4/4 n=8). The volunteers or legally acceptable representatives (in case of youths) gave written informed consent for the participation in this study. The volunteers did not suffer from any skin disease or any other serious systematic disease such as diabetes mellitus and were not using any medicaments. The sampling was conducted during June before the main summer season and all the volunteers had avoided extensive sunlight exposure 14 days prior to the skin sampling.

9.3.2 Non-invasive *in vivo* biophysical skin analysis

Prior to SB, both skin sites, sun-protected (volar) and sun-exposed (dorsal), of each volunteer's forearm were probed by a Tewameter® TM300 probe (Courage + Khazaka electronic, Cologne, Germany) and by a Vivascope reflectance confocal microscope (Mavig, Munich, Germany) after 30 minutes of acclimation. The same settings were utilized for each imaging.

9.3.3 Microarray analysis

TS samples of the epidermis of young (18 ± 1 years, n=4) and aged (57 ± 2 years, n=4) donors were collected from sun-protected lower part of back neck. RNA was isolated from twenty TS discs (RNeasy Micro Kit, Qiagen, Hilden, Germany), amplified (Ovation® RNA Amplification System V2, NuGEN, USA), fluorescently-labeled (WGA2 - GenomePlex® Complete Whole Genome Amplification (WGA) Kit, Sigma-Aldrich, St.Louis, MO, USA) and hybridized to a microarray (Human Gene Expression 4x44K v2 chip, Agilent Technologies, Santa Clara, CA, USA). Data were analyzed with software R (R Development Team) and differential gene expression was determined between the two age groups using R statistical package limma.

9.3.4 Epidermal sampling

After the non-invasive skin analysis, SB was performed on sun-protected (volar) and sun-exposed (dorsal) skin sites of the left forearm of the volunteers by one person, an acknowledged medical laboratory technician. A modified syringe with an inner diameter of 0.9 cm was utilized to form the blister as described elsewhere (Svoboda et al. 2017). Briefly, the syringe was connected to a vacuum pump with a CVC 3000 vacuum controller (Vacuubrand, Essex, CT, USA) through a two-way valve. Once a negative pressure of 250 mmHg was developed, the two-way valve was sealed. The blister fluid was discarded and the blister roof (the epidermis) collected. The samples of collected epidermis were divided into three parts, i.e., one half and two quarters. The half of the sample was used for the protein and RNA extraction and the two quarters were used for IHC and lipid analysis.

9.3.5 Protein and RNA isolation

The obtained material was homogenized in RNAzol® RT (MRC, Cincinnati, OH, USA) reagent by a TissueLyser II homogenizer (Qiagen, Hilden, Germany) with RNAse free stainless-steel beads. The total RNA and protein isolation as described in chapter 9.2.4. with little adjustments. Briefly, diethylpyrocarbonate-treated water was added to a RNAzol® sample lysate and the mixture was vortexed for 20 seconds and stored for 20 minutes at RT. Protocol then continued as in 9.2.4.

9.3.6 Quantitative real-time RT PCR

The concentration and purity of isolated RNA were determined by a Cary50 UV-VIS spectrophotometer (Agilent Technologies, Santa Clara, CA, USA) using the 260/280 absorption ratio. A reverse transcription reaction was performed with 1 µg of isolated RNA using the High Capacity RNA-to-cDNA Kit (ThermoFischer Scientific, Waltham, MA, USA) as suggested by the manufacturer. Subsequent qPCR was performed with TaqMan gene expression assays (ThermoFischer Scientific, Waltham, MA, USA) for *CLDN1* (Hs00221623_m1), *OCLN* (Hs00170162_m1), *TJP2* (Hs00910543_m1) and *RPL13A* (Hs04194366_g1) genes in case of the human epidermis, and for *OCLN* (Ss03377507) and *RPL13A* (Ss003376908_u1) in case of the porcine epidermis. The threshold cycle was determined for the genes of interest and the relative mRNA level in each sample was calculated using the $2^{-\Delta\Delta CT}$ method (Livak and Schmittgen 2001).

9.3.7 SDS-PAGE and western blotting

Same protocol was performed as described in chapter 9.2.5. only that the membranes were incubated with the primary antibodies against claudin-1 (clone 2H10D10, 1:500, cat.no. 37-4900), occludin (clone OC-3F10, 1:300, cat.no. 33-1500), ZO-2 (polyclonal, 1:200, cat.no. 71-1400) (ThermoFischer Scientific, Waltham, MA, USA) and GAPDH (polyclonal, Sigma-Aldrich, St.Louis, MO, USA, 1:1000, cat.no. G8795) overnight at 4°C.

9.3.8 Immunohistochemistry and confocal microscopy

Tissue samples were frozen in a Cryomount optimal cutting temperature compound (Histolab, Göteborg, Sweden) and stored at -80°C until further use. Cross-sections (7 µm) were obtained by a Leica CM1950 cryostat (Leica Biosystems, Wetzlar, Germany) and fixed in acetone at -20°C for 10 minutes. The sections were then blocked by 5% BSA in 0.1% TBS-T solution for 60 minutes at RT and probed with the primary antibodies against claudin-1 for 90 minutes (clone 2H10D10, 1:200, cat.no. 37-4900), occludin for 30 minutes (clone OC-3F10, 1:100, cat.no. 33-1500) or ZO-2 for 60 minutes (polyclonal, 1:200, cat.no. 71-1400) at RT. After washing with TBS-T, the sections were incubated with the appropriate secondary antibody conjugated with Alexa 647 (1:500, cat.no. A-21235) or Alexa 488 (1:500, cat.no. A-11008) for 60 minutes at RT. After subsequent washing with TBS-T, the sections were mounted in Prolong Diamond with DAPI (all ThermoFischer Scientific, Waltham, MA, USA). Images were acquired by a Leica TCS SP8 X confocal laser scanning microscope (Leica Microsystems, Wetzlar, Germany). Representative images were obtained using HyVolution mode and deconvoluted by HuygensEssential software (Scientific Volume Imaging, Hilversum,

Netherlands). For quantification purpose, images were acquired using the Leica Hybrid Detector Photon Counter along with the white light laser and retaining the same settings for each image. A stack of 7.2 µm was acquired for each cross-section and the fluorescent signal was quantified in the whole stack.

9.3.9 Lipid analysis

For lipid analysis, please see chapter 7.2.8 and 7.2.9.

9.3.10 *Ex vivo* porcine epidermal culture

Fresh porcine auricles were purchased from a local slaughterhouse and immediately used for the experiments. After the auricle was cleansed, samples (5 x 5 cm) of the full-thickness skin were obtained from the inner side of the auricle. The samples were disinfected and incubated in 2.4 U mL^{-1} Gibco® Dispase II (Thermo Fisher Scientific, Waltham, USA) solution over night at 4°C in a Petri dish with a dermal side facing the bottom of the dish while the epidermis was exposed to air. Epidermal samples were obtained after 18 hours, washed in a sterile PBS solution and inserted into modified Franz diffusion cells containing a porous polyamide membrane and a culture medium. The culture medium consisted of a MCDB 153 medium with 0.3 mg mL^{-1} adenine, 4.9 ng mL^{-1} apo-transferrin, 1.4 ng mL^{-1} triiodo-L-thyronine, 0.8 µg mL^{-1} hydrocortisone, 10 ng mL^{-1} insulin, 2 ng mL^{-1} cholera toxin, 2 ng mL^{-1} hEGF and supplemented with penicillin, streptomycin and amphotericin B. The resultant *ex vivo* porcine epidermis was cultured at "air-liquid interface" with 5% CO2 at 37°C for the next 6 days.

9.3.11 NPWDQ peptide synthesis

A casein-derived peptide NPWDQ was synthetized following standard Fmoc/HBTU/DIPEA protocols using 2-chlorotrityl resin (Agilent Technologies, Santa Clara, CA). Fmoc-amino acids and chemicals used in the synthesis and cleavage were obtained from Iris Biotech GmbH (Marktredwitz, Germany). The crude peptide was precipitated with diethylether and purified. The purity was confirmed by LC-MS 2020 (Shimadzu Europa, Duisburg, Germany) using a Jupiter® Proteo 90 Å reverse phase column (Phenomenex, Torrance, CA), see Supplementary Figure 3.

9.3.12 Skin barrier disruption model

Ex vivo porcine epidermis specimens were placed into the modified Franz cells as described above and cultivated at 37°C, 5% CO2 in a humidified atmosphere for 24 hours. Subsequently, initial TEWL values of the *ex vivo* porcine epidermis were measured by a Tewameter® TM300 probe (Courage + Khazaka electronic, Cologne, Germany). After the TEWL measurement, the

ex vivo porcine epidermis was delipidated using acetone as described elsewhere to yield an epidermal model with the delipidated SC (Rissmann et al. 2009). Briefly, acetone-soaked cotton swabs were moved back and forth over the surface of the model. Afterwards, a surface of the delipidated epidermal model was rinsed with a sterile PBS solution. TEWL rates of the delipidated epidermal model were measured 24 hours after the delipidation. Subsequently, the *ex vivo* porcine epidermis was treated with 1.6×10^{-4} M NPWDQ peptide in the culture medium or control (culture medium), which were placed in both the donor and acceptor chambers of Franz diffusion cells. Another TEWL rates were measured 48 and 120 hours after the delipidation. The Franz diffusion cells were then dismantled, and the *ex vivo* porcine epidermis retrieved for the total RNA isolation and IHC analysis by the aforementioned protocols.

9.3.13 Statistical analysis

Data analysis was performed using Prism 7 software (GraphPad Software, San Diego, CA, USA). Data are presented as means ± SEM. Normality of the data was checked by D'Agostino-Pearson normality test and statistical significance was calculated using paired or unpaired t-test. $P < 0.05$ was considered significant.

10 RESULTS

10.1 Methods Optimization

10.1.1 Protein extraction optimization

Enhanced manufacturer's protocol procedure for extracting RNA and proteins from the porcine or human epidermis worked the best – both adding SDS/heat and urea improved yield of ZO-2, claudin-1 and GAPDH, see Figure 13. Chloroform based coextraction of RNA and proteins showed very low yields of proteins in comparison to water based coextraction. Anti-GAPDH antibody was shown to be inappropriate for the porcine epidermis.

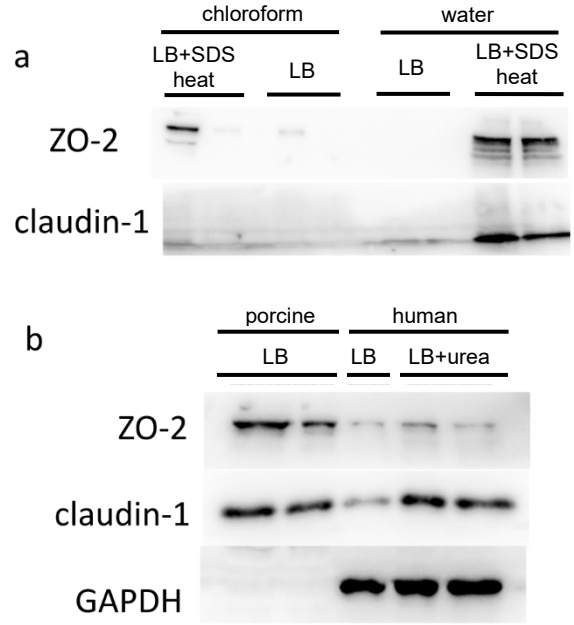

Figure 13: Optimization of a protein extraction from the epidermis samples*. (a) Different extraction procedures from porcine epidermis samples based either on chloroform or water. (b) Effect of enhanced lysis buffer (LB) on the extraction of either porcine or human epidermis.*

10.1.2 Immunohistochemistry optimization

The ideal set up for the claudin-1 detection was dilution of primary antibody (2H10D10) 1:200 incubated for 90 minutes at RT. No difference in the staining was observed when using human or porcine skin (data not shown). The ideal set up for occludin was dilution of primary antibody (OC-3F10) 1:100 incubated for 30 minutes at RT. Anti-occludin worked on the human skin specimens with no problem. But, in the porcine skin occludin was detectable only with OC-3F10. Other anti-occludin antibodies were not efficient in detection of occludin in the porcine

skin, see Figure 14. Ideal ZO-2 set up included dilution of primary antibody 1:100 for 60 minutes at RT (data not shown).

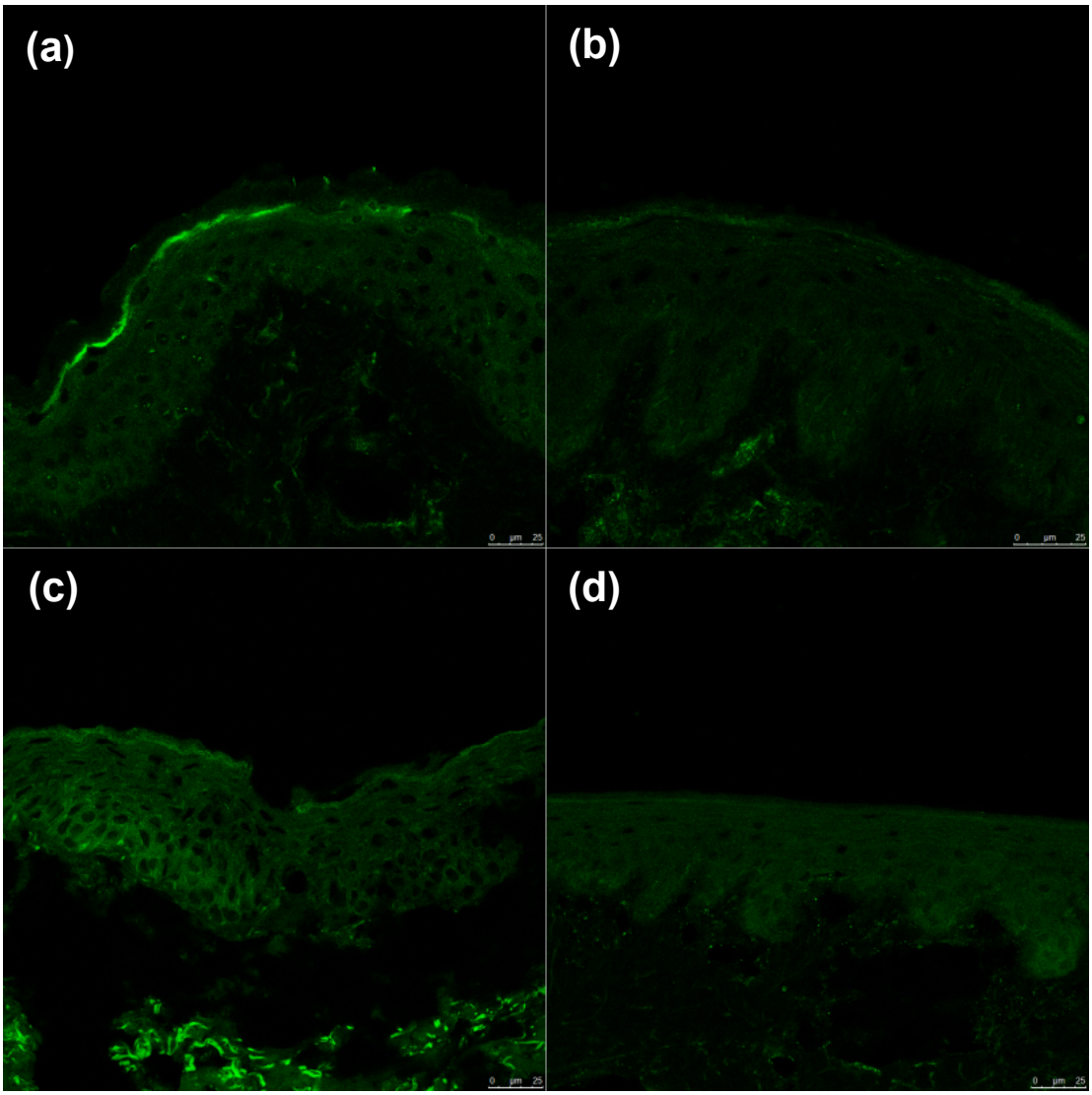

Figure 14: IHC staining of occludin *in the human (a,c) and porcine (b,d) skin using either antibody anti-occludin 40-4700 (a,b) or 701161 (c,d).*

10.1.3 Lipidomics

More than 100 m/z have been identified of which 15 belonged to sphingomyelins (SM), 26 to triacylglycerols (TG), 10 to phosphatidylcholines (PC), 3 to phosphatidylserines, 8 to phosphatidylinositols and 4 to phosphatidic acid and phosphatidylethanolamines, see Table 4. SM were identified and confirmed in positive-ion mode using DHB matrix where they exhibited much greater relative abundance than other lipid classes. TG were identified and confirmed in negative-ion mode using AA matrix with sodium acetate. PC class was selectively identified in

positive-ion mode using AA matrix while rest of the glycerophospholipids were identified in positive-ion mode using AA matrix. Also, more than 30 ceramides were identified in positive-ion mode of DHB. However, most of ceramides could not be confirmed due to mass overlap, low relative abundance and low fragmentation potential of ceramides. Moreover, no long-chain ceramides were detected at all, see Supplementary Figure 1.

Table 4: Confirmed lipid masses (m/z) in the porcine epidermis by MALDI-MS.

Experimental m/z	Theoretical m/z	Species
703.5763	703.5748	SM 34:1$[M+Na]^+$
753.5859	753.5881	SM 36:1$[M+Na]^+$
781.6213	781.6194	SM 38:1$[M+Na]^+$
809.6527	809.6507	SM 40:1$[M+Na]^+$
835.6688	835.6663	SM 40:2 $[M+Na]^+$
855.7370	855.7412	TG 50:1 $[M+Na]^+$
853.7229	853.7256	TG 50:2 $[M+Na]^+$
823.6771	823.6786	TG 48:3 $[M+Na]^+$
883.7648	883.7725	TG 52:1 $[M+Na]^+$
881.7537	881.7569	TG 52:2 $[M+Na]^+$
879.7397	879.7412	TG 52:3 $[M+Na]^+$
905.7531	905.7569	TG 54:4 $[M+Na]^+$
782.5652	782.5670	PC 34:1 $[M+Na]^+$
780.5502	780.5514	PC 34:2 $[M+Na]^+$
808.5810	808.5827	PC 36:2 $[M+Na]^+$
786.5214	786.5291	PS 36:2 $[M+Na]^+$
842.5411	842.5917	PC 40:2 $[M+Na]^+$
861.5411	861.5499	PI 36:2 $[M+Na]^+$

PC, phosphatidylcholine; PI, phosphatidylinositol; PS, phosphatidylserine; SM, sphingomyeline; TG, triacylglycerols.

10.2 Suction blistering and tape-stripping characterization

Sampling durations of both techniques were roughly comparable (SB average 62 minutes, range 39-105 minutes; TS average 50 minutes, range 47-55 minutes). According to the subjective evaluation, both SB and TS were equally painful, more precisely, little or no pain was reported by the volunteers. The skin of some volunteers developed a slight local hyperpigmentation after SB as well as TS procedure. The hyperpigmentation lasted for less than month in case of TS and over a six month in case of SB (Supplementary Figure 2). Both techniques left no permanent damage.

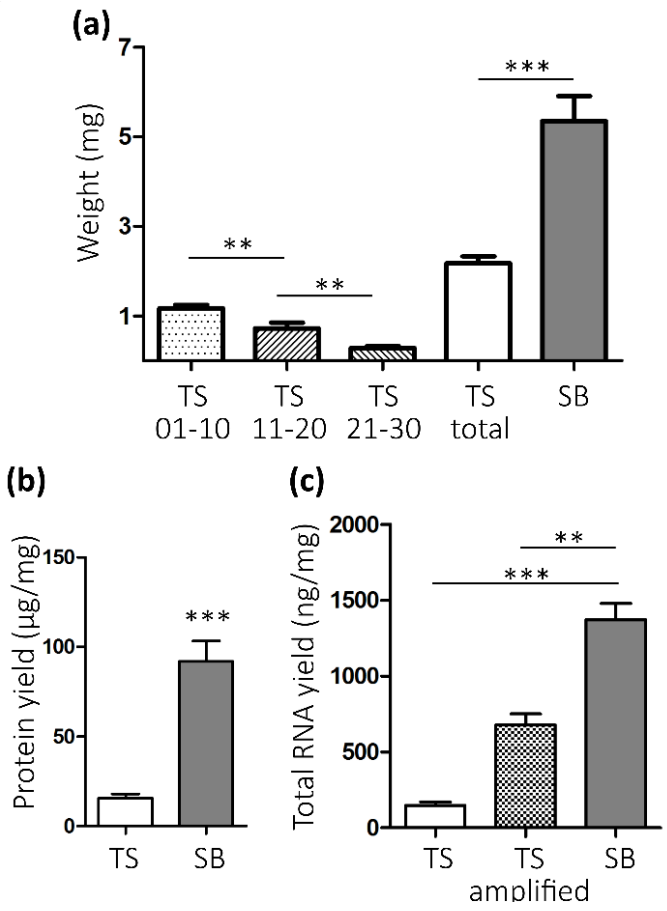

Figure 15: Comparison of the RNA and protein yields of the TS and SB sampling techniques*. Weight of the obtained material from 30 consecutive strips (TS) and SB from volar forearm of 10 volunteers for each technique (a). Protein yield per mg of obtained material (b). Total RNA yield per mg of obtained material (c). The data represent mean ± SEM; **P<.01; ***P<.0001*

The SB samples provided more biological material than the TS samples (Figure 15a) even though TS covered a larger area, 1.54 cm^2, than the SB samples, which ranged from 0.2 cm^2 to 0.5 cm^2. Results also showed that significantly less material is obtained towards the living part of the epidermis by TS. The yield of the protein and RNA was disproportionally higher in SB than in TS regarding the weight of biological material obtained, suggesting that the extraction of the TS samples was not very effective (Figure 15b and 15c).

(a)

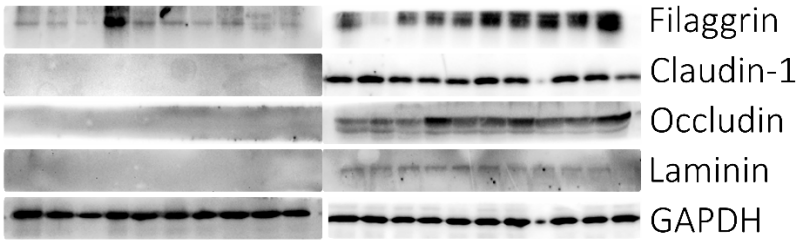

(b)

Gene	TS (Ct)	TS amplified (Ct)	½ SB (Ct)
FLG	ND	26.4 ± 1.5	21.6 ± 0.8
CLDN1	ND	ND	23.0 ± 0.6
OCLN	ND	ND	26.7 ± 0.5
LAMA3	ND	ND	24.6 ± 0.6
RPL13A	ND	30.4 ± 4.9	20.9 ± 0.4

ND- not determined

Figure 16: Expression of the representative proteins and genes*. WB detection of filaggrin, occludin, claudin-1, laminin and GAPDH in TS and one half of each SB samples obtained from volar forearm of 10 volunteers (a). Expression of genes FLG, OCLN, CLDN-1, LAMA3 and RPL13A detected by qRT-PCR in TS and one half of each SB samples obtained from volar forearm of 10 volunteers (b).*

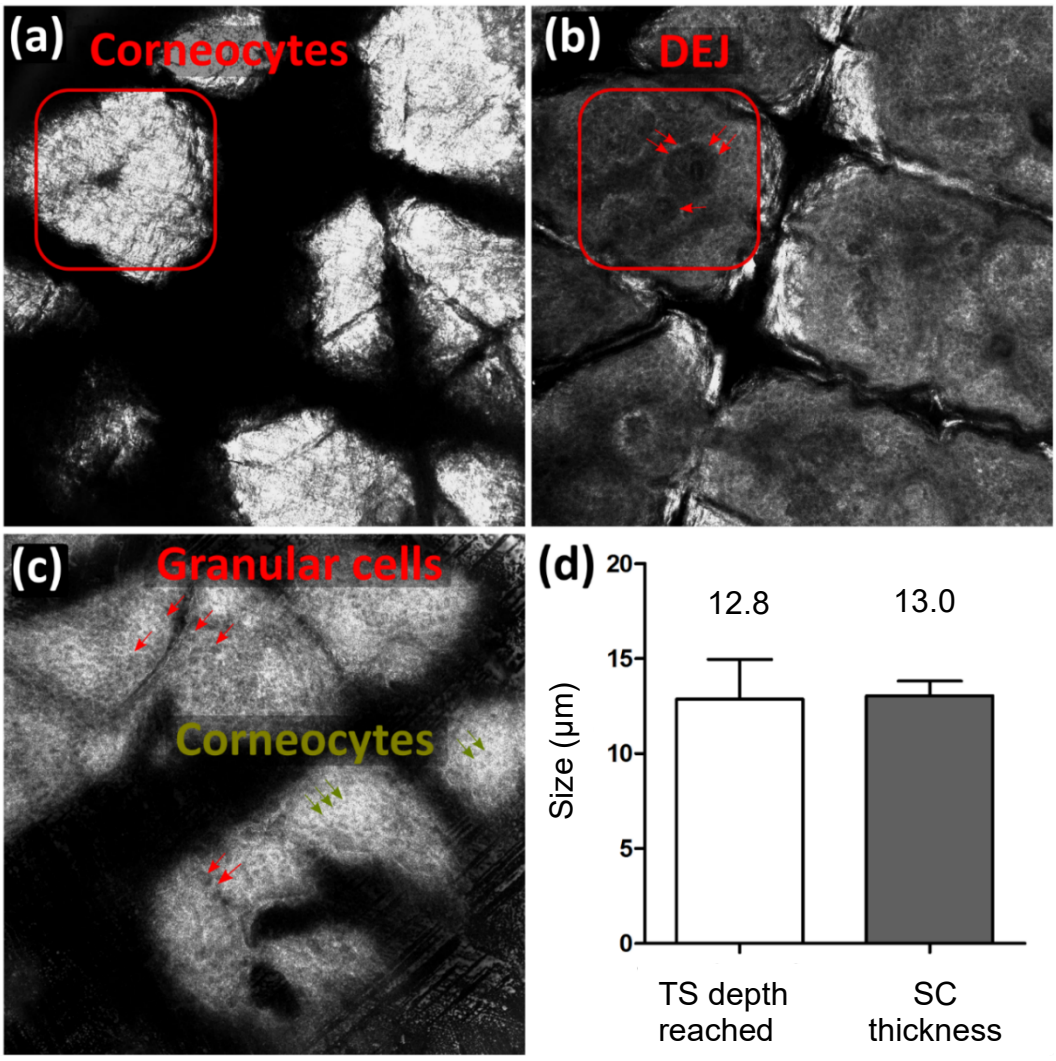

Figure 17: RCM imaging of the tape-stripped skin*. The uppermost image prior to TS indicating undamaged SC with clusters of corneocytes (a). Image indicating start of the dermo-epidermal junction (DEJ) which is the endpoint for thickness measurement (b). The uppermost image after TS indicating presence of the SG (honeycomb pattern) with granular cells (red arrows) and residual corneocytes (green arrows) (c). Size comparison of the depth reached by TS and SC thickness in 10 healthy volunteers (d). RCM image = 0.5 x 0.5 mm. The data represent mean ± SEM. DEJ, dermo-epidermal junction.*

All genes analyzed by qRT-PCR were detected in the SB samples (Figure 16a). However, only *FLG* and *RPL13A* were successfully detected in the TS samples since *OCLN*, *CLDN1* and *LAMA3* remained undetermined. A similar trend was observed on a protein level as well. The WB analysis showed that all the analyzed proteins are detectable in the SB samples, whereas only GAPDH and filaggrin were detected in the TS samples (Figure 16b). This suggests that 30 consecutive TS discs were sufficient to reach the SG but were not effective to detach it. RCM

imaging showed characteristic structures of the human epidermis before and after TS and confirms the fact that TS did not detach the SG layer (Figure 17).

The epidermal structure seemed to be intact and the expression pattern of claudin-1 in the SB samples is congruent with the literature (Figure 18), while in the TS samples a very faint fluorescent signal occurs that cannot be considered as a specific signal of claudin-1. Also, no signal for cell nuclei is present in the TS samples as expected, only clusters of corneocytes are visible within a transmission detector channel (Figure 18).

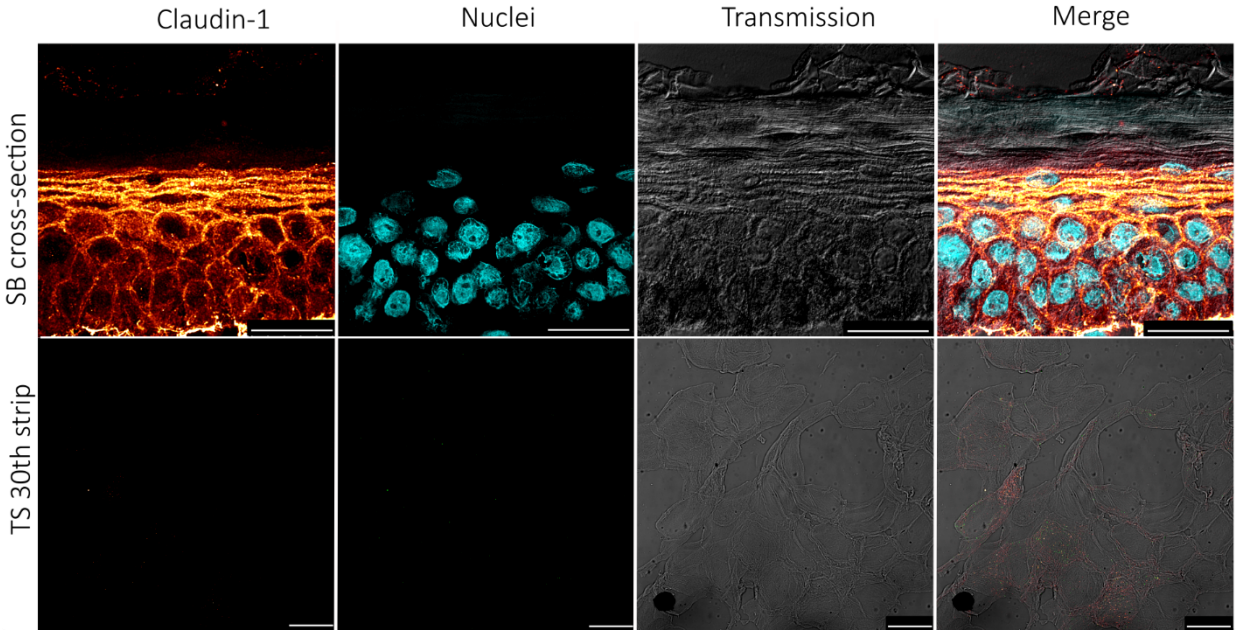

Figure 18: Representative IHC staining *of a SB cross-section and the 30th TS disc both acquired from left volar forearm. Images of merged channels show the localization of claudin-1 (orange), cell nuclei (teal) and epidermal structure by transmission detector. Bar = 25 µm.*

IR spectroscopy of the SB samples (one quarter of the blister collected) showed the presence of highly ordered SC lipids (as indicated by methylene stretching wavenumbers) and the co-existence of a very tight orthorhombic chain with slightly looser hexagonal lipid packing (Figure 19a). HPTLC analysis showed the presence of all barrier lipids in correct proportions (8 ceramide subclasses, FFA, cholesterol and cholesteryl sulfate) and their precursors (SM, glucosylceramides and phospholipids (PL)) (Figure 19b). However, PL class was notably decreased.

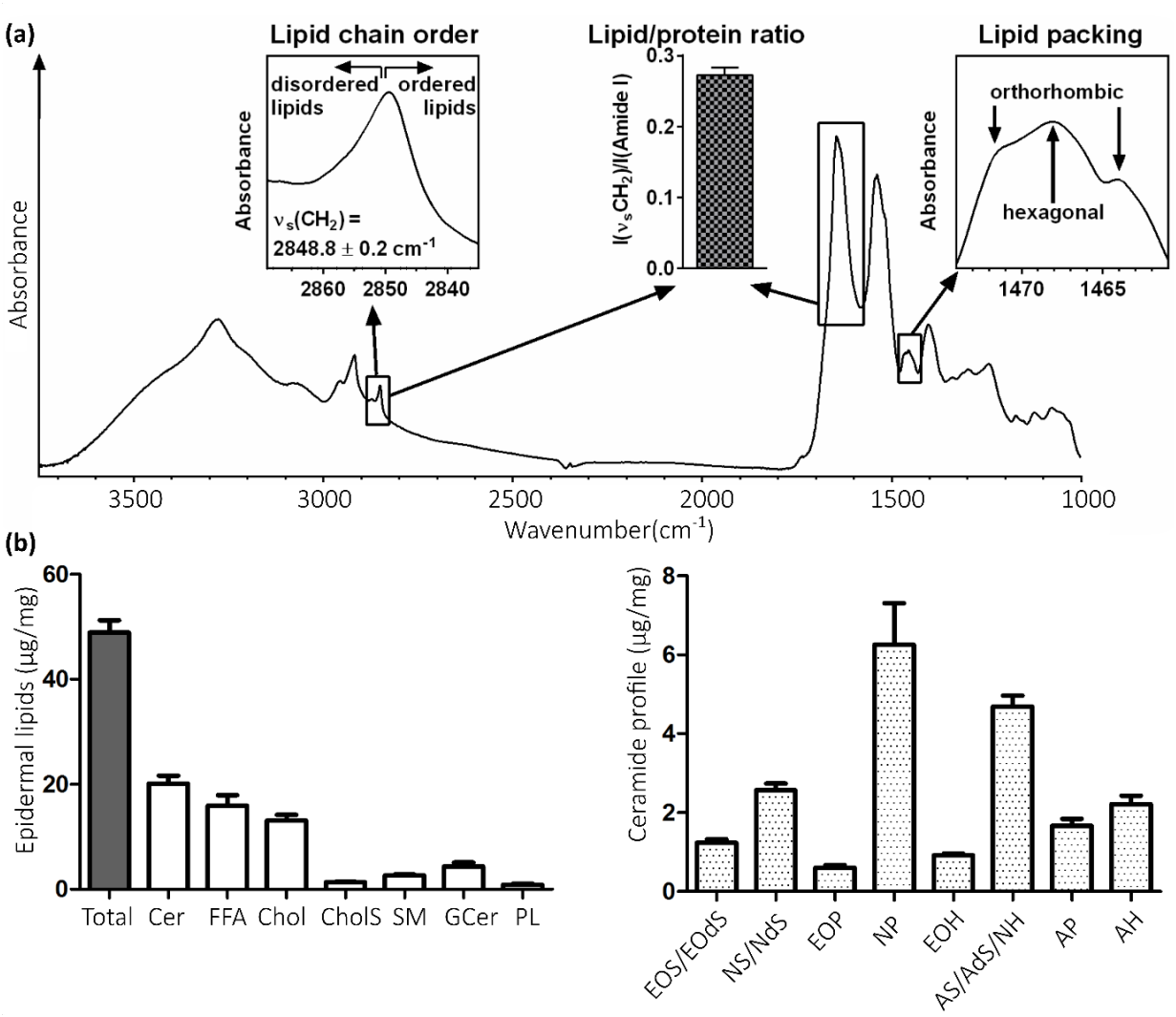

Figure 19: Representative IR spectra of the SC side of the SB sample *highlighting the lipid chain order, lipid packing and lipid/protein ratio. Lipid analysis of the SB samples using HPTLC separation. Composition of epidermal lipids (a) and ceramide profile (b). The data represent mean ± SEM (n=10). Cer, ceramides; Chol, cholesterol; CholS, cholesteryl sulfate; FFA, free fatty acids; GCer, glucosylceramides; PL, phospholipids; SM, sphingomyelins.*

10.3 Skin barrier and tight junctions analysis in the sun-protected and sun-exposed, young and aged human epidermis

10.3.1 Lipid barrier is deteriorated in aged sun-exposed skin without altered water permeability

To assess the condition of the skin barrier we analyzed the lipid composition and organization and TEWL in the sun-protected and sun-exposed forearm skin of aged and young donors. TEWL showed no differences either between the young and aged or between the sun-protected and sun-exposed skin (Figure 21a). Furthermore, a structure of the young and aged epidermis

was analyzed *in vivo* by the reflectance confocal microscopy. Apart from an increased melanin content in melanocytes and basal keratinocytes in the sun-exposed area, we noticed fewer structures corresponding to rete pegs at dermo-epidermal junctions in the aged skin (Figure 20).

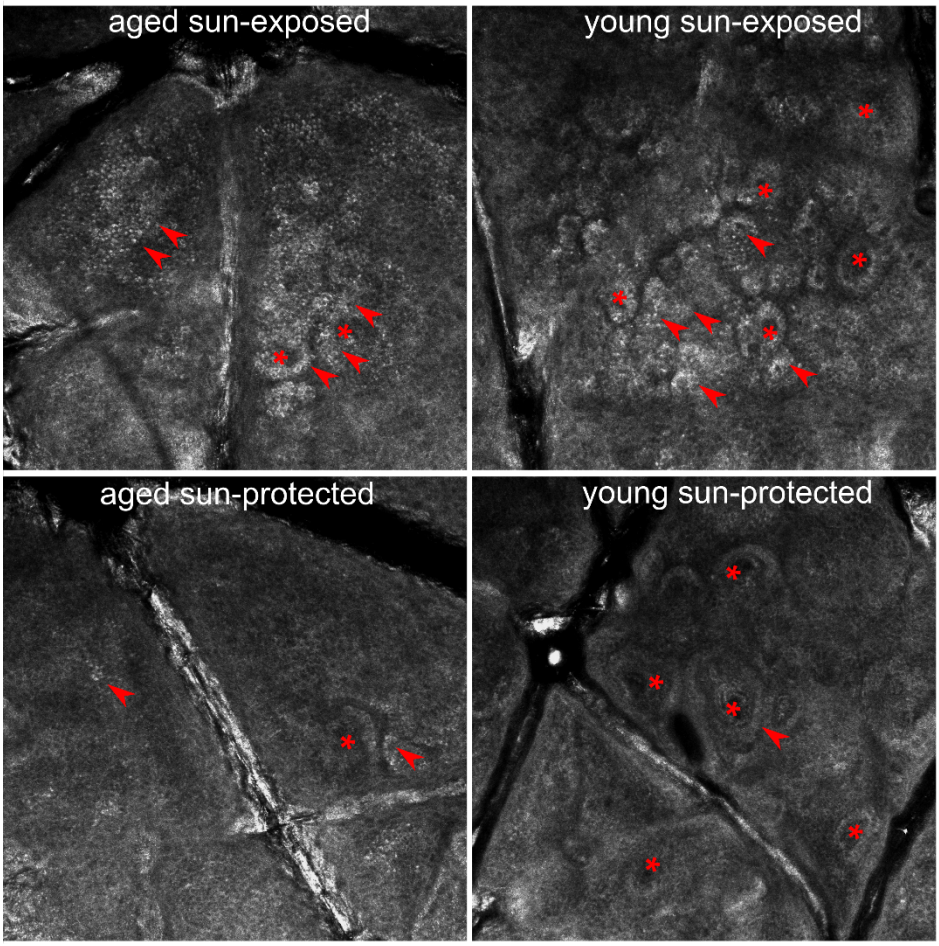

***Figure 20**: **Non-invasive in vivo RCM analysis of the volar (sun-protected) and dorsal (sun-exposed) skin of human donors performed prior the suction blistering**. Representative images show higher content of melanin (arrow) in the basal layer of the epidermis in the sun-exposed skin when compared to the sun-protected skin. Fewer structures corresponding to rete pegs (asterisk) are visible in the aged skin when compared to the young skin.*

The HPTLC analysis showed 15% lesser amount of the total barrier lipids in the aged sun-exposed skin than in the young sun-exposed skin and aged sun-protected skin (Figure 21b), which is congruent with lipid/protein ratio. The lesser amount of total barrier lipids in the aged sun-exposed skin is reflected by a lowered amount of free fatty acids and cholesterol (Figure 21d). In contrast, total ceramides as the main constituents of the lipid barrier (Coderch et al. 2003) did not differ between the studied groups (Figure 21d). Furthermore, detailed ceramide analysis did not reveal any significant changes in ceramide subclasses (Figure 22c).

Interestingly, the young sun-protected skin had fewer barrier lipids than the aged sun-protected or young sun-exposed skin (Figure 21b).

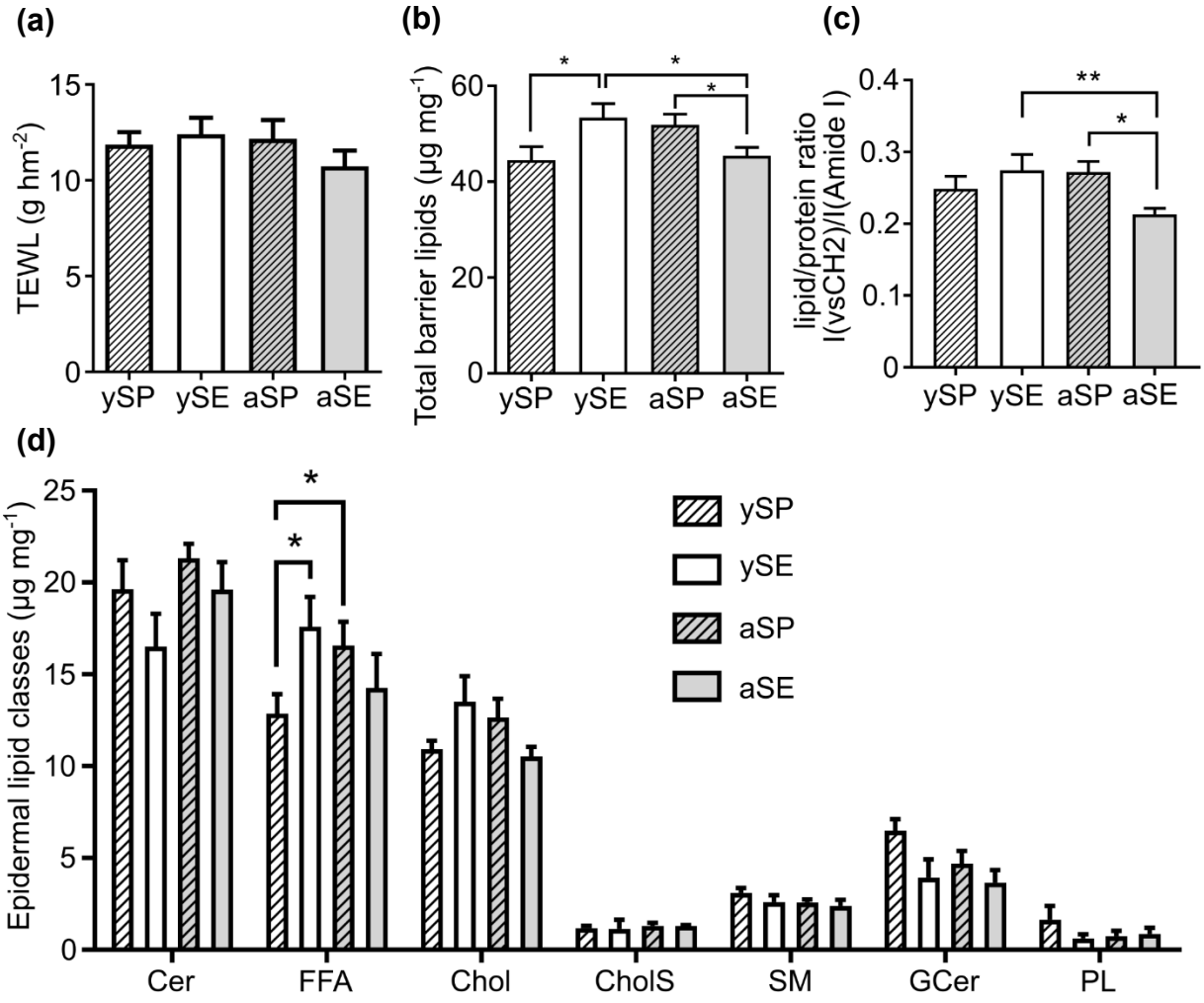

Figure 21: Condition of the young and aged skin barrier in sun-exposed and sun-protected skin of human donors as indicated by TEWL and lipid analysis*. (a) TEWL rates measured in vivo by an open-chamber method prior to the suction blister sampling. (b) Total epidermal lipids in suction blister samples quantified by densitometry after HPTLC separation. (c) The lipid/protein ratio in suction blister samples evaluated by IR spectroscopy as a ratio of intensities of methylene symmetric stretching vibration that originates mostly from lipids and Amide I band that originates mostly from the peptide bond. (d) Composition of barrier lipids (Cer, FFA, Chol) and their precursors (GCer, SM, CholS, PL) in the suction blister samples quantified by densitometry after HPTLC separation. The data are shown as mean ± SEM (young n=12, aged n=8). Statistical significance * P < 0.05, ** P < 0.01. aSE, aged sun-exposed; aSP, aged sun-protected; CholS, cholesterol sulfate; FFA, free fatty acids; GCer, glucosylceramide; PL, phospholipid; SM, sphingomyelin; TEWL, transepidermal water loss; ySE, young sun-exposed; ySP, young sun-protected.*

Complementary information from IR shows that young sun-exposed skin is less ordered than young sun-protected (Figure 22a), and that the broader lipid chain order can be found in aged sun-exposed when compared to young sun-exposed (Figure 22b).

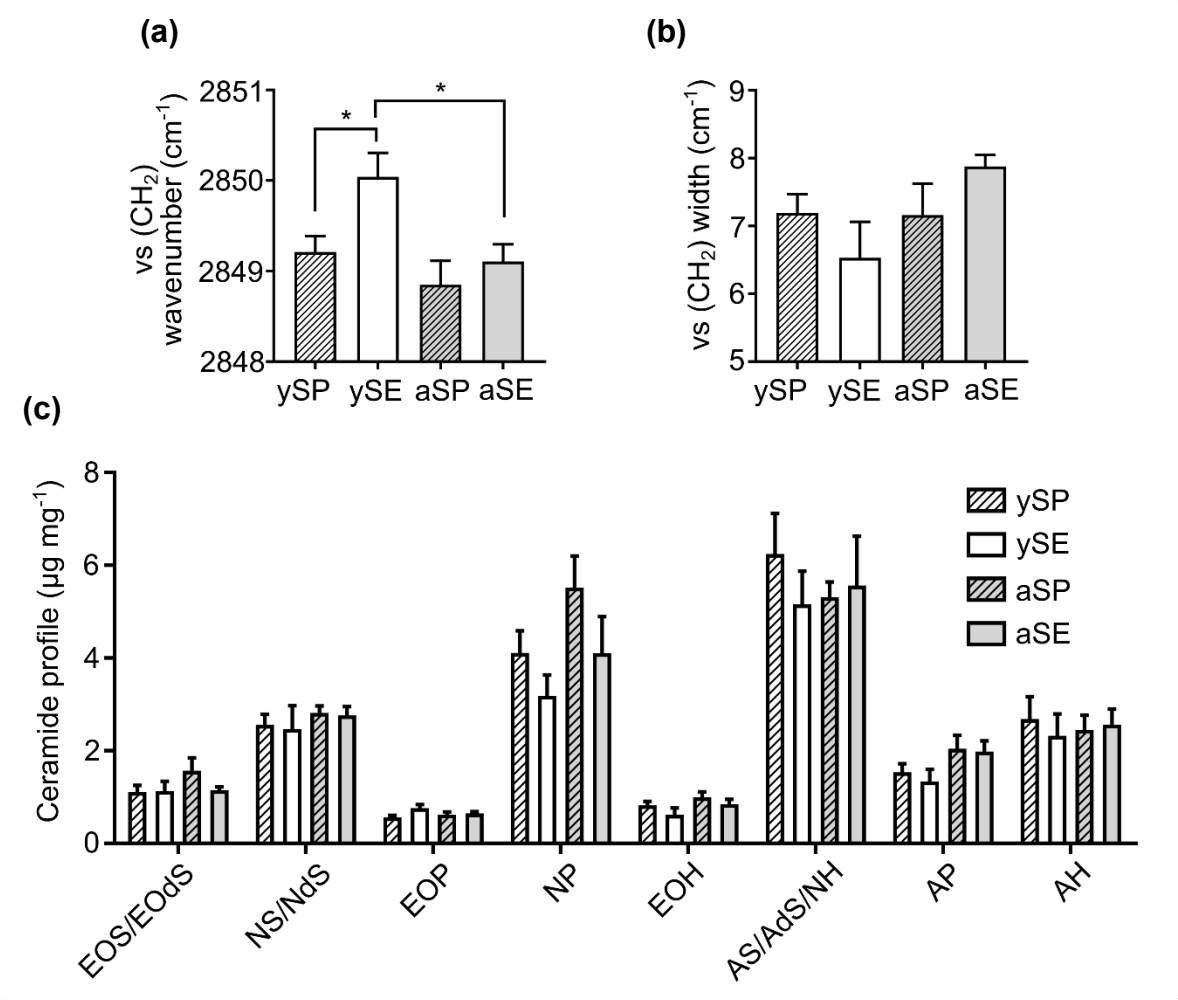

Figure 22: Lipid chain conformation and order, and subclasses of ceramides in the skin of human donors as analyzed by IR and HPTLC/densitometry, respectively*. (a) Methylene symmetric stretching vibrations, which are sensitive to lipid chain conformations: lipids in young sun-exposed epidermis are less ordered than in young sun-protected samples. (b) Complementary information evaluated as the methylene symmetric stretching band width at half height. Broader methylene symmetric stretching peak in aged sun exposed epidermis compared to young sun exposed epidermis means broader distribution of the lipid chain order. (c) No differences in the ceramide profile determined by densitometry after HPTLC separation are present between the young and aged skin. The data are shown as mean ± SEM (young n=12, aged n=8). Statistical significance *P < 0.05. aSE, aged sun-exposed; aSP, aged sun-protected; ySE, young sun-exposed; ySP, young sun-protected.*

10.3.2 Occludin expression is elevated in the human photoaged skin and ZO-2 expression is increased in the sun-exposed and sun-protected aged skin

Claudin-1, occludin and ZO-2 selection was based on a microarray analysis (Supplementary Table 1) and previously described roles of TJ proteins in the skin barrier. Claudin-1-/- mice exerted lethal TEWL after birth (Furuse et al. 2002), the occludin overexpression was present in the recovering epidermal barrier (Malminen et al. 2003; Yamamoto et al. 2008), and the ZO-2 knockdown deteriorated barrier function (Roy et al. 2014). Next, we determined the expression of claudin-1, occludin and ZO-2 on the mRNA as well as protein level. The expression of *CLDN1*/claudin-1 on the mRNA and protein levels was not consistent. Although *CLDN1* mRNA was expressed significantly more in the aged sun-exposed skin in comparison to other groups (Figure 23a), the expression of claudin-1 on the protein level was significantly increased in the young sun-protected area as analyzed by WB (Figure 23b). For a representative WB image showing detection of claudin-1, occludin, ZO-2 and GAPDH in the skin of human donors see Figure 24. A similar trend of the claudin-1 expression on the protein level was acquired by IHC (Figure 23c and 25), although with no statistical significance.

All methods confirmed that *OCLN*/occludin was expressed significantly more in the aged sun-exposed skin when compared to the young skin (Figure 23). Other significant differences were also observed, although trends were inconsistent. *OCLN* gene expression levels were elevated in the aged skin – both sun-protected and sun-exposed in comparison to their young counterparts (Figure 23a). On the protein level, WB indicated the elevated occludin expression in the young and aged sun-exposed skin (Figure 23b), while IHC confirmed the upregulation of occludin only in the aged sun-exposed skin (Figure 23c and 25). These results suggest that the photoaging affects the occludin expression in the skin.

The *TJP2*/ZO-2 expression was elevated on the mRNA as well as protein level in the aged skin of both areas, which was confirmed by all the used methods (Figure 23 and 25). Apparently, the intrinsic aging rather than photoaging affects the ZO-2 expression.

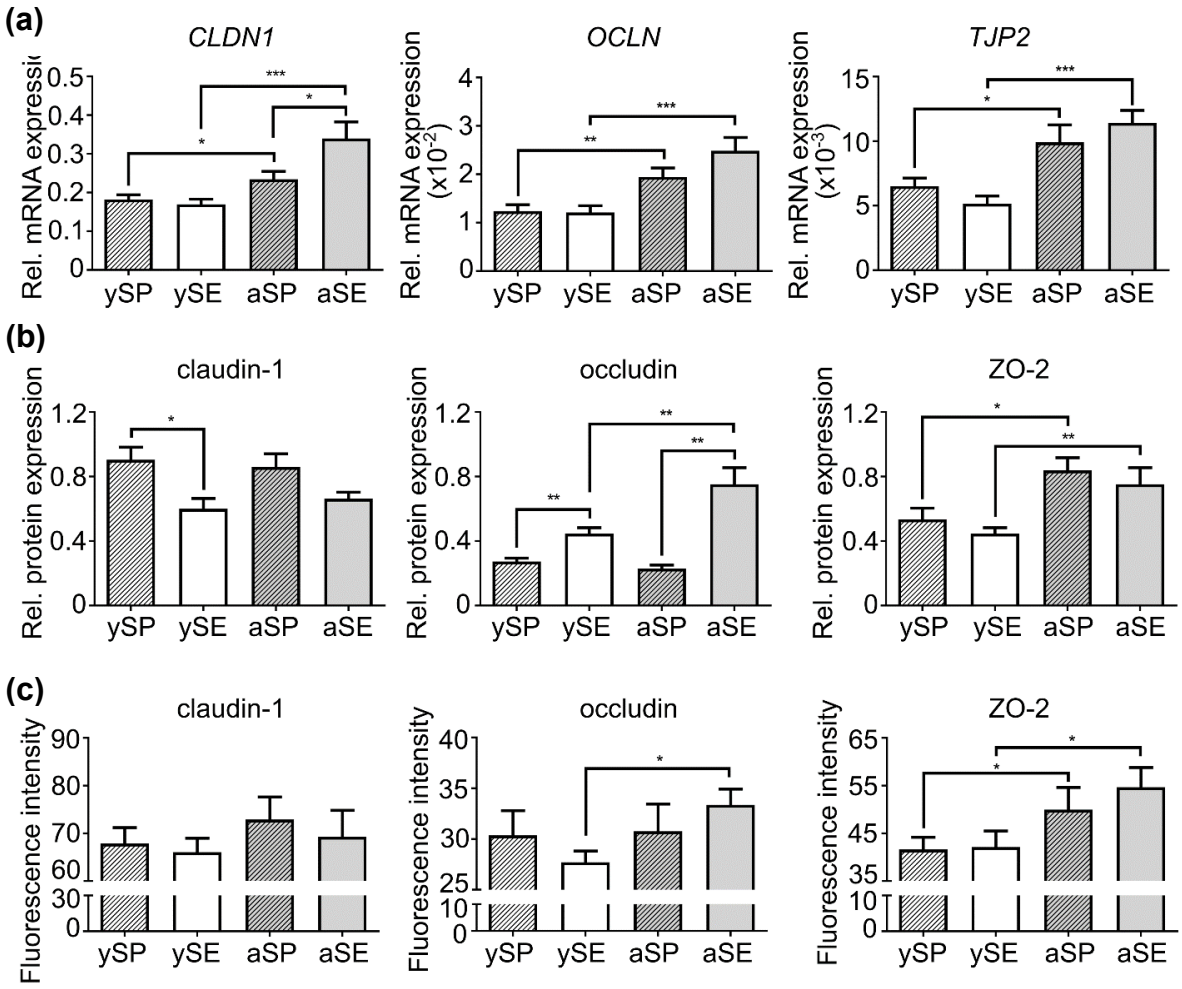

Figure 23: Expression of claudin-1, occludin and ZO-2 in the sun-exposed and sun-protected epidermis of young and aged human forearm skin on the mRNA and protein level. *Samples of human epidermis were acquired by suction blistering from healthy volunteers. (a) Relative expression of CLDN1, OCLN and TJP2 assessed by qRT-PCR. (b) Relative expression of claudin-1, occludin and ZO-2 on the protein level assessed by western blotting. (c) Quantification of fluorescence intensities of claudin-1, occludin and ZO-2 expression from 7.2 µm stacks from histological cross-sections using the Leica Hybrid Detector Photon Counter. Data are shown as mean ± SEM (young n=12, aged n=8), statistical significance *P < 0.05, **P < 0.01, ***P < 0.001.*

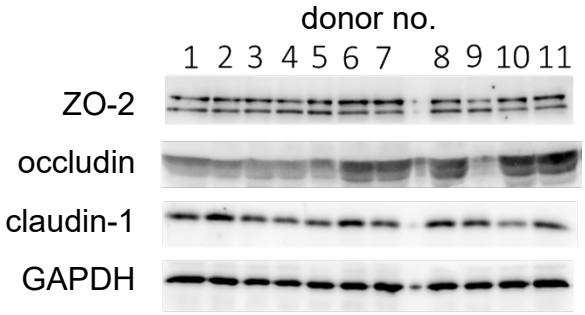

Figure 24: Representative western blotting image of claudin-1, occludin and ZO-2 protein expression *in human epidermis of 11 donors (this image was acquired for representative purpose only).*

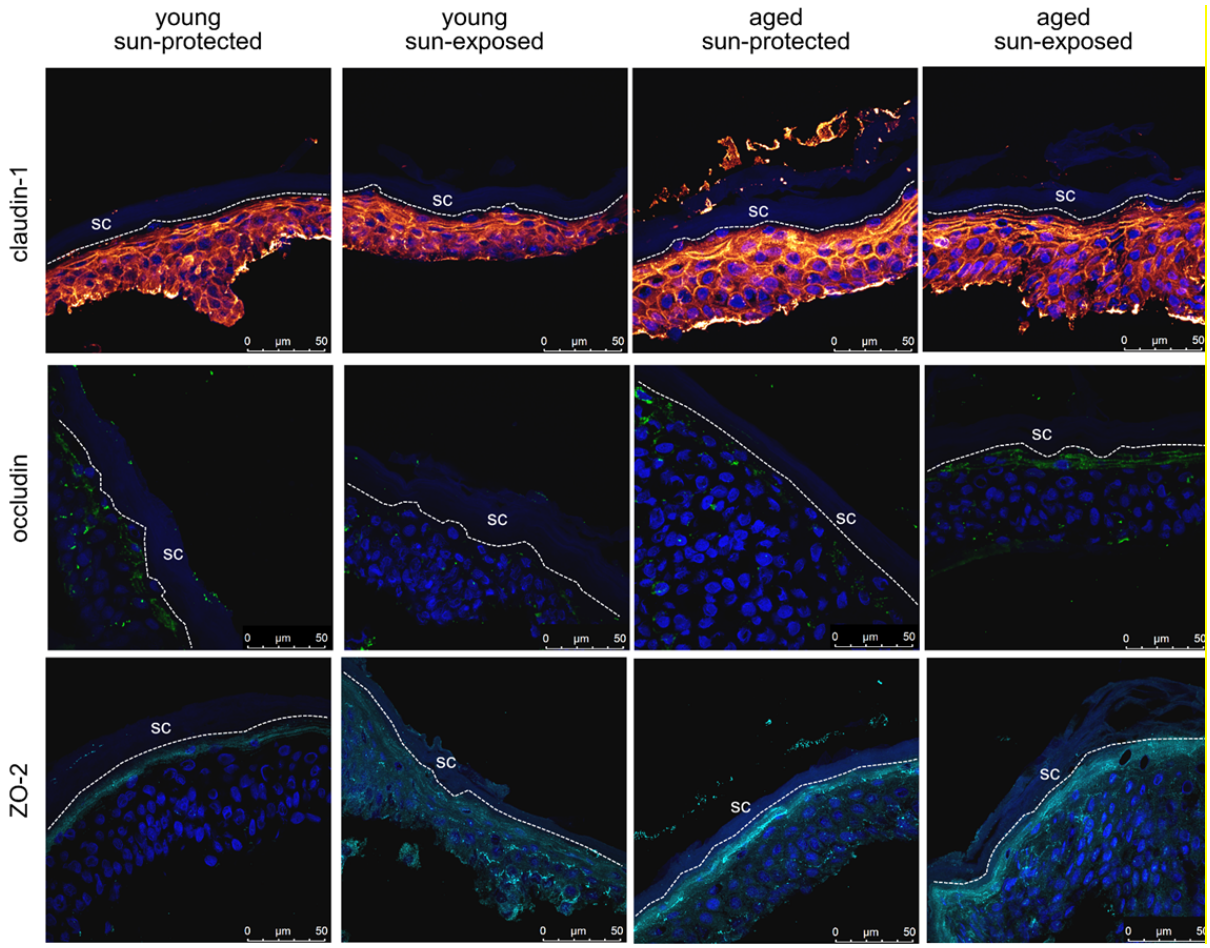

Figure 25: Representative IHC images of claudin-1, occludin and ZO-2 expression in young and aged sun-exposed and sun-protected human forearm skin. *Skin cross-sections were prepared using optimized IHC protocol and visualized with confocal laser scanning microscope. Orange – claudin-1, green – occludin, teal – ZO-2, blue – cell nuclei. Bar=50 µm.*

10.3.3 Occludin overexpression lowers TEWL of *ex vivo* porcine epidermis after delipidation

Since the occludin expression was clearly increased in the photoaged skin where the decreased lipid content was found, we examined the occludin link to the water barrier. To examine whether occludin plays a role in the maintenance of the water barrier in the photoaged skin with decreased lipid content, we used an *ex vivo* porcine epidermis with delipidated SC as the experimental model. The epidermis was previously shown to re-establish the water barrier after an acute damage. TEWL reached the peak in 3 days, started to decline after 5 days being fully restored within 10 days after the damage (Jiang et al. 2007; Kottner et al. 2013a; Malminen et al. 2003). The *ex vivo* porcine epidermis exhibited a similar trend after the delipidation with acetone. TEWL doubled 24 hours after the delipidation and further increased 48 hours after the delipidation. 120 hours after the delipidation, the *ex vivo* porcine epidermis shows partially

recovered TEWL (Figure 26a). To evaluate the potential role of occludin in the re-establishment of the water barrier, we stimulated the occludin expression 24 hours after the delipidation step by a casein-derived peptide NPWDQ, which was shown to be highly specific occludin inducer in epithelial cells in a previous study (Yasumatsu and Tanabe 2010). The stimulation of the occludin expression in the *ex vivo* porcine epidermis was confirmed by qRT-PCR and IHC showing its broader distribution in the epidermis (Figure 26b and 26c). The NPWDQ peptide treatment of the *ex vivo* porcine epidermis resulted in a faster decrease of the TEWL when compared to control. TEWL of the NPWDQ treated model was significantly lower than control model 120 hours after the delipidation (Figure 26a).

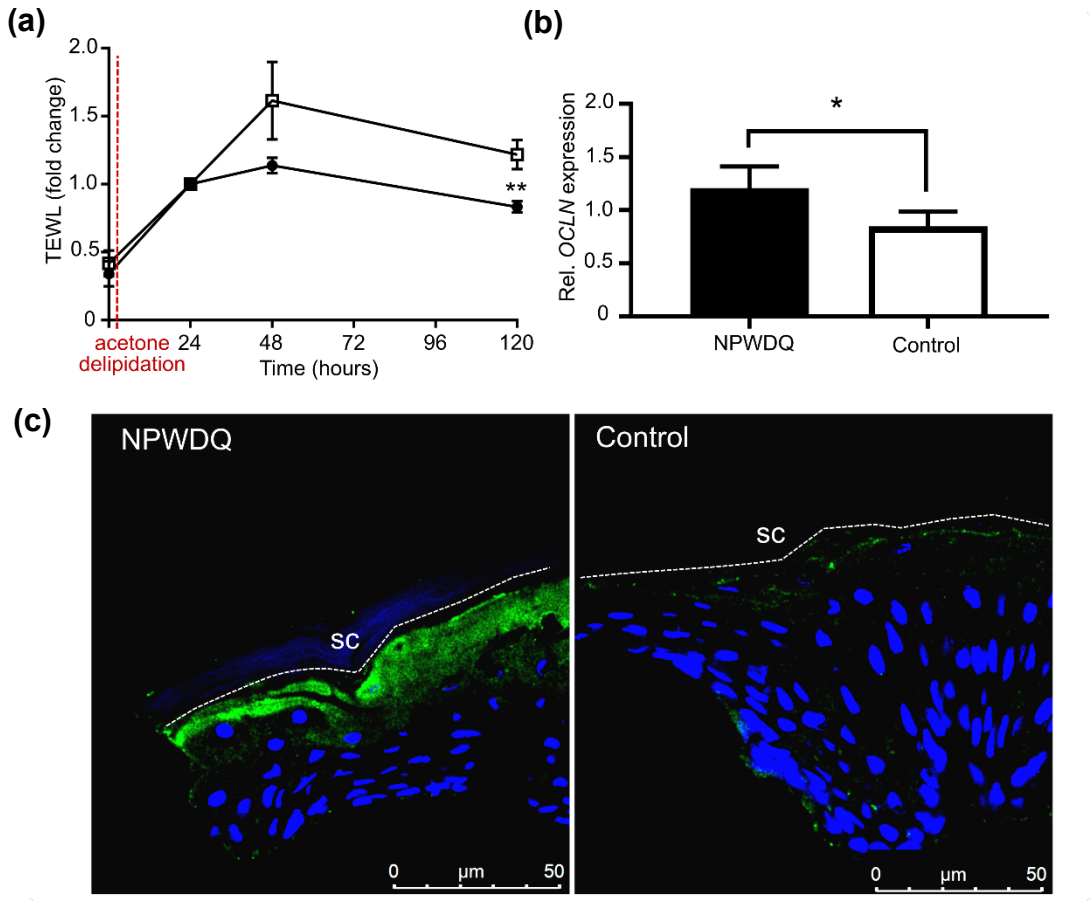

Figure 26: Casein-derived peptide NPWDQ treatment *resulted in occludin overexpression and faster TEWL restoration in ex vivo porcine epidermis after acetone delipidation. Ex vivo porcine epidermis specimens placed in modified Franz diffusion cells were delipidated using acetone and after 24 hours treated with 1.6 µM NPWDQ solution for 96 hours. (a) TEWL was monitored during the experiment using an open-chamber method at following timepoints: prior acetone delipidation (0 hours), and 24, 48 and 120 hours after acetone delipidation. The data are expressed as fold change (TEWL 24 hours after damage=1) and shown as mean ± SEM. (b) Occludin expression in the NPWDQ treated model and control 120 hours after acetone delipidation assessed by qRT-PCR (data shown as mean ± SEM; n=5) and IHC (representative images are shown; n=5; green – occludin, blue – cell nuclei, bar=50 µm). Statistical significance *P < 0.05, **P < 0.001. SC, stratum corneum.*

11 DISCUSSION

The skin is an inhomogeneous organ whose various parameters differ both inter-individually and intra-individually. Therefore, a selection of adequate skin sites is crucial when dealing with skin analysis. SB and TS are promising less-invasive alternatives than punch biopsy, which cause permanent damage. Since both SB and TS, are not widely used for epidermal analysis, method optimization and characterization of the sample acquired was done prior to any other analysis.

Co-extraction with a phenol-based reagent (RNAzol) enables a reliable extraction of both, RNA and proteins from the same sample, and reduces an amount of the sample needed. RNAzol manufacturer's protocol had to be enhanced and used with QIAcube automated extractor to maximize the yield of both proteins and RNA. Addition of chloroform to phenol-based reagent may be useful when extracting RNA only (Reimann et al. 2019), but hampered further protein extraction in our case. For IHC detection only antibodies with experimentally verified functionality were used. Regarding the approach, we preferred frozen specimens with acetone fixation, which provided better outcomes of TJ proteins detection than paraffin embedded specimens with heat antigen retrieval.

Number of studies utilized shotgun lipidomics on various biological samples such as human blood plasma without prior HPLC separation using various approaches (e.g. ESI-QqQ, ESI-QTOF, ESI-Orbitrap, MALDI-TOF). We analyzed lipid profile in porcine epidermis using MALDI-Orbitrap and conventional DHB, CHCA and AA matrixes. Although over 100 m/z were identified with 30 m/z potentially belonging to ceramides, none of the ceramide species were confirmed due to significant mass overlap. As discussed elsewhere, MALDI approach is lacking reproducibility and fact that there is no universal matrix (Hsu 2018).

SB and TS represent different samples to work with; therefore, a different approach is needed. The duration of TS depends on the number of strips used. We also noticed that the duration of the SB sampling varied from individual to individual more than in TS. Panoutsopoulou et al. implied that the duration of SB is too long for a routine usage in the clinical practice as his team reported duration necessary to form a blister 47-85 minutes on the calf, 63-158 minutes on the foot (Panoutsopoulou et al. 2009), 42-129 minutes on distal thigh and 63-193 minutes on distal leg (Panoutsopoulou et al. 2015). Other groups reported 90-120 minutes on upper inner arm (Benfeldt et al. 1999; Leitch et al. 2016). This time is, indeed,

tolerable in research laboratories, though the unpredictability of the time necessary to form a blister is rather inconvenient.

A SB roof is the sole epidermis. Therefore, no special approach is needed. TS generally provides a lesser amount of material which, in addition, is stuck to the glue of the strip hindering whole extraction process. Probably, a certain amount of the material was not detached from a sticky surface of the TS discs. Still, our yield of RNA that was roughly 300 ng from 30 TS discs is more than other groups have reported as their total RNA yield was 0.92 ng using four tape strips on the healthy skin (Wong et al. 2004) and 11 ng using twelve tape strips on the forearm (Wong et al. 2006). Nevertheless, the RNA concentration from the TS samples was too low to perform a reliable qRT-PCR analysis. Therefore, isolated RNA from the TS samples was amplified to yield a sufficient amount of RNA (Fig. 1c). With regard to the protein yield, Clausen et al. reported approximate amount <1 μg (Clausen et al. 2013) and later 10 μg of protein per a D-Squame disc (Clausen et al. 2016), and our protein amount per a TS disc was 1.1 ± 0.13 μg on average. However, our extraction protocol was designed to extract both RNA and proteins in one procedure. During the extraction, the RNAzol® reagent caused swelling of the glue, which might have rendered the extraction of RNA and proteins more difficult. Moreover, Clausen et al. did not clearly state a diameter of the D-Squame discs and a total amount of material sampled by TS, which also might have caused the difference.

Furthermore, representative proteins of different epidermal layers were analyzed by WB and qRT-PCR: filaggrin/*FLG* for the SC, occludin/*OCLN* for the SG, claudin-1/*CLDN1* for all living epidermal cell layers, laminin/*LAMA3* for the stratum basale, and GAPDH/*RPL13A* as the housekeepers.

Although filaggrin present in the TS samples may have been sampled from the SG layer, neither claudin-1 nor occludin, which reside in the SG layer (Yuki et al. 2011), have been detected. Therefore, filaggrin that is present in the lower SC (Nachat et al. 2005) was rather obtained by TS. Upper layers of the SC do not contain filaggrin as showed by other investigators (Egawa et al. 2013). Images by RCM are congruent with our results from qRT-PCR and WB as they indicated that the SG was reached but not obtained by TS. Taken together, our results do not provide any direct evidence of collecting SG cells, rather the opposite.

The question is whether it is possible to detach living layers of the epidermis by TS. Pinkus et al. observed by light microscopy a missing SG layer in a cross-section of the skin that was biopsied after TS with a Scotch tape, but it was not confirmed with a complete certainty (Pinkus

1952). According to the literature, the SG layer starts 15-20 µm below the skin surface (Puig et al. 2012). Since the biological material obtained by TS rapidly decreased with increasing depth of the epidermis, we may anticipate that the SG is hardly obtainable even with larger amounts of tape-strips. Other studies that have used different tape-strips reached the SG using 50-70 tape-strips with a non-linear decrease of obtained material as well (Jacobi et al. 2005; Lademann et al. 2012; Weigmann et al. 1999). As far as we know, no study has ever confirmed a successful yield of a human granular layer by TS up to date. A humid surface and increasing cohesion of the SC layers towards the living epidermis decreases the effectiveness of the TS (Chapman et al. 1991; Weigmann et al. 1999).

Although proteins from all layers of the epidermis were detected in the SB samples, there is one major shortcoming of the SB technique for the epidermal analysis. Early studies characterizing the SB sampling found that the epidermis is detached from the dermis at the interface between the lamina lucida and lamina densa, leaving the lamina densa and its components attached to the dermis. Therefore, SB samples provide incomplete information about the basal membrane of the epidermis. Some of the proteins such as collagen type IV were not present in the epidermis obtained by SB (Oikarinen et al. 1982) and laminin expression was visible on a dermal as well as epidermal side after SB (Saksela et al. 1981). Alongside the qRT-PCR and WB analyses, we were also able to successfully perform IHC and lipid analyses on the same SB samples.

IR spectroscopy of the SB samples showed the presence of highly ordered SC lipids and the co-existence of a very tight orthorhombic chain with slightly looser hexagonal lipid packing, which is consistent with the literature (Boncheva et al. 2008). A simple lipid/protein ratio for comparative purpose between samples could be obtained by a ratio of the intensity of methylene symmetric stretching and Amide I band. IR spectroscopy is non-destructive and enables further sample processing, in our case, the lipid extraction and analysis. HPTLC analysis showed the presence of all barrier lipids in correct proportions (8 ceramide subclasses, free fatty acids, cholesterol and cholesteryl sulfate) and their precursors (sphingomyelins, glucosylceramides and phospholipids (PL)) (Schreiner et al. 2000). Interestingly, decreased PL were observed in the SB samples, which could be caused by their secretion into the blister fluid or their degradation and consequent secretion of degradation products into the blister fluid. PL are precursors for many bioactive lipid mediators involved in the skin inflammation and immunity response (Kendall and Nicolaou 2013). Lysophosphatidic acid had been detected in the blister fluid in higher concentration than in plasma, which suggested that lysophosphatidic acid is

produced in the blister fluid by LPLD-dependent hydrolysis of lysophosphatidylcholine (Mazereeuw-Hautier et al. 2005). Also, similarities between lipid profiles in the blister fluid and epidermis indicated a primarily epidermal origin of the SB fluid (Kendall et al. 2015).

IHC and lipid analyses are performable on the TS samples as well (Camera et al. 2010b; Jungersted et al. 2013; van Smeden et al. 2011a), but reliable results from all the used methods are hardly achievable from a single TS sampling due to lack of material and a highly demanding workup. Indeed, multiple TS can provide enough of material. However, IHC on a single strip provides only limited information in contrast to the typical vertical cross-sections covering the whole epidermis obtained from SB. Therefore, one would have to analyze all the consecutive strips to gain complete information about the whole SC. Moreover, TS discs may not provide optimal optical conditions for microscopy and may cause non-specific binding or auto-fluorescence. For these reasons, we do find a TS sample rather unsuitable for IHC.

Also, it should be noted that both methods cause a certain level of the irritation or damage that triggers respective cellular responses during the procedure. Therefore, some of the molecules such as early immune response markers can be significantly affected even within 60 minutes of either SB or TS sampling procedure. After all, a low PL content was found in our SB samples. This should be taken into a consideration when selecting an application of SB and TS. When all outcomes of the characterization were taken into account, SB was chosen for our further study as the epidermal sampling technique.

The unimpaired water barrier in the aged skin has been an unexplained phenomenon for over years. A comprehensive meta-analysis shows that TEWL remains the same or rather decreases with age. Authors further explained this by a decreased water diffusion coefficient due to the overall reduction of lipids in the aged skin (Kottner et al. 2013b). However, the epidermis has been shown to reduce TEWL even if the SC is completely missing (Celli et al. 2012; Malminen et al. 2003). TJs represent a potential key player as they compensate for the impaired skin barrier function after the acute damage (Svoboda et al. 2016). Identification of TJ proteins induced by the skin photoaging and the evidence of their direct link to the water barrier led to a hypothesis that TJs proteins, especially occludin, might contribute to the maintenance (or even decrease) of TEWL in the photoaged or intrinsically aged skin.

Next part of the research was focused on analysis of the human lipid composition, TEWL rates and TJ proteins expression in the young and aged skin, both the sun-protected and sun-exposed. Selected sun-exposed and sun-protected zones of the aged and young skin were

confirmed to have respective typical structural features (Ganceviciene et al. 2012). Skin barrier analysis confirmed a stable water barrier in both aged skin areas, and revealed the deteriorated lipid content in the photoaged skin but not in the intrinsically aged skin suggesting a detrimental effect of the UV irradiation on the skin barrier lipid content, which is consistent with (Bak et al. 2011). However, no significant changes were detected in the ceramide subclasses. In spite of the generally accepted idea of the aged skin lacking 30% of ceramides, the literature on this matter is inconsistent (Coderch et al. 2003). Some studies do report the decrease of ceramides in the skin barrier as a function of age (Imokawa et al. 1991; Rogers et al. 1996; Schreiner et al. 2000) but this is not supported by other studies (Mutanu Jungersted et al. 2010; De Paepe et al. 2004; Sadowski et al. 2017). Clearly, there are changes in the lipid composition during the skin aging. However, other factors such as gender, site or seasons appear to have an impact on the lipid composition of the SC as well, making the results throughout the literature hardly comparable. Thus, the only trend pronounced almost in all studies is the decrease of the overall SC lipid content.

Further analysis of the skin barrier revealed significant differences in the TJ proteins expression between the young and aged skin. We observed the significant occludin overexpression that was present only in the photoaged skin, where the decreased lipid content was also found. Our results do not reconcile with a recent work, where a decreased expression of occludin was observed in the aged skin and no difference in the occludin expression between sun-exposed and sun-protected skin sites. However, young donors were rather middle aged (range 26-31years). Moreover, the comparison of sun-exposed and sun-protected involved different skin sites, buttock and forearm (Jin et al. 2016). A decreased occludin expression was also detected in squamous cell carcinoma but not in its precursor states such as the chronically sun-exposed skin (Rachow et al. 2013). Occludin as a transmembrane protein contributes to the epidermal barrier function (Furuse et al. 1993). Although its knockdown decreased the transepithelial resistance in cultured cells (Kirschner et al. 2013), no fatal TEWL phenotype was seen in mice lacking occludin. On the other hand, the occludin overexpression was detected in the regenerating human epidermis, which was accompanied with the gradually ameliorating water barrier (Malminen et al. 2003). The occludin expression was also found to be increased 3 days after an exposure to the UVB irradiation which was followed by a skin barrier improvement (Yamamoto et al. 2008). This compensation-like overexpression of occludin was also observed in the developing fetal epidermis (Celli et al. 2012) or infected epidermis (Ohnemus et al. 2008). However, to the best of our knowledge, the direct link of occludin to

the water barrier (TEWL) has never been confirmed. Therefore, we utilized the *ex vivo* porcine epidermal model to address this issue. By using the acetone delipidation and the stimulation of occludin by a casein-derived peptide, NPWDQ, we demonstrated that the occludin overexpression contributes to the restoration of the water barrier in the skin with an impaired lipid barrier, which is a typical feature of the photoaged skin as well. Taken together, these results suggest that occludin is an important molecule in the maintenance of the water barrier of the photoaged skin. The peptide retained its functionality in the epidermis and enhanced the water barrier on the level of TEWL. Previously, the NPWDQ peptide was shown to enhance the barrier in epithelial cells by upregulating the occludin expression (Tanabe 2012).

From other TJ proteins, claudin-1 is the most characterized. Acute UV exposure studies lead to an increase of claudin-1 on the protein level 3 days after the exposure (Yamamoto et al. 2008). Other investigators reported a decrease of claudin-1 in the aged skin. Claudin-1 null mice exhibited fatal TEWL rates (Furuse et al. 2002) and aberrant SC (Sugawara et al. 2013; Yuki et al. 2013). However, our results of the claudin-1 expression were inconsistent since mRNA levels of claudin-1 were increased in the photoaged skin whereas on the protein levels it showed rather a decrease suggesting a post-translational regulation. Therefore, we suggest that claudin-1 probably does not play a significant role in the water barrier maintenance in the photoaged skin.

ZO-2 is a scaffolding protein of TJs whose function is associated with the establishment and fine tuning of TJs (Shin and Margolis 2006). However, information on ZO-2 and its involvement in the epidermal barrier is scarce. Attenuation of ZO-2 along with ZO-1 induced by miRNA-146a and miRNA-106b has been shown to diminish the water barrier (Roy et al. 2014). Our results suggest that the intrinsic aging process rather than photoaging causes the elevation of the ZO-2 expression in the skin. Is the ZO-2 overexpression in the intrinsically aged skin important for a skin barrier integrity? ZO-2 seems to be an interesting target for future studies regarding the skin barrier.

12 CONCLUSION

In summary, we established a methodological basis for dermatological research in the field of the skin barrier and tight junctions in Contipro a.s. Theoretical part is focused on a state-of-the-art of analytic methods and procedures used in dermatological research and thorough review of TJs role in the skin barrier. This brought us before unchallenged hypothesis "Could tight junctions regulate barrier function of the aged skin?"

To answer this hypothesis several methods and models were developed and optimized. Suction blistering has shown itself as a valuable tool for epidermal sampling, being painless, reproducible technique and providing intact epidermal samples at the same time. Although skin represents one of the toughest and most complex organic samples, the protein/RNA co-extraction has been successfully resolved and utilized for further experiments. IHC procedure has been optimized for use with CLSM that provided us with ultra-quality images and reliable quantification of fluorescent signal via a photon counter. A conventional "gold -standard" HPTLC has been used to analyze lipid composition. MS based approach was far too time-consuming as it would require a development of whole new protocol and post-analysis processing of results, which was not an objective of this project. But, MS based analysis of epidermal lipids is one of the potential future directions of this research.

Next part of the project dealt directly with the hypothesis suggesting an important role of TJ in the maintenance of TEWL in the aged skin. Clinical aspect of the protocol has been carefully designed to ensure the safety and well-being of volunteers. Microarray analysis of aged vs young skin shown significant differences in the expression of TJ proteins. Our experiments confirmed unchanged/reduced TEWL in the aged skin and detrimental effect of photoaging on the skin lipid content in our volunteers. Further experiments demonstrated that occludin overexpression was associated with faster recovery of the water barrier in the delipidated porcine epidermis suggesting a role of occludin and TJs in the epidermis with the impaired lipid content which is a typical feature of the photoaged skin as well. Whether the maintenance of the water barrier is mediated directly by occludin creating a physical barrier or indirectly by other mechanisms warrants further studies. Furthermore, modifications of occludin such as phosphorylation or ubiquitination were shown to be essential for the barrier permeability (Murakami et al. 2009).

Despite the common epithelial character of the intestine and epidermal tissues, further studies are needed to confirm the specificity of NPWDQ towards TJs proteins and occludin in

our model and the skin as such. Furthermore, occludin seems to be a promising target for the treatment of the perturbed skin barrier. Other inducers of the occludin overexpression can be tested as well. Apart from occludin, claudin-1 and ZO-2, there are also other TJ proteins worth investigating such as cingulin, claudin-6 or claudin-7 whose expression in aged skin significantly differed from young skin as shown by microarray analysis. However, knowledge of their connection to skin barrier function is rather limited. Also, as mentioned above, MS based analysis of epidermal lipids could help identify potential disturbances in lipid species profile, which conventional HPTLC fail to show.

13 REFERENCES

Abcam. Protocols book [Internet - cited 2020 Jul 28]. p. 1–100 Available from: https://www.abcam.com/protocols/limited-edition-protocols-book

Ackermann K, Lombardi Borgia S, Korting HC, Mewes KR, Schäfer-Korting M. The phenion® full-thickness skin model for percutaneous absorption testing. *Skin Pharmacol. Physiol.* 2010;23(2):105–12

Ahlgrimm-Siess V, Massone C, Koller S, Fink-Puches R, Richtig E, Wolf I, Gerger A, Hofmann-Wellenhof R. In vivo confocal scanning laser microscopy of common naevi with globular, homogeneous and reticular pattern in dermoscopy. *Br. J. Dermatol*. 2008;158(5):1000–7

Alépée N, Bahinski A, Daneshian M, Wever B De, Fritsche E. State-of-the-Art of 3D Cultures (Organs-on-a-Chip) in Safety Testing and Pathophysiology. *ALTEX* 2014;31:441–77

Alexander H, Brown S, Danby S, Flohr C. Research Techniques Made Simple: Transepidermal Water Loss Measurement as a Research Tool. *J. Invest. Dermatol.* 2018;138(11):2295–300

Alguire PC, Mathes BM. Skin biopsy techniques for the internist. *J. Gen. Intern. Med.* 1998;13(1):46–54

Anderson JM, Van Itallie CM, Fanning AS. Setting up a selective barrier at the apical junction complex. *Curr. Opin. Cell Biol*. 2004;16(2):140–5

Bailey J, Thew M, Balls M. An analysis of the use of animal models in predicting human toxicology and drug safety. *Altern Lab Anim*. 2014;42(3):181–99

Bak H, Hong S phil, Jeong SK, Choi EH, Lee SE, Lee SH, Sung-Ku A. Altered epidermal lipid layers induced by long-term exposure to suberythemal-dose ultraviolet. *Int. J. Dermatol.* 2011;50(7):832–7

Benfeldt E, Serup Jø, Menné T. Microdialysis vs. suction blister technique for in vivo sampling of pharmacokinetics in the human dermis. *Acta Derm. Venereol.* 1999;79(5):338–42

Berglund SR, Schwietert CW, Jones AA, Stern RL, Lehmann J, Goldberg Z. Optimized methodology for sequential extraction of RNA and protein from small human skin biopsies. *J. Invest. Dermatol.* 2007;127(2):349–53

Bhattacharya SK. *Lipidomics: Methods and Protocols*. New Jersey: Humana Press; 2017. ISBN: 978-1-4939-6995-1

Bleck O, Abeck D, Ring J, Hoppe U, Vietzke JP, Wolber R, Brandt O, Schreiner V. Two ceramide subfractions detectable in Cer(AS) position by HPTLC in skin surface lipids of non-lesional skin of atopic eczema. *J. Invest. Dermatol*. 1999;113(6):894–900

Bligh EG, Dyer WJ. A rapid Method of total Lipid extraction and purification. *Can. J. Biochem. Physiol.* 1959;37(8):911–7

Bogen SA, Vani K, Sompuram SR. Molecular mechanisms of antigen retrieval : antigen retrieval reverses steric interference caused by formalin-induced cross-links. *Biotech. Histochem.* 2009;84(5):207–15

Boncheva M, Damien F, Normand V. Molecular organization of the lipid matrix in intact Stratum corneum using ATR-FTIR spectroscopy. *Biochim. Biophys. Acta - Biomembr.* 2008;1778(5):1344–55

Bordeaux J, Welsh AW, Agarwal S, Killiam E, Baquero MT, Hanna JA, Anagnostou V, Rimm D. Antibody validation. *Biotechniques.* 2010;48(3):197–209

Borlinghaus RT. MRT letter: High speed scanning has the potential to increase fluorescence yield and to reduce photobleaching. Microsc. Res. Tech. 2006;69(9):689–92

Boyman O, Hefti HP, Conrad C, Nickoloff BJ, Suter M, Nestle FO. Spontaneous Development of Psoriasis in a New Animal Model Shows an Essential Role for Resident T Cells and Tumor Necrosis Factor-α. *J. Exp. Med.* 2004;199(5):731–6

Brandner JM. Pores in the epidermis: Aquaporins and tight junctions. *Int. J. Cosmet. Sci.* 2007;29(6):413–22

Brandner JM. Tight junctions and tight junction proteins in mammalian epidermis. *Eur. J. Pharm. Biopharm.* 2009;72(2):289–94

Brandner JM, Poetzl C, Schmage P, Hauswirth U, Moll I. A (leaky?) barrier: Tight junction proteins in skin diseases. *Drug Discov. Today Dis. Mech*. 2008;5(1):39–45

Branzan AL, Landthaler M, Szeimies RM. In vivo confocal scanning laser microscopy in dermatology. *Lasers Med. Sci*. 2007;22(2):73–82

Breiden B, Sandhoff K. The role of sphingolipid metabolism in cutaneous permeability barrier formation. *Biochim. Biophys. Acta.* 2014;1841(3):441–52

Broccardo CJ, Mahaffey SB, Strand M, Reisdorph NA, Leung DYM. Peeling off the layers: Skin taping and a novel proteomics approach to study atopic dermatitis. *J. Allergy Clin. Immunol.* 2009; 124(5):1113-5.e1-11

Brönneke S, Brückner B, Söhle J, Siegner R, Smuda C, Stäb F, Wenck H, Kolbe L, Grönniger E, Winnefeld M. Genome-wide expression analysis of wounded skin reveals novel genes involved in angiogenesis. *Angiogenesis*. 2015;18(3):361–71

Buesa RJ. Histology without formalin? Ann. Diagn. Pathol. 2008;12(6):387–96

Burr S, Penzer R. Promoting skin health. *Nurs. Stand*. 2005;19(36):57–65

Calzavara-Pinton P, Longo C, Venturini M, Sala R, Pellacani G. Reflectance confocal microscopy for in vivo skin imaging. *Photochem. Photobiol.* 2008;84(6):1421–30

Camera E, Ludovici M, Galante M, Sinagra J-L, Picardo M. Comprehensive analysis of the

major lipid classes in sebum by rapid resolution high-performance liquid chromatography and electrospray mass spectrometry. *J. Lipid Res.* 2010a;51(11):3377–88

Camera E, Ludovici M, Galante M, Sinagra J-L, Picardo M. Comprehensive analysis of the major lipid classes in sebum by rapid resolution high-performance liquid chromatography and electrospray mass spectrometry. J. Lipid Res. 2010b;51(11):3377–88

Celli A, Zhai Y, Jiang YJ, Crumrine D, Elias PM, Feingold KR, Mauro TM. Tight junction properties change during epidermis development. *Exp. Dermatol*. 2012;21(10):798–801

Chao YCE, Nylander-French LA. Determination of Keratin Protein in a Tape-stripped Skin Sample from Jet Fuel Exposed Skin. *Ann. Occup. Hyg.* 2004;48(1):65–73

Chapman SJ, Walsh A, Jackson SM, Friedmann PS. Lipids, proteins and corneocyte adhesion. *Arch. Dermatol. Res*. 1991;283(3):167–73

Chen C, Ridzon DA, Broomer AJ, Zhou Z, Lee DH, Nguyen JT, Barbisin M, Xu NL, Mahuvakar VR, Andersen MR, Lao KQ, Livak KJ, Guegler KJ. Real-time quantification of microRNAs by stem-loop RT-PCR. *Nucleic Acids Res*. 2005;33(20):1–9

Clausen ML, Jungersted JM, Andersen PS, Slotved HC, Krogfelt KA, Agner T. Human β-defensin-2 as a marker for disease severity and skin barrier properties in atopic dermatitis. *Br J Dermatol.* 2013;169(3):587–93

Clausen M-L, Slotved H-C, Krogfelt KA, Agner T. Tape Stripping Technique for Stratum Corneum Protein Analysis. *Sci. Rep.* 2016;6:19918

Coderch L, López O, De La Maza A, Parra JL. Ceramides and skin function. *Am. J. Clin. Dermatol.* 2003;4(2):107–29

Cole RB. *Electrospray and MALDI Mass Spectrometry: Fundamentals, Instrumentation, Practicalities, and Biological Applications - 2nd ed.* New Jersey: John Wiley & Sons, Inc.. 2010 ISBN: 978-0-471-74107-7

Deepak SA, Kottapalli KR, Rakwal R, Oros G, Rangappa KS, Iwahashi H, Masuo Y, Agraval GK. Real-Time PCR: Revolutionizing Detection and Expression Analysis of Genes. *Curr. Genomics*. 2007;8(4):234–51

Delgado-Charro MB. Skin sampling; a challenging but worth taking endeavour. *J. Appl. Bioanal.* 2015;1(4):112–5

Denk W, Strickler JH, Webb WW, Series N, Apr N. Two-Photon Laser Scanning Fluorescence Microscopy. *Sci. New Ser.* 1990;248(4951):73–6

Denning MF. Tightening the epidermal barrier with atypical PKCs. *J. Invest. Dermatol*. 2007;127(4):742–4

Earthslab. Cells and Layers of the Epidermis [Internet - cited 2020 Jul 28]. Available from: https://www.earthslab.com/physiology/cells-layers-epidermis/

Eaton LH, Chularojanamontri L, Ali FR, Theodorakopoulou E, Dearman RJ, Kimber I, Grifiths CEM. Guttate psoriasis is associated with an intermediate phenotype of impaired Langerhans cell migration. *Br. J. Dermatol.* 2014;171(2):409–11

Ebnet K. Junctional adhesion molecules (JAMs): more molecules with dual functions? *J. Cell Sci.* 2004;117(1):19–29

Eckert RL, Yaffe MB, Crish JF, Murthy S, Rorke EA, Welter JF. Involucrin-structure and role in envelope assembly. *J. Invest. Dermatol.* 1993;100(5):613–7

Egawa G, Doi H, Miyachi Y, Kabashima K. Skin tape stripping and cheek swab method for a detection of filaggrin. *J. Dermatol. Sci.* 2013;69(3):263–5

Elias PM. Stratum corneum defensive functions: An integrated view. *J. Invest. Dermatol*. 2005;125(2):183–200

Elias PM, Wakefield JS. Mechanisms of abnormal lamellar body secretion and the dysfunctional skin barrier in patients with atopic dermatitis. *J. Allergy Clin. Immunol.* 2014;134(4):781-791

Epp N, Fürstenberger G, Müller K, De Juanes S, Leitges M, Hausser I, Thieme F, Liebisch G, Schimtz G, Krieg P. 12R-lipoxygenase deficiency disrupts epidermal barrier function. *J. Cell Biol*. 2007;177(1):173–82

Fahy E, Subramaniam S, Brown HA, Glass CK, Merrill AH, Murphy RC, et al. A comprehensive classification system for lipids. J. Lipid Res. 2005;46(5):839–62

Farage MA, Miller KW, Elsner P, Maibach HI. Functional and physiological characteristics of the aging skin. *Aging Clin. Exp. Res*. 2008;20(4):195–200

Farahmand S, Tien L, Hui X, Maibach HI. Measuring transepidermal water loss: A comparative in vivo study of condenser-chamber, unventilated-chamber and open-chamber systems. *Ski. Res. Technol.* 2009;15(4):392–8

Feingold KR. The Role of Epidermal Lipids in Cutaneous Permeability Barrier Homeostasis. *J Lipid Res.* 2007;48:2531–46

Fluhr, Feingold, Elias. Transepidermal water loss reflects permeability barrier status: validation in human and rodent in vivo and ex vivo models. *Exp. Dermatol.* 2006;15(7):483–92

Fourtanier A, Moyal D, Seité S. Sunscreens containing the broad-spectrum UVA absorber, Mexoryl® SX, the cutaneous detrimental effects of UV exposure: A review of clinical study results. *Photodermatol. Photoimmunol. Photomed.* 2008;24(4):164–74

Frade MAC, Aguiar AFCL, Leite MN, Coelho EB, De Moretti Andrade TA, Guedes FA, Leite MN, Passos WR, Coelho EB, Das PK. Prolonged viability of human organotypic skin explant in culture method (hOSEC). *An. Bras. Dermatol.* 2015;90(3):347–50

Freeman WM, Walker SJ, Vrana KE. Quantitative RT-PCR: Pitfalls and potential.

Biotechniques. 1999;26(1):112–25

Fuchs B, Süß R, Nimptsch A, Schiller J. MALDI-TOF-MS directly combined with TLC: A Review of the current state. *Chromatographia*. 2009;69:95

Fuchs B, Süß R, Teuber K, Eibisch M, Schiller J. Lipid analysis by thin-layer chromatography-A review of the current state. *J. Chromatogr. A*. 2011;1218(19):2754–74

Furuse M, Hata M, Furuse K, Yoshida Y, Haratake A, Sugitani Y, et al. Claudin-based tight junctions are crucial for the mammalian epidermal barrier: A lesson from claudin-1-deficient mice. *J. Cell Biol.* 2002;156(6):1099–111

Furuse M, Hirase T, Itoh M, Nagafuchi A, Yonemura S, Tsukita S, et al. Occludin: A novel integral membrane protein localizing at tight junctions. *J. Cell Biol*. 1993;123(6 II):1777–88

Ganceviciene R, Liakou AI, Theodoridis A, Makrantonaki E, Zouboulis CC. Skin anti-aging strategies. *Dermatoendocrinol.* 2012;4(3)

Gardner H, Shearstone JR, Bandaru R, Crowell T, Lynes M, Trojanowska M, Pannu J, Smith E, Jablonska S, Blaszczyk M, Tan FK, Mayes MD. Gene profiling of scleroderma skin reveals robust signatures of disease that are imperfectly reflected in the transcript profiles of explanted fibroblasts. *Arthritis Rheum.* 2006;54(6):1961–73

Gazel A, Ramphal P, Rosdy M, De Wever B, Tornier C, Hosein N, Lee B, Tomic-Canic M, Blumenberg M. Transcriptional Profiling of Epidermal Keratinocytes: Comparison of Genes Expressed in Skin, Cultured Keratinocytes, and Reconstituted Epidermis, Using Large DNA Microarrays. *J. Invest. Dermatol.* 2003;121(6):1459–68

Gilchrest BA. Photoaging. *J. Invest. Dermatol.* 2013;133:E2–6

Ginzinger DG. Gene quantification using real-time quantitative PCR: An emerging technology hits the mainstream. *Exp. Hematol.* 2002;30(6):503–12

González-Mariscal L, Tapia R, Chamorro D. Crosstalk of tight junction components with signaling pathways. *Biochim. Biophys. Acta - Biomembr*. 2008;1778(3):729–56

González S, Gilaberte-Calzada Y. In vivo reflectance-mode confocal microscopy in clinical dermatology and cosmetology. *Int. J. Cosmet. Sci*. 2008;30(1):1–17

Goto-Inoue N, Hayasaka T, Zaima N, Setou M. Imaging mass spectrometry for lipidomics. *Biochim. Biophys. Acta*. 2011;1811(11):961–9

Gupta S, Shroff S, Gupta S. Modified technique of suction blistering for epidermal grafting in vitiligo. *Int. J. Dermatol.* 1999;38(4):306–9

Haftek M, Callejon S, Sandjeu Y, Padois K, Falson F, Pirot F, Portes P, Demarne F, Jannin V. Compartmentalization of the human stratum corneum by persistent tight junction-like structures. *Exp. Dermatol*. 2011;20(8):617–21

Hartung T. Food for thought ... on validation. *ALTEX*. 2007;67–73

Hartung T, Hoffmann S, Stephens M. Mechanistic validation. *ALTEX.* 2013;30(2):119–30

Hatano Y, Terashi H, Arakawa S, Katagiri K. Interleukin-4 suppresses the enhancement of ceramide synthesis and cutaneous permeability barrier functions induced by tumor necrosis factor-α and interferon-γ in human epidermis. *J. Invest. Dermatol.* 2005;124(4):786–92

Helmchen F, Denk W. Deep tissue two-photon microscopy. *Nat. Methods*. 2005;2(12):932–40

Hewitt SM, Baskin DG, Frevert CW, Stahl WL, Rosa-Molinar E. Controls for Immunohistochemistry: The Histochemical Society's Standards of Practice for Validation of Immunohistochemical Assays. *J. Histochem. Cytochem*. 2014;62(10):693–7

Hirose T, Izumi Y, Nagashima Y, Tamai-Nagai Y, Kurihara H, Sakai T, Suzuki Y, Yamanaka T, Suzuki A, Mizuno K, Ohno S. Involvement of ASIP/PAR-3 in the promotion of epithelial tight junction formation. *J Cell Sci.* 2002;115:2485–95

Hofmann-Wellenhof R, Pellacani G, Malvehy J, Soyer HP. *Reflectance Confocal Microscopy for Skin Diseases*. Berlin: Springer; 2012. ISBN: 978-3-642-21996-2

Hofmann-Wellenhof R, Wurm EMT, Ahlgrimm-Siess V, Richtig E, Koller S, Smolle J, Gerger A. Reflectance Confocal Microscopy-State-of-Art and Research Overview. *Semin. Cutan. Med. Surg.* 2009;28(3):172–9

Holčapek M, Jandera P, Zderadička P, Hrubá L. Characterization of triacylglycerol and diacylglycerol composition of plant oils using high-performance liquid chromatography-atmospheric pressure chemical ionization mass spectrometry. *J. Chromatogr. A.* 2003;1010(2):195–215

Holčapek M, Jirásko R, Lísa M. Recent developments in liquid chromatography-mass spectrometry and related techniques. *J. Chromatogr. A*. 2012;1259:3–15

Holčapek M, Liebisch G, Ekroos K. Lipidomic Analysis. *Anal. Chem.* 2018;90(7):4249–57

Horikoshi Y, Suzuki A, Yamanaka T, Sasaki K, Mizuno K, Sawada H, Yonemura S, Ohno S. Interaction between PAR-3 and the aPKC-PAR-6 complex is indispensable for apical domain development of epithelial cells. *J. Cell Sci.* 2009;122(10):1595–606

Hsu F-F. Mass spectrometry based shotgun lipidomics-a critical review from the technical point of view. *Anal. Bioanal. Chem.* 2018;410(25):6387–6409

Huang SN, Minassian H, More JD. Application of immunofluorescent staining on paraffin sections improved by trypsin digestion. *Lab. Investig.* 1976;35(4):383–90

Hung CF, Fang CL, Al-Suwayeh SA, Yang SY, Fang JY. Evaluation of drug and sunscreen permeation via skin irradiated with UVA and UVB: Comparisons of normal skin and chronologically aged skin. *J. Dermatol. Sci.* 2012;68(3):135–48

Hutchins PM, Barkley RM, Murphy RC. Separation of cellular nonpolar neutral lipids by normal-phase chromatography and analysis by electrospray ionization mass spectrometry. *J. Lipid Res.* 2008;49(4):804–13

Ichihashi M, Ueda M, Budiyanto A, Bito T, Oka M, Fukunaga M, Tsuru K, Horikawa T. UV-induced skin damage. *Toxicology*. 2003;189(1–2):21–39

Ikenouchi J, Furuse M, Furuse K, Sasaki H, Tsukita S, Tsukita S. Tricellulin constitutes a novel barrier at tricellular contacts of epithelial cells. *J. Cell Biol.* 2005;171(6):939–45

Imhof RE. In-vivo and in-vitro applications of closed-chamber TEWL measurements. *Intensive Course Dermato-cosmetic Sci*. 2007;1–29

Imhof RE, Berg EP, Chilcott RP, Ciortea LI, Pascut FC, Xiao P. New Instrument for Measuring Water Vapor Flux Density from Arbitrary Surfaces. *Ifscc*. 2002;5(4):297–301

Imhof RE, De Jesus MEP, Xiao P, Ciortea LI, Berg EP. Closed-chamber transepidermal water loss measurement: Microclimate, calibration and performance. *Int. J. Cosmet. Sci*. 2009;31(2):97–118

Imokawa G, Abe A, Jin K, Higaki Y, Kawashima M, Hidano A. Decreased Level of Ceramides in Stratum Corneum of Atopic Dermatitis: An Etiologic Factor in Atopic Dry Skin? *J. Invest. Dermatol.* 1991;96(4):523–6

Indra AK, Leid M. Epidermal permeability barrier measurement in mammalian skin. *Methods Mol. Biol.* 2011;763:73–81

Ishida-Yamamoto A, Simon M, Kishibe M, Miyauchi Y, Takahashi H, Yoshida S, O'Brian TJ, Serre G, Iizuka H. Epidermal lamellar granules transport different cargoes as distinct aggregates. *J. Invest. Dermatol.* 2004;122(5):1137–44

Jacobi U, Weigmann H-J, Ulrich J, Sterry W, Lademann J. Estimation of the relative stratum corneum amount removed by tape stripping. *Ski. Res Technol.* 2005;11(10):91–6

Jadoon S, Karim S, Akram MR, Kalsoom Khan A, Zia MA, Siddiqi AR, Murtaza G. Recent developments in sweat analysis and its applications. *Int. J. Anal. Chem.* 2015;2015

James W, Berger T, Elston D, Neuhaus I. *Andrews' Diseases of the Skin - Clinical Dermatology - 12th ed*. Philadelphia: Elsevier Saunders; 2006. ISBN: 9780323319690

Jansen van Rensburg S, Franken A, Du Plessis JL. Measurement of transepidermal water loss, stratum corneum hydration and skin surface pH in occupational settings: A review. *Ski. Res. Technol.* 2019;25:595–605

Janssens M, van Smeden J, Gooris GS, Bras W, Portale G, Caspers PJ, Vreeken RJ, Hankemeier T, Kezic S, Wolterbeek R, Lavrijsen AP, Bouwstra JA. Increase in short-chain ceramides correlates with an altered lipid organization and decreased barrier function in atopic eczema patients. *J. Lipid Res.* 2012;53(12):2755–66

Jensen EC. The basics of western blotting. *Anat. Rec*. 2012;295:369–71

Jiang SJ, Chu AW, Lu ZF, Pan MH, Che DF, Zhou XJ. Ultraviolet B-induced alterations of the skin barrier and epidermal calcium gradient. *Exp. Dermatol*. 2007;16(12):985–92

Jin SP, Han SB, Kim YK, Park EE, Doh EJ, Kim KH, Lee DH, Chung JH. Changes in tight junction protein expression in intrinsic aging and photoaging in human skin in vivo. *J. Dermatol. Sci.* 2016;84:99–101

Jones PH, Bishop LA, Watt FM. Functional significance of CD9 association with beta 1 integrins in human epidermal keratinocytes. *Cell Adhes. Commun.* 1996;4(4–5):297–305

Jonkman J, Brown CM. Any way you slice it—A comparison of confocal microscopy techniques. *J. Biomol. Tech*. 2015;26(2):54–65

Jungersted JM, Bomholt J, Bajraktari N, Hansen JS, Klærke DA, Pedersen PA, Hedfalk K, Nielsen KH, Agner T, Hélix-Nielsen C. In vivo studies of aquaporins 3 and 10 in human stratum corneum. *Arch. Dermatol. Res*. 2013;305(8):699–704

Jungersted JM, Scheer H, Mempel M, Baurecht H, Cifuentes L, Høgh JK, Hellgren LI, Jemec GBE, Agner T, Weidinger S. Stratum corneum lipids, skin barrier function and filaggrin mutations in patients with atopic eczema. *Allergy.* 2010;65(7):911–8

Kalinin AE, Kajava A V., Steinert PM. Epithelial barrier function: Assembly and structural features of the cornified cell envelope. *BioEssays.* 2002;24(9):789–800

Kammeyer A, Luiten RM. Oxidation events and skin aging. *Ageing Res. Rev*. 2015;21:16–29

Kanitakis J. Anatomy , histology and immunohistochemistry of normal human skin. *Eur. J. Dermatology.* 2002;12(4):5–8

Kap M, Smedts F, Oosterhuis W, Winther R, Christensen N, Reischauer B, Viertler C, Groelz D, Becker KF, Zatloukal K, Langer R, Slotta-Huspenina J, Bodo K, de Jong B, Oelmuller U, Riegman P . Histological assessment of paxgene tissue fixation and stabilization reagents. *PLoS One*. 2011;6(11):e27704

Kebarle P, Verkerk UH. On the Mechanism of Electrospray Ionization Mass Spectrometry (ESIMS). In: Cole RB (ed.). *Electrospray and MALDI Mass Spectrometry: Fundamentals, Instrumentation, Practicalities, and Biological Applications - 2nd ed*. New Jersey: John Wiley & Sons, Inc.. 2010; p. 1-48. ISBN: 978-0-471-74107-7

Keermann M, Kõks S, Reimann E, Prans E, Abram K, Kingo K. Transcriptional landscape of psoriasis identifies the involvement of IL36 and IL36RN. *BMC Genomics.* 2015;16(1):1–11

Kendall AC, Nicolaou A. Bioactive lipid mediators in skin inflammation and immunity. *Prog. Lipid Res.* 2013;52(1):141–64

Kendall AC, Pilkington SM, Massey K a, Sassano G, Rhodes LE, Nicolaou A. Distribution of Bioactive Lipid Mediators in Human Skin. *J. Invest. Dermatol.* 2015;135(6):1510–20

Kim YH, Woodley DT, Wynn KC, Giomi W, Bauer EA. Recessive dystrophic epidermolysis bullosa phenotype is preserved in xenografts using scid mice: Development of an experimental in vivo model. *J. Invest. Dermatol.* 1992;98(2):191–7

Kindt R, Jorge L, Dumont E, Couturon P, David F, Sandra P, Sandra K. Profiling and Characterizing Skin Ceramides Using Reversed-Phase Liquid Chromatography − Quadrupole Time-of-Flight Mass Spectrometry. *Anal Chem*. 2012;84:403–11

Kirschner N, Rosenthal R, Furuse M, Moll I, Fromm M, Brandner JM. Contribution of Tight Junction Proteins to Ion , Macromolecule , and Water Barrier in Keratinocytes. *J. Invest. Dermatol.* 2013;133(5):1161–9

Klopfleisch R, von Deetzen M, Weiss AT, Weigner J, Weigner F, Plendl J, Gruber AD. Weigners fixative: an alternative to formalin fixation for histology with improved preservation of nucleic acids. *Vet. Pathol.* 2012;50(1):191–9

Knochenmuss R. MALDI Ionization Mechanisms: An Overview. In: Cole RB (ed.). *Electrospray and MALDI Mass Spectrometry: Fundamentals, Instrumentation, Practicalities, and Biological Applications - 2nd ed.* New Jersey: John Wiley & Sons, Inc.. 2010;147–83 ISBN: 978-0-471-74107-7

Koch S, Stappenbeck N, Cornelissen CG, Flanagan TC, Mela P, Sachweh J, et al. Tissue engineering: Selecting the optimal fixative for immunohistochemistry. *Tissue Eng. - Part C Methods*. 2012;18(12):976–83

Köfeler HC, Fauland A, Rechberger GN, Trötzmüller M. Mass spectrometry based lipidomics: An overview of technological platforms. *Metabolites*. 2012;2(1):19–38

Kohl E, Steinbauer J, Landthaler M, Szeimies RM. Skin ageing. *J. Eur. Acad. Dermatology Venereol.* 2011;25(8):873–84

Kolarsick PAJ, Kolarsick MA, Goodwin C. Anatomy and Physiology of the Skin. *J. Dermatol. Nurses. Assoc.* 2011;3(4):203–13

Kottner J, Hillmann K, Fimmel S, Seité S, Blume-Peytavi U. Characterisation of epidermal regeneration in vivo: a 60-day follow-up study. *J. Wound Care*. 2013a;22(8):395–400

Kottner J, Lichterfeld A, Blume-Peytavi U. Transepidermal water loss in young and aged healthy humans: A systematic review and meta-analysis. *Arch. Dermatol. Res*. 2013b;305(4):315–23

Kováčik A, Opálka L, Šilarová M, Roh J, Vávrová K. Synthesis of 6-hydroxyceramide using ruthenium-catalyzed hydrosilylation–protodesilylation. Unexpected formation of a long periodicity lamellar phase in skin lipid membranes. *RSC Adv*. 2016;6(77):73343–50

Krause G, Winkler L, Mueller SL, Haseloff RF, Piontek J, Blasig IE. Structure and function of claudins. *Biochim. Biophys. Acta - Biomembr.* 2008;1778(3):631–45

Kubo A, Nagao K, Yokouchi M, Sasaki H, Amagai M. External antigen uptake by Langerhans

cells with reorganization of epidermal tight junction barriers. *J. Exp. Med.* 2009;206(13):2937–46

Kurien BT, Scofield RH. A brief review of other notable protein detection methods on blots. *Methods Mol Biol.* 2009; 536:557-71

Laboureur L, Ollero M, Touboul D. Lipidomics by supercritical fluid chromatography. *Int. J. Mol. Sci.* 2015;16(6):13868–84

Lademann J, Ilgevicius a, Zurbau O, Liess HD, Schanzer S, Weigmann HJ, Antoniou C, von Pelchrzim R, Sterry W. Penetration studies of topically applied substances: Optical determination of the amount of stratum corneum removed by tape stripping. *J. Biomed. Opt.* 2012;11(5):054026

Lam SM, Shui G. Lipidomics as a Principal Tool for Advancing Biomedical Research. *J. Genet. Genomics*. 2013;40(8):375–90

Langbein L, Grund C, Kuhn C, Praetzel S, Kartenbeck J, Brandner JM, Moll I, Franke WW. Tight junctions and compositionally related junctional structures in mammalian stratified epithelia and cell cultures derives therefrom. *Eur. J. Cell Biol*. 2002;81(8):419–35

Langbein L, Pape UF, Grund C, Kuhn C, Praetzel S, Moll I, Moll R, Frank WW. Tight junction-related structures in the absence of a lumen: Occludin, claudins and tight junction plaque proteins in densely packed cell formations of stratified epithelia and squamous cell carcinomas. *Eur. J. Cell Biol.* 2003;82(8):385–400

Laudanska H, Reduta T, Szmitkowska D. Evaluation of skin barrier function in allergic contact dermatitis and atopic dermatitis using method of the continuous TEWL measurement. *Rocz Akad Med Bialymst.* 2003;48:123–7

Lebonvallet N, Pennec JP, Le Gall-Ianotto C, Chéret J, Jeanmaire C, Carré JL, Pauly G, Misery L. Activation of primary sensory neurons by the topical application of capsaicin on the epidermis of a re-innervated organotypic human skin model. *Exp. Dermatol.* 2014;23(1):73–5

Leboulanger B, Guy RH, Delgado-Charro MB. Reverse iontophoresis for non-invasive transdermal monitoring. *Physiol. Meas.* 2004;25(3)R35-50

Leica. Leica HyD for Confocal Imaging [Internet - cited 2020 Jul 28]. pp.1-24 Available from: https://downloads.leica-microsystems.com/Leica%20TCS%20SP5%20II/Brochures/Leica%20HyD-Brochure_EN.pdf

Leitch CS, Natafji E, Yu C, Abdul-Ghaffar S, Madarasingha N, Venables ZC, Chu R, Fitch PM, Muinonen-Martin AJ, Campbell LE, McLean WHI, Schwarze J, Howie SEM, Weller RB. Filaggrin-null mutations are associated with increased maturation markers on Langerhans cells. *J. Allergy Clin. Immunol.* 2016;138(2):482-490.e7

Levin J, Maibach HI. The correlation between transepidermal water loss and percutaneous absorption: an overview. J. *Control. Release.* 2005;103:291–9

Levine A, Markowitz O. In Vivo Reflectance Confocal Microscopy. *Cutis.* 2017;99:399–402

Levine A, Markowitz O. Introduction to reflectance confocal microscopy and its use in clinical practice. *JAAD Case Reports.* 2018;4(10):1014–23

Li W, Sandhoff R, Kono M, Zerfas P, Hoffmann V, Ding BCH, Proia RL, Deng CX. Depletion of ceramides with very long chain fatty acids causes defective skin permeability barrier function, and neonatal lethality in ELOVL4 deficient mice. *Int. J. Biol. Sci.* 2007;3(2):120–8

Lin LL, Prow TW, Raphael AP, Harrold III RL, Primiero CA, Ansaldo AB, et al. Microbiopsy engineered for minimally invasive and suture-free sub-millimetre skin sampling. *F1000Research*. 2013;2:120

Lísa M, Holčapek M. Triacylglycerols profiling in plant oils important in food industry, dietetics and cosmetics using high-performance liquid chromatography-atmospheric pressure chemical ionization mass spectrometry. *J. Chromatogr. A*. 2008;1198–1199(1–2):115–30

Livak KJ, Schmittgen TD. Analysis of Relative Gene Expression Data Using Real-Time Quantitative PCR and the 2−ΔΔCT Method. *Methods*. 2001;25(4):402–8

De Luca C, Valacchi G. Surface lipids as multifunctional mediators of skin responses to environmental stimuli. *Mediators Inflamm*. 2010;2010

Luebberding S, Krueger N, Kerscher M. Skin physiology in men and women: In vivo evaluation of 300 people including TEWL, SC hydration, sebum content and skin surface pH. *Int. J. Cosmet. Sci*. 2013a;35(5):477–83

Luebberding S, Krueger N, Kerscher M. Age-related changes in skin barrier function - Quantitative evaluation of 150 female subjects. *Int. J. Cosmet. Sci.* 2013b;35(2):183–90

Macdonald N, Cumberbatch M, Singh M, Moggs JG, Orphanides G, Dearman RJ, Griffiths CEM, Kimber I. Proteomic analysis of suction blister fluid isolated from human skin. *Clin. Exp. Dermatol*. 2006;31(3):445–8

MacPhee DJ. Methodological considerations for improving Western blot analysis. *J. Pharmacol. Toxicol. Methods.* 2010;61(2):171–7

Madison KC. Barrier Function of the Skin: ‘‘La Raison d’Etre" of the Epidermis. *J. Invest. Dermatol.* 2003;121(2):231–41

Mahmood T, Yang PC. Western blot: Technique, theory, and trouble shooting. *N. Am. J. Med. Sci.* 2012;4(9):429–34

Mallbris L, Granath F, Hamsten A, Ståhle M. Psoriasis is associated with lipid abnormalities at the onset of skin disease. *J. Am. Acad. Dermatol.* 2006;54(4):614–21

Malminen M, Koivukangas V, Peltonen J, Karvonen SL, Oikarinen A, Peltonen S. Immunohistological distribution of the tight junction components ZO-1 and occludin in regenerating human epidermis. *Br. J. Dermatol.* 2003;149(2):255–60

Matter K, Aijaz S, Tsapara A, Balda MS. Mammalian tight junctions in the regulation of epithelial differentiation and proliferation. *Curr. Opin. Cell Biol*. 2005;17:453–8

Mazereeuw-Hautier J, Gres S, Fanguin M, Cariven C, Fauvel J, Perret B, Chap H, Salles JP, Saulnier-Blache JB. Production of lysophosphatidic acid in blister fluid: Involvement of a lysophospholipase D activity. *J. Invest. Dermatol*. 2005;125(3):421–7

McLafferty E, Hendry C, Farley A. The integumentary system: anatomy, physiology and function of skin. *Nurs. Stand.* 2012;27(3):35–42

Motta S, Monti M, Sesana S, Caputo R, Carelli S, Ghidoni R. Ceramide composition of the psoriatic scale. *Biochim Biophys Acta.* 1993;1182(2):147–51

Murakami T, Felinski EA, Antonetti DA. Occludin phosphorylation and ubiquitination regulate tight junction trafficking and vascular endothelial growth factor-induced permeability. *J. Biol. Chem*. 2009;284(31):21036–46

Mutanu Jungersted J, Hellgren LI, Høgh JK, Drachmann T, Jemec GBE, Agner T. Ceramides and barrier function in healthy skin. *Acta Derm. Venereol*. 2010;90(4):350–3

Nachat R, Méchin M-C, Takahara H, Chavanas S, Charveron M, Guy S, et al. Peptidylarginine Deiminase Isoforms 1–3 Are Expressed in the Epidermis and Involved in the Deimination of K1 and Filaggrin. *J. Invest. Dermatol.* 2005;124:384–93

Nagy K, Bongiorno D, Avellone G, Agozzino P, Ceraulo L, Vékey K. High performance liquid chromatography-mass spectrometry based chemometric characterization of olive oils. *J. Chromatogr. A*. 2005;1078(1–2):90–7

Nagy K, Jakab A, Fekete J, Vékey K. An HPLC-MS Approach for Analysis of Very Long Chain Fatty Acids and Other Apolar Compounds on Octadecyl-Silica Phase Using Partly Miscible Solvents. *Anal. Chem*. 2004;76(7):1935–41

Nakano K, Kiyokane K, Benvenuto-Andrade C, González S. Real-time reflectance confocal microscopy, a noninvasive tool for in vivo quantitative evaluation of comedolysis in the rhino mouse model. *Skin Pharmacol. Physiol*. 2006;20(1):29–36

Natsuga K. Epidermal barriers. *Cold Spring Harb. Perspect. Med.* 2014;4(4)

Netzlaff F, Lehr CM, Wertz PW, Schaefer UF. The human epidermis models EpiSkin®, SkinEthic® and EpiDerm®: An evaluation of morphology and their suitability for testing phototoxicity, irritancy, corrosivity, and substance transport. *Eur. J. Pharm. Biopharm*. 2005;60(2):167–78

Ng KW, Lau WM. Skin Deep: The Basics of Human Skin Structure and Drug Penetration. In: Dragicevic N., Maibach H. (eds) *Percutaneous Penetration Enhancers Chemical Methods in Penetration Enhancement.* Berlin: Springer, 2015;pp.3–11. ISBN: Print ISBN: 978-3-662-45012-3

Ninfa A, Ballou D, Benore M. *Fundamental laboratory approaches for biochemistry and*

biotechnology -2nd ed. Chichester: John Wiley and Sons Ltd; 2009. ISBN: 978-0-470-08766-4

Nischal U, Nischal K, Khopkar U. Techniques of skin biopsy and practical considerations. *J. Cutan. Aesthet. Surg.* 2008;1(2):107

Nithya S, Radhika T, Jeddy N. Loricrin - an overview. *J. Oral Maxillofac. Pathol.* 2015;19(1):64

Nosbaum A, Prevel N, Truong H-A, Mehta P, Ettinger M, Scharschmidt TC, Ali NH, Pauli ML, Abbas AK, Rosenblum MD. Cutting Edge: Regulatory T Cells Facilitate Cutaneous Wound Healing. *J. Immunol.* 2016;196(5):2010–4

Nuutinen J, Alanen E, Autio P, Lahtinen MR, Harvima I, Lahtinen T. A closed unventilated chamber for the measurement of transepidermal water loss. *Ski. Res. Technol.* 2003;9(2):85–9

O'Leary TJ, Fowler CB, Evers DL, Mason JT. Protein fixation and antigen retrieval: Chemical studies Protein fixation. *Biotech. Histochem*. 2009;84(5):217–21

O'Neill CA, Garrod D. Tight junction proteins and the epidermis. *Exp. Dermatol*. 2011;20(2):88–91

OECD. Test No. 428: Skin Absorption: In Vitro Method. O*ECD Guideline for the Testing of Chemicals, Section 4.*. 2004:1–8 [Internet - cited 2020 Jul 28] Available from: https://www.oecd-ilibrary.org/environment/test-no-428-skin-absorption-in-vitro-method_9789264071087-en

Oh JW, Hsi TC, Fernando C, Ramos R, Plikus M V. Organotypic skin culture. *J. Invest. Dermatol.* 2013;133(11)

Ohnemus U, Kohrmeyer K, Houdek P, Rohde H, Wladykowski E, Vidal S, Horstkotte MA, Aepfelbacher M, Kirschner N, Behne MJ, Moll I, Brandner JM. Regulation of Epidermal Tight-Junctions (TJ) during Infection with Exfoliative Toxin-Negative Staphylococcus Strains. *J. Invest. Dermatol.* 2008;128(4):906–16

Oikarinen A, Savolainen ER, Tryggvason K, Foidart JM, Kiistala U. Basement membrane components and galactosylhydroxylysyl glucosyltransferase in suction blisters of human skin. *Br. J. Dermatol.* 1982;106(3):257–66

Opálka L, Kováčik A, Sochorová M, Roh J, Kuneš J, Lenčo J, Vávrová K. Scalable Synthesis of Human Ultralong Chain Ceramides. *Org. Lett.* 2015;17(21):5456–9

De Paepe K, Houben E, Adam R, Wiessemann F, Rogiers V. Validation of the VapoMeter, a closed unventilated chamber system to assess transepidermal water loss vs. the open chamber Tewameter®. *Ski. Res. Technol.* 2005;11(1):61–9

De Paepe K, Weerheim A, Houben E, Roseeuw D, Ponec M, Rogiers V. Analysis of Epidermal Lipids of the Healthy Human Skin: Factors Affecting the Design of a Control Population. *Skin Pharmacol. Physiol.* 2004;17(1):23–30

Panoutsopoulou IG, Luciano CA, Wendelschafer-Crabb G, Hodges JS, Kennedy WR. Epidermal innervation in healthy children and adolescents. *Muscle and Nerve.* 2015;51(3):378–84

Panoutsopoulou IG, Wendelschafer-Crabb G, Hodges JS, Kennedy WR. Skin blister and skin biopsy to quantify epidermal nerves: A comparative study. *Neurology*. 2009;72(14):1205–10

Park GH, Chang SE, Bang S, Won KH, Won CH, Lee MW, Choi JH, Moon KC. Usefulness of skin explants for histologic analysis after fractional photothermolysis. *Ann. Dermatol.* 2015;27(3):283–90

Park J, Pande P, Shrestha S, Clubb F, Applegate BE, Jo JA. Biochemical characterization of atherosclerotic plaques by endogenous multispectral fluorescence lifetime imaging microscopy. *Atherosclerosis.* 2012;220(2):394–401

Patterson GH. Photoactivation and imaging of photoactivatable fluorescent proteins. *Curr. Protoc. Cell Biol.* 2008;38:21.6.1-21.6.10

Peltonen S, Riehokainen J, Pummi K, Peltonen J. Tight junction components occludin, ZO-1, and claudin-1, -4 and -5 in active and healing psoriasis. *Br. J. Dermatol.* 2007;156(3):466–72

Phillips PL, Yang Q, Schultz GS. The effect of negative pressure wound therapy with periodic instillation using antimicrobial solutions on Pseudomonas aeruginosa biofilm on porcine skin explants. *Int. Wound J.* 2013;10(S1):48–55

Pillai S, Oresajo C, Hayward J. Ultraviolet radiation and skin aging: Roles of reactive oxygen species, inflammation and protease activation, and strategies for prevention of inflammation-induced matrix degradation - A review. *Int. J. Cosmet. Sci.* 2005;27(1):17–34

Pinkus H. Examination of the Epidermis By the Strip Method II. Biometric Data on Regeneration of the Human Epidermis. *J. Invest. Dermatol.* 1952;19:431–47

Pinnagoda J, Tupkek RA, Agner T, Serup J. Guidelines for transepidermal water loss (TEWL) measurement: A Report from the Standardization Group of the European Society of Contact Dermatitis. *Contact Dermatitis.* 1990;22(3):164–78

Polak J, Van Noorden S. *Introduction to Immunocytochemistry. 3rd ed.* Oxford: Bios Scientific Publishers Ltd; 2003. ISBN: 1 85996 208 4

Ponec M, Boelsma E, Gibbs S, Mommaas M. Characterization of reconstructed skin models. *Skin Pharmacol. Appl. Skin Physiol*. 2002;15:4–17

Ponec M, Gibbs S, Pilgram G, Boelsma E, Koerten H, Bouwstra J, et al. Barrier function in reconstructed epidermis and its resemblance to native human skin. *Skin Pharmacol. Appl. Skin Physiol.* 2001;14:63–71

Ponec M, Weerheim A, Lankhorst P, Wertz P. New acylceramide in native and reconstructed epidermis. *J. Invest. Dermatol.* 2003;120(4):581–8

Pouillot A, Dayan N, Polla AS, Polla LL, Polla BS. The stratum corneum: A double paradox. *J. Cosmet. Dermatol*. 2008;7(2):143–8

Proksch E, Brandner JM, Jensen JM. The skin: An indispensable barrier. *Exp. Dermatol*. 2008;17(12):1063–72

Puig S, Carrera C, Salerni G, Rocha-Portela J. Epidermis, dermis and epidermal appendages. In: Hofmann-Wellenhof R, Pellacani G, Malvehy J, Soyer HP. *Reflectance Confocal Microscopy for Skin Diseases*. Berlin: Springer; 2012. p. 21–31; ISBN: 978-3-642-21996-2.

Pummi K, Malminen M, Aho H, Karvonen SL, Peltonen J, Peltonen S. Epidermal tight junctions: ZO-1 and occludin are expressed in mature, developing, and affected skin and in vitro differentiating keratinocytes. *J. Invest. Dermatol.* 2001;117(5):1050–8

Rabionet M, Gorgas K, Sandhoff R. Ceramide synthesis in the epidermis. *Biochim. Biophys. Acta*. 2014;1841(3):422–34

Rachow S, Zorn-Kruppa M, Ohnemus U, Kirschner N, Vidal-y-Sy S, von den Driesch P, Börnen C, Eberle J, Mildner M, Vettorazzi E, Rosenthal R, Moll I, Brandner JM. Occludin Is Involved in Adhesion, Apoptosis, Differentiation and Ca^{2+}-Homeostasis of Human Keratinocytes: Implications for Tumorigenesis. *PLoS One*. 2013;8(2)

Radner FPW, Fischer J. The important role of epidermal triacylglycerol metabolism for maintenance of the skin permeability barrier function. *Biochim. Biophys. Acta*. 2014;1841(3):409–15

Rainville PD, Stumpf CL, Shockcor JP, Plumb RS, Nicholson JK. Novel application of reversed-phase UPLC-oaTOF-MS for lipid analysis in complex biological mixtures: A new tool for lipidomics. *J. Proteome Res.* 2007;6(2):552–8

Rajadhyaksha M, Marghoob A, Rossi A, Halpern AC, Nehal KS. Reflectance confocal microscopy of skin in vivo: From bench to bedside. *Lasers Surg. Med.* 2017;49(1):7–19

Ramos-Vara JA. Technical Aspects of Immunohistochemistry. *Vet. Pathol.* 2005;42(1):405–26

Ramos-Vara JA, Miller MA. When Tissue Antigens and Antibodies Get Along: Revisiting the Technical Aspects of Immunohistochemistry-The Red, Brown, and Blue Technique. *Vet. Pathol.* 2014;51(1):42–87

Reijnders CMA, Van Lier A, Roffel S, Kramer D, Scheper RJ, Gibbs S. Development of a Full-Thickness Human Skin Equivalent in Vitro Model Derived from TERT-Immortalized Keratinocytes and Fibroblasts. *Tissue Eng. - Part A.* 2015;21(17–18):2448–59

Reimann E, Abram K, Kõks S, Kingo K, Fazeli A. Identification of an optimal method for extracting RNA from human skin biopsy, using domestic pig as a model system. *Sci. Rep*. 2019;9(1):1–10

Reimann E, Kingo K, Karelson M, Reemann P, Loite U, Sulakatko H, Keerman M, Raud K, Abram K, Vasar E, Silm H, Koks S. The mRNA expression profile of cytokines connected to

the regulation of melanocyte functioning in vitiligo skin biopsy samples and peripheral blood mononuclear cells. *Hum. Immunol.* 2012;73(4):393–8

Rissmann R, Oudshoorn MHM, Hennink WE, Ponec M, Bouwstra JA. Skin barrier disruption by acetone: Observations in a hairless mouse skin model. *Arch. Dermatol. Res.* 2009;301(8):609–13

Rittié L, Fisher GJ. UV-light-induced signal cascades and skin aging. *Ageing Res. Rev*. 2002;1(4):705–20

Rogers J, Harding C, Mayo A, Banks J, Rawlings A. Stratum corneum lipids: The effect of ageing and the seasons. *Arch. Dermatol. Res*. 1996;288(12):765–70

Roy S, Elgharably H, Sinha M, Ganesh K, Chaney S, Mann E, et al. Mixed-species biofilm compromises wound healing by disrupting epidermal barrier function. *J. Pathol.* 2014;233(4):331–43

Rutledge RG. Sigmoidal curve-fitting redefines quantitative real-time PCR with the prospective of developing automated high-throughput applications. *Nucleic Acids Res.* 2004;32(22)e178

Sadowski T, Klose C, Gerl MJ, Wójcik-Maciejewicz A, Herzog R, Simons K, Reich A, Surma MA. Large-scale human skin lipidomics by quantitative, high-throughput shotgun mass spectrometry. *Sci. Rep.* 2017;7:43761

Saksela O, Alitalo K, Knstala U, Aheri A V. Basal Lamina Components in Experimentally Induced Skin Blisters. *J. Invest. Dermatol.* 1981;77:283–6

Salgado G, Ng YZ, Koh LF, Goh CSM, Common JE. Human reconstructed skin xenografts on mice to model skin physiology. *Differentiation.* 2017;98:14–24

Samadani AA, Nikbakhsh N, Fattahi S, Pourbagher R, Aghajanpour Mir SM, Mousavi Kani N, et al. RNA Extraction from Animal and Human's Cancerous Tissues: Does Tissue Matter? *Int. J. Mol. Cell. Med.* 2015;4(1):54–9

Sandby-Møller J, Poulsen T, Wulf HC. Epidermal Thickness at Different Body Sites: Relationship to Age, Gender, Pigmentation, Blood Content, Skin Type and Smoking Habits. *Acta Derm. Venereol.* 2003;83(6):410–3

Sandilands AC, Irvine AD, McLean W. I. Filaggrin in the frontline: role in skin barrier function and disease. *J. Cell Sci.* 2009;122:1285–94

Sandra K, Sandra P. Lipidomics from an analytical perspective. *Curr. Opin. Chem. Biol*. 2013;17(5):847–53

Saper CB. A guide to the perplexed on the specificity of antibodies. *J. Histochem. Cytochem*. 2009;57(1):1–5

Schäfer-Korting M, Bock U, Diembeck W, Düsing HJ, Gamer A, Haltner-Ukomadu E, Hoffmann C, Kaca M, Kamp H, Kersen S, Kietzmann M, Korting HC, Krächter HU, Lehr CM,

Liebsch M, Mehling A, Müller -Goymann C, Netzlaf F, Niedorf F, Rübbelke MK, Schäfer U, Schmidt E, Schreiber S, Spielmann H, Vuia A, Weimer M. The use of reconstructed human epidermis for skin absorption testing: Results of the validation study. *Altern. Lab. Anim*. 2008a;36(2):161–87

Schäfer-Korting M, Mahmoud A, Borgia SL, Brüggener B, Kleuser B, Schreiber S, Mehnert W. Reconstructed epidermis and full-thickness skin for absorption testing: Influence of the vehicles used on steroid permeation. *Altern. Lab. Anim*. 2008b;36(4):441–52

Schlüter H, Moll I, Wolburg H, Franke WW. The different structures containing tight junction proteins in epidermal and other stratified epithelial cells, including squamous cell metaplasia. *Eur. J. Cell Biol.* 2007;86(11–12):645–55

Schmittgen TD, Livak KJ. Analyzing real-time PCR data by the comparative CT method. *Nat. Protoc.* 2008;3(6):1101–8

Schreiner V, Gooris GS, Pfeiffer S, Lanzendo G, Wenck H, Diembeck W. Barrier Characteristics of Different Human Skin Types Investigated with X-Ray Diffraction, Lipid Analysis, and Electron Microscopy Imaging. *J.Invest Dermatol.* 2000;114(1994):654–60

Seok J, Warren H, Cuenca A, Mindrinos M, Baker H, Xu W. Genomic responses in mouse models poorly mimic human inflammatory diseases. *Proc Natl Acad Sci USA*. 2013;110(9):3507–12

Serup Jø, Jemec GBE, Grove GL. *Handbook of Non-Invasive Methods and the Skin. 2nd ed*. Boca Raton: CRC Press; 2006. ISBN: 9780849314377

Shah H, Rawal Mahajan S. Photoaging: New insights into its stimulators, complications, biochemical changes and therapeutic interventions. *Biomed. Aging Pathol*. 2013;3(3):161–9

Shi SR, Cote RJ, Taylor CR. Antigen retrieval immunohistochemistry: Past, present, and future. J. Histochem. *Cytochem*. 1997;45(3):327–43

Shin K, Margolis B. ZOning out Tight Junctions. *Cell.* 2006;126(4):647–9

van Smeden J, Hoppel L, van der Heijden R, Hankemeier T, Vreeken RJ, Bouwstra JA. LC/MS analysis of stratum corneum lipids: ceramide profiling and discovery. *J. Lipid Res*. 2011a;52(6):1211–21

van Smeden J, Hoppel L, van der Heijden R, Hankemeier T, Vreeken RJ, Bouwstra JA. LC/MS analysis of stratum corneum lipids: ceramide profiling and discovery. *J. Lipid Res*. 2011b;52(6):1211–21

Sommer U, Herscovitz H, Welty FK, Costello CE. LC-MS-based method for the qualitative and quantitative analysis of complex lipid mixtures. *J. Lipid Res.* 2006;47(4):804–14

Sontheimer RD. Skin is not the largest organ. *J. Invest. Dermatol.* 2014;134(2):581–2

Sparvero LJ, Amoscato AA, Dixon CE, Long JB, Kochanek PM, Pitt BR, Bayir H, Kagan VE.

Mapping of phospholipids by MALDI imaging (MALDI-MSI): Realities and expectations. *Chem. Phys. Lipids*. 2012;165(5):545–62

Sugawara T, Iwamoto N, Akashi M, Kojima T, Hisatsune J, Sugai M, Furuse M. Tight junction dysfunction in the stratum granulosum leads to aberrant stratum corneum barrier function in claudin-1-deficient mice. *J. Dermatol. Sci.* 2013;70(1):12–8

Suzuki A. aPKC kinase activity is required for the asymmetric differentiation of the premature junctional complex during epithelial cell polarization. *J. Cell Sci.* 2002;115(18):3565–73

Svoboda M, Bílková Z, Muthný T. Could tight junctions regulate the barrier function of the aged skin? *J. Dermatol. Sci.* 2016. p. 147–52

Svoboda M, Hlobilová M, Marešová M, Sochorová M, Kováčik A, Vávrová K, Dolečková I. Comparison of suction blistering and tape stripping for analysis of epidermal genes, proteins and lipids. *Arch. Dermatol. Res*. 2017; 309:757–765

Tagami H. Location-related differences in structure and function of the stratum corneum with special emphasis on those of the facial skin. *Int. J. Cosmet. Sci*. 2008;30(6):413-34

Tanabe S. Short Peptide Modules for Enhancing Intestinal Barrier Function. *Curr. Pharm. Des*. 2012;18(6):776–81

Thiele JJ, Hsieh SN, Briviba K, Sies H. Protein oxidation in human stratum corneum: Susceptibility of keratins to oxidation in vitro and presence of a keratin oxidation gradient in vivo. *J. Invest. Dermatol.* 1999;113(3):335–9

Torres A, Niemeyer A, Berkes B, Marra D, Schanbacher C, González S, Owens M, Morgan B. 5% Imiquimod cream and reflectance-mode confocal microscopy as adjunct modalities to Mohs micrographic surgery for treatment of basal cell carcinoma. *Dermatologic Surg.* 2004;30(12 I):1462–9

Tortora G, Derrickson B. *Principles of Anatomy and Physiology. 12th ed*. New Jersey: John Wiley & Sons; 2009. ISBN: 978-0470084717

Tsukita S, Furuse M, Itoh M. Multifunctional strands in tight junctions. *Nat. Rev. Mol. Cell Biol.* 2001;2(4):285–93

Turksen K. Barriers built on claudins. *J. Cell Sci*. 2004;117(12):2435–47

Varila E, Rantala I, Oikarinen A, Risteli J, Reunala T, Oksanen H, Punnonen R. The effect of topical oestradiol on skin collagen of postmenopausal women. *Br J Obstet Gynaecol* 1995;102(12):985–9

Vávrová K, Henkes D, Strüver K, Sochorová M, Skolová B, Witting MY, Friess W, Schreml S, Meier RJ, Schäfer-Korting M, Fluhr JW, Küchler S. Filaggrin deficiency leads to impaired lipid profile and altered acidification pathways in a 3D skin construct. *J. Invest. Dermatol*. 2014;134(3):746–53

Venus M, Waterman J, McNab I. Basic physiology of the skin. *Surgery*. 2011;29(10):471–4

Vinson J, Anamandla S. Comparative topical absorption and antioxidant effectiveness of two forms of coenzyme q10 after a single dose and after long-term supplementation in the skin of young and middle-aged subjects. *Int. J. Cosmet. Sci*. 2006;28(2):148

Wallmeyer L, Lehnen D, Eger N, Sochorová M, Opálka L, Kováčik A, Vávrová K, Hedtrich S. Stimulation of PPARα normalizes the skin lipid ratio and improves the skin barrier of normal and filaggrin deficient reconstructed skin. *J. Dermatol. Sci*. 2015;80(2):102–10

Wang CY, Maibach HI. Why minimally invasive skin sampling techniques? A bright scientific future. *Cutan. Ocul. Toxicol.* 2011;30(1):1–6

Waters JC. Accuracy and precision in quantitative fluorescence microscopy. *J. Cell Biol*. 2009;185(7):1135–48

Watson AD. Thematic review series: Systems Biology Approaches to Metabolic and Cardiovascular Disorders. Lipidomics: a global approach to lipid analysis in biological systems. *J. Lipid Res.* 2006;47(10):2101–11

Weigmann HJ, Lademann J, Meffert H, Schaefer H, Sterry W. Determination of the horny layer profile by tape stripping in combination with optical spectroscopy in the visible range as a prerequisite to quantify percutaneous absorption. *Skin Pharmacol. Appl. Skin Physiol*. 1999;12(1–2):34–45

Wenk MR. The emerging field of lipidomics. *Nat. Rev. Drug Discov*. 2005;4(7):594–610

Wolf C, Quinn PJ. Lipidomics: Practical aspects and applications. *Prog. Lipid Res*. 2008;47(1):15–36

Wong R, Tran V, Morhenn V, Hung SP, Andersen B, Ito E, Hatfield GW, Benson NR. Use of RT-PCR and DNA microarrays to characterize RNA recovered by non-invasive tape harvesting of normal and inflamed skin. *J. Invest. Dermatol.* 2004;123(1):159–67

Wong R, Tran V, Talwalker S, Benson NR. Analysis of RNA recovery and gene expression in the epidermis using non-invasive tape stripping. *J. Dermatol. Sci.* 2006;44(2):81–92

Xu Y, Fisher GJ. Ultraviolet (UV) light irradiation induced signal transduction in skin photoaging. *J. Dermatological Sci. Suppl.* 2005;2(1):S1–8

Yaar M, Gilchrest BA. Photoageing: Mechanism, prevention and therapy. *Br. J. Dermatol.* 2007;157(5):874–87

Yamamoto T, Kurasawa M, Hattori T, Maeda T, Nakano H, Sasaki H. Relationship between expression of tight junction-related molecules and perturbed epidermal barrier function in UVB-irradiated hairless mice. *Arch. Dermatol. Res.* 2008;300(2):61–8

Yamashita T, Kuwahara T, González S, Takahashi M. Non-invasive visualization of melanin and melanocytes by reflectance-mode confocal microscopy. *J. Invest. Dermatol*.

2005;124(1):235–40

Yan HC, Juhasz I, Pilewski J, Murphy GF, Herlyn M, Albelda SM. Human/severe combined immunodeficient mouse chimeras: An experimental in vivo model system to study the regulation of human endothelial cell-leukocyte adhesion molecules. *J. Clin. Invest.* 1993;91(3):986–96

Yasumatsu H, Tanabe S. The casein peptide Asn-Pro-Trp-Asp-Gln enforces the intestinal tight junction partly by increasing occludin expression in Caco-2 cells. *Br. J. Nutr.* 2010;104(7):951–6

Yoneda K, McBride OW, Korge BP, Kim IG, Steinert PM. The cornified cell envelope: Loricrin and transglutaminases. *J. Dermatol.* 1992;19(11):761–4

Yoshida K, Yokouchi M, Nagao K, Ishii K, Amagai M, Kubo A. Functional tight junction barrier localizes in the second layer of the stratum granulosum of human epidermis. *J. Dermatol. Sci.* 2013;71(2):89–99

Yuki T, Hachiya A, Kusaka A, Sriwiriyanont P, Visscher MO, Morita K, et al. Characterization of Tight Junctions and Their Disruption by UVB in Human Epidermis and Cultured Keratinocytes. *J. Invest. Dermatol.* 2011;131(3):744–52

Yuki T, Haratake A, Koishikawa H, Morita K, Miyachi Y, Inoue S. Tight junction proteins in keratinocytes: Localization and contribution to barrier function. *Exp. Dermatol.* 2007;16(4):324–30

Yuki T, Komiya A, Kusaka A, Kuze T, Sugiyama Y, Inoue S. Impaired tight junctions obstruct stratum corneum formation by altering polar lipid and profilaggrin processing. *J. Dermatol. Sci*. 2013;69(2):148–58

Zheng Y, Yin H, Boeglin WE, Elias PM, Crumrine D, Beier DR, Brash AR. Lipoxygenases mediate the effect of essential fatty acid in skin barrier formation: A proposed role in releasing omega-hydroxyceramide for construction of the corneocyte lipid envelope. *J. Biol. Chem*. 2011;286(27):24046–56

Ziboh V a, Cho Y, Mani I, Xi S. Biological significance of essential fatty acids/ prostanoids/lipoxygenase-derived monohydroxy fatty acids in the skin. *Arch. Pharm. Res.* 2002;25(6):747–58

Zoschke C, Ulrich M, Sochorová M, Wolff C, Vávrová K, Ma N, Ulrich C, Brandner JM, Schäfer-Korting M. The barrier function of organotypic non-melanoma skin cancer models. *J. Control. Release.* 2016;233:10–8

Zuber TJ. Punch biopsy of the skin. *Am. Fam. Physician.* 2002;65(6):1155-1158+1164+1167

14 SUPPLEMENT

Supplementary Table 1: Difference in tight junction proteins gene expression in the aged skin in comparison to the young skin.

Protein Name	Gene Name	% change[1]	P[2]
Claudin-1	CLDN1	49	0.066613
Claudin-12	CLDN12	50	0.062081
Claudin-14	CLDN14	134	0.443192
Claudin-15	CLDN15	180	0.196604
Claudin-19	CLDN19	130	0.606717
Claudin-2	CLDN2	93	0.791794
Claudin-22	CLDN22	127	0.436552
Claudin-23	CLDN23	94	0.84548
Claudin-25	CLDN25	104	0.897453
Claudin-3	CLDN3	113	0.680981
Claudin-4	CLDN4	131	0.766747
Claudin-5	CLDN5	100	0.988526
Claudin-6	CLDN6	201	0.098568
Claudin-7	CLDN7	220	0.061234
Claudin-9	CLDN9	126	0.712389
Occludin	OCLN	146	0.394748
Tricellulin	MARVELD2	100	0.998974
JAM-A	F11R	99	0.203679
JAM-B	JAM2	125	0.452228
ZO-1	TJP1	90	0.81784
ZO-2	TJP2	152	0.08018
ZO-3	TJP3	95	0.885548
Symplekin	SYMPK	83	0.517268
Cingulin	CGN	381	0.031543
Par3	PARD3	131	0.197697
Par6	PARD6A	152	0.197121
aPKC iota	PRKCI	42	0.082615
aPKC zeta	PRKCZ	144	0.213673

[1]*young = 100 %*

[2]*Unadjusted p value*

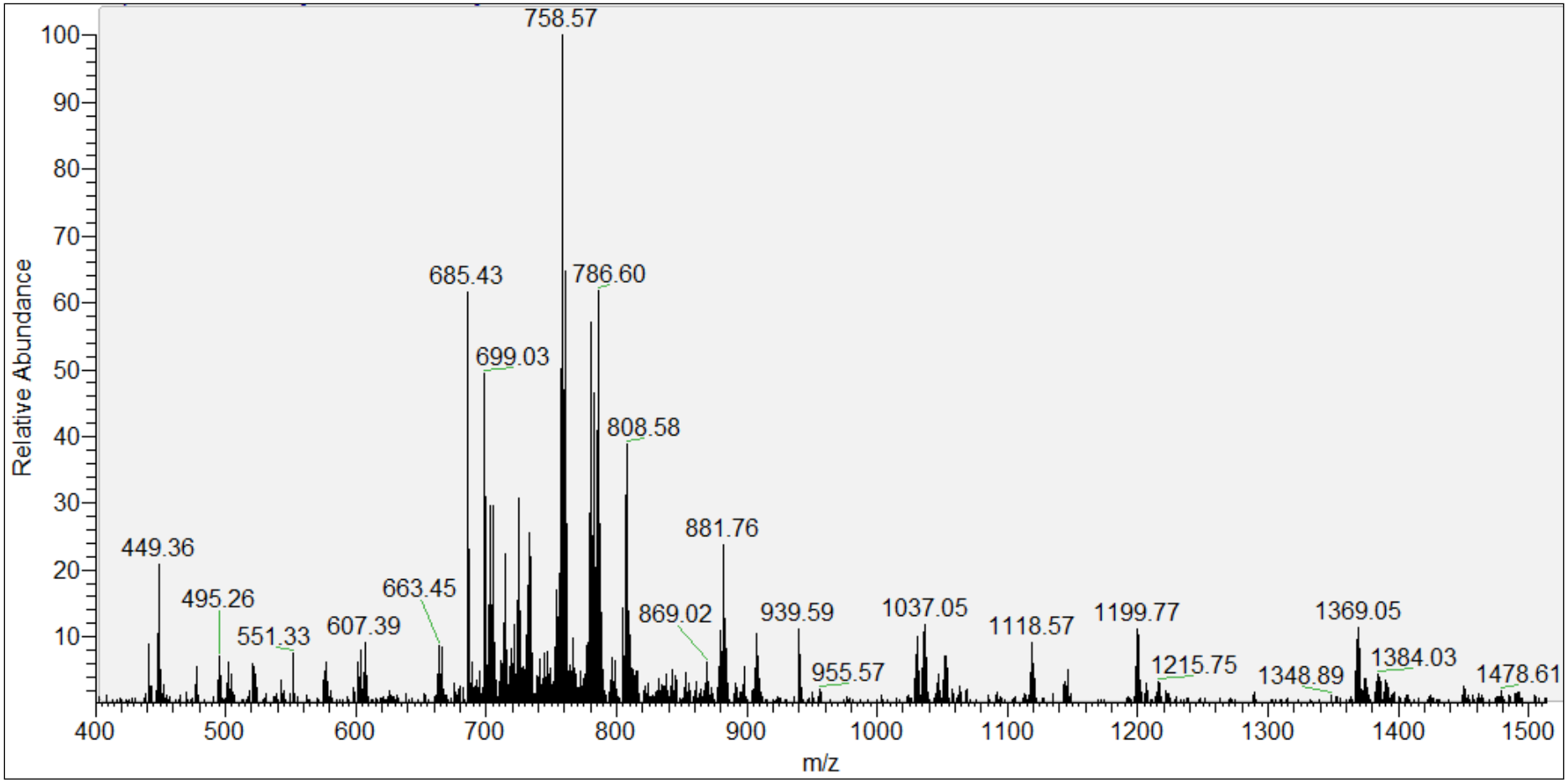

Supplementary Figure 1: MALDI fullscan of the porcine epidermis after Bligh Dyer extraction using DHB matrix (10 mg/mL). Positive ion mode with range 400-1600 of m/z.

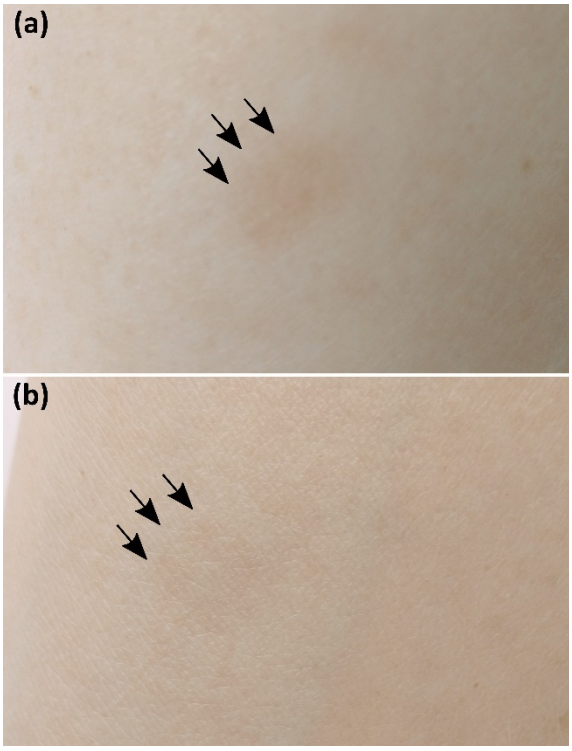

Supplementary Figure 2: Hyperpigmentation after the suction blistering procedure occured in some of the volunteers. Images show hyperpigmented zones (arrows) one month (a) and six months (b) after the suction blistering procedure

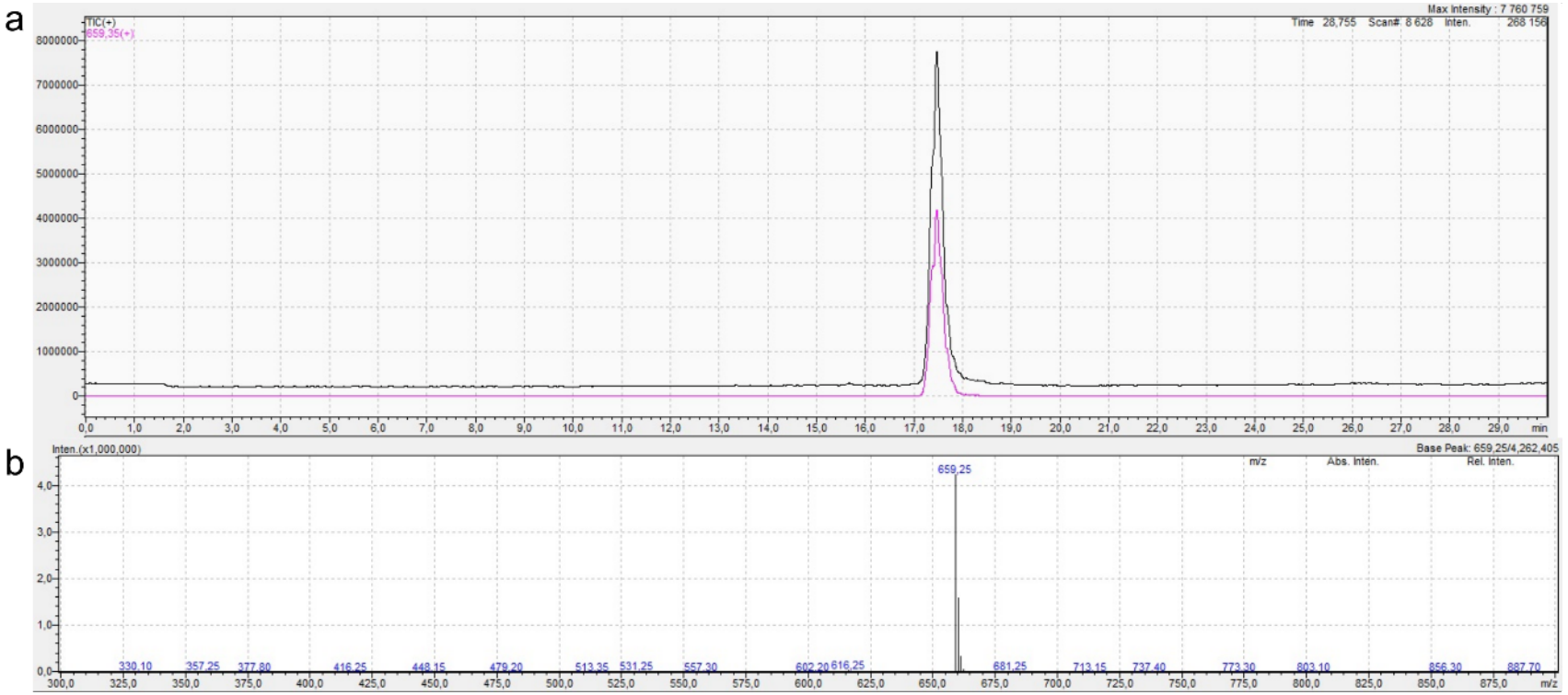

Supplementary Figure 3: Characterization of a synthetized NPWDQ peptide by HPLC/MS. No impurities were detected either in the chromatogram (a) or MS spectrum (b). Dominant peak 659,25 [M+H]+ corresponds to an NPWDQ peptide.

15 TABLE OF PUBLICATIONS

Publication Type	Authors	Title	Publish Place	Publish Date
Original Article	Svoboda M, Vávrová K, Marešová M, Čechová M, Pavlík V, Šuláková R, Sochorová M, Kováčik A, Fryčák R, Muthný T, Dolečková I	Occludin contributes to the water barrier maintenance in the photoaged skin	-	Submitted to JID in 2018
Original Article	Svoboda M, Hlobilová M, Marešová M, Sochorová M, Kováčik A, Vávrová K, Dolečková I	Comparison of suction blistering and tape stripping for analysis of epidermal genes, proteins and lipids	Archives of Dermatological Research	11/2017
Original Article	Šmejkalová D, Muthný T, Nešporová K, Hermannová M, Achbergerová E, Huerta-Angeles G, Svoboda M, Čepa M, Machalová V, Luptáková D, Velebný V	Hyaluronan Polymeric Micelles for Topical Drug Delivery	Carbohydrate Polymers	01/2017
Review Article	Svoboda M, Bílková Z, Muthný T	Could tight junctions regulate the barrier function of the aged skin?	Journal of Dermatological Science	3/2016
Presentation	Svoboda M, Dolečková I	Aged skin barrier and TEWL phenomenon	MKK 2017 Mikulov	05.10.2017
Poster	Svoboda, M, Pavlík V, Hlobilová M, Dolečková I	Expression of tight junction proteins claudin-1, occludin and ZO-2 in aged skin	ESDR 2016 Munich	07.-10.09.2016
Presentation	Svoboda, M, Pavlík V, Hlobilová M, Dolečková I	Structural analysis and relative quantification of tight junction proteins: claudin-1 in human skin biopsy using confocal microscope.	CeCe 2015 Brno	21.-23.09.2015
Poster	Svoboda M, Muthný T	Lipidomic profile of porcine epidermis by maldi-orbitrap mass spectrometry using shotgun approach.	CeCe 2015 Brno	21.-23.09.2015

Poster	Svoboda M, Salvetová E, Šmejkalová D, Muthný T	Preanalytic phase optimization of ethyl ferulate analysis after penetration experiments into the skin within various delivery systems	Cece 2014 Brno	20.-22.10.2014
Poster	Svoboda M, Salvetová E, Šmejkalová D, Muthný T	Percutaneous delivery of ethylferulate in HA based polymeric micelles	Stratum Corneum Conference, Cardiff	17.-19.09.2014